

The Penn State–Toruń Centre for Astronomy Planet Search stars [★]

I. Spectroscopic analysis of 348 red giants

P. Zieliński¹, A. Niedzielski¹, A. Wolszczan^{2,3}, M. Adamów¹, and G. Nowak¹

¹ Toruń Centre for Astronomy, Nicolaus Copernicus University, Gagarina 11, 87-100 Toruń, Poland

e-mail: pawziel@astri.umk.pl, aniedzi@astri.umk.pl, adamow@astri.umk.pl, grzenow@astri.umk.pl

² Department of Astronomy and Astrophysics, Pennsylvania State University, 525 Davey Laboratory, University Park, PA 16802

e-mail: alex@astro.psu.edu

³ Center for Exoplanets and Habitable Worlds, Pennsylvania State University, 525 Davey Laboratory, University Park, PA 16802

Received ; accepted

ABSTRACT

Aims. We present basic atmospheric parameters (T_{eff} , $\log g$, v_t and [Fe/H]) as well as luminosities, masses, radii and absolute radial velocities for 348 stars, presumably giants, from the ~ 1000 star sample observed within the Penn State–Toruń Centre for Astronomy Planet Search with the High Resolution Spectrograph of the 9.2 m Hobby-Eberly Telescope. The stellar parameters (luminosities, masses, radii) are key ingredients in proper interpretation of newly discovered low-mass companions while a systematic study of the complete sample will create a basis for future statistical considerations concerning low-mass companions appearance around evolved low and intermediate-mass stars.

Methods. The atmospheric parameters were derived using a strictly spectroscopic method based on the LTE analysis of equivalent widths of Fe I and Fe II lines. With existing photometric data and the Hipparcos parallaxes we estimated stellar masses and ages via evolutionary tracks fitting. The stellar radii were calculated from either estimated masses and the spectroscopic $\log g$ or from the spectroscopic T_{eff} and estimated luminosities. The absolute radial velocities were obtained by cross-correlating spectra with a numerical template.

Results. We completed the spectroscopic analysis for 332 stars of which 327 were found to be giants. For the remaining 16 stars with incomplete data a simplified analysis was applied. The results show that our sample is composed of stars with effective temperatures ranging from 4055 K to 6239 K, and $\log g$ between 1.39 and 4.78 (5 dwarfs were identified). The estimated luminosities ranging between $\log L/L_\odot = -1.0$ and 3 lead to masses ranging from 0.6 to $3.4 M_\odot$. Only 63 stars with masses larger than $2 M_\odot$ were found. The radii of our stars range from 0.6 to $52 R_\odot$ with vast majority between 9 – $11 R_\odot$. The stars in our sample are generally less metal abundant than the Sun with median [Fe/H] = -0.15 . The estimated uncertainties in the atmospheric parameters were found to be comparable to those reached in other studies. However, due to lack of precise parallaxes the stellar luminosities and, in turn, the masses are far less precise, within $0.2 M_\odot$ in best cases, and $0.3 M_\odot$ on average.

Key words. Stars: fundamental parameters - Stars: atmospheres - Stars: late-type - Techniques: spectroscopic - Planetary systems

1. Introduction

Since the discovery of the first extrasolar planetary systems by Wolszczan & Frail (1992); Mayor & Queloz (1995) and Marcy & Butler (1996) over 700 planets were found around other stars. The richness of exoplanets and the architectures of planetary systems that are today emerging is amazing and rises questions about a general picture of planet formation and evolution. Before such a general picture will be available, studies of planetary systems in various environments are essential.

The observational techniques applied in searches for exoplanets are all limited to their areas of competence – a range in stellar or planetary parameters (effective temperatures, masses, planetary periods or orbital separations etc.) that are available to them. Due to the current detectors limitations the direct imaging searches for exoplanets deliver typically massive planets at large orbital distances from low-mass stars (cf. 2M1207 b –

Chauvin et al. 2004 or HD 8799 system – Marois et al. 2008). The transit planet searches, conveniently operating in the $\sin i \approx 1$ domain (i being orbital inclination), discover exoplanets with relatively short orbital periods (orbital separations) due to the natural limit of the observable transit length set by the lengths of a night (a condition now being relaxed with the multi-site or space observations, cf. HD 80606 b – Hidas et al. 2010, Hébrard et al. 2010, Kepler 11g – Lissauer et al. 2011). The searches for planets based on the radial velocity (RV) technique are the most versatile. They detect planetary candidates at various orbital separations and in a wide range of planetary minimum masses, as long as $\sin i \neq 0$ (cf. for example GJ 581 system – Mayor et al. 2009 and 47 UMa d – Gregory & Fischer 2010). Even this method has its limitations, though. Since it requires a large number of narrow spectral lines it focuses on the slowly rotating cool stars of late-F to M spectral type what sets an upper limit to the Main Sequence planetary hosts masses ($M \lesssim 1.5 M_\odot$). This technique is unfortunately also seriously affected by the stellar activity (Queloz et al. 2001) which, if not resolved, adds noise (jitter) and limits the precision in RV (Carney et al. 2003; Hekker et al. 2006; Cumming et al. 2008). It is, however the most suitable in searches for planets around

* Based on observations obtained with the Hobby-Eberly Telescope, which is a joint project of the University of Texas at Austin, the Pennsylvania State University, Stanford University, Ludwig-Maximilians-Universität München, and Georg-August-Universität Göttingen.

stars more massive than $\sim 1.5M_{\odot}$. In turn of evolution these stars slow down their rotation and decrease their effective temperatures becoming red giants available for precise RV measurements.

The Penn State–Toruń Centre for Astronomy Planet Search (PTPS) is aiming at detection and characterization of planetary systems around stars at various evolutionary stages (Niedzielski & Wolszczan 2008) with the long-term goal of description of the evolution of planetary systems with aging stars. To this end over 1000 stars are monitored with the Hobby-Eberly Telescope (HET) for RV variations using the high precision iodine-cell technique (Butler et al. 1996). The sample is mainly composed of evolved low-mass and intermediate-mass stars: ~ 575 giants (including presented here 348 stars from the Red Giant Clump (RGC) sample) and ~ 225 subgiants but it also contains ~ 200 slightly evolved dwarfs. Several stars with planetary-mass companions were already discovered, mainly around red giants (Niedzielski et al. 2007, 2009a,b; Gettel et al. 2012b,a). These findings supplemented the slowly growing population of ~ 50 planets currently known around evolved stars, discovered in such projects like: the McDonald Observatory Planet Search (Cochran & Hatzes 1993; Hatzes & Cochran 1993), the Okayama Planet Search (Sato et al. 2003), the Tautenburg Planet Search (Hatzes et al. 2005), the Lick K-giant Survey (Frink et al. 2002), the ESO FEROS planet search (Setiawan et al. 2003a,b), the Retired A Stars and Their Companions (Johnson et al. 2007), the CORALIE & HARPS search (Lovis & Mayor 2007), the Boyunsen Planet Search (Lee et al. 2011) and several others.

With this paper we start a series devoted to a detailed description of stars incorporated in the complete PTPS sample, their atmospheric parameters, elemental abundances, rotation velocities, kinematical properties, masses, radii, ages etc. The derived parameters will not only describe our sample but also will allow for proper interpretation of the planet search results. The stellar masses are essential in extracting the planetary mass companions minimum masses ($m_p \sin i$), the radii and projected rotation velocities are key ingredients in the stellar activity considerations etc. Since the complete sample contains ~ 1000 stars randomly distributed in the skies it is of interest for general stellar and galactic astrophysics as well. It may be used for studies of galactic structure and evolution, galactic distribution of planetary systems (Haywood 2009) and the galactic habitable zone (Gonzalez et al. 2001; Lineweaver et al. 2004; McCabe & Lucas 2010; Gowanlock et al. 2011).

The purposes of present paper is to determine atmospheric parameters, such as effective temperatures (T_{eff}), stellar gravitational accelerations ($\log g$), microturbulence velocities (v_t) and metallicities ([Fe/H]) for 348 GK-type stars, presumably Red Clump giants observed within the PTPS survey. Together with existing photometric data and parallaxes (when available) they will allow us to estimate stellar masses (M/M_{\odot}), radii (R/R_{\odot}) and ages.

The RGC, together with the Main Sequence (MS) and the red giant branch (RGB) is one of the most characteristic features of the Hertzsprung-Russell diagram (HRD). It was identified by Cannon (1970) and Faulkner & Cannon (1973) as the location of the steady core helium burning. That finding was elaborated in detail by Girardi (1999). Jimenez et al. (1998) used the RGC stars to estimate the age of the Galaxy. Due to very similar intrinsic brightness of all stars at that stage the RGC was proposed as a standard candle in distance estimates and applied to the Galactic Center (Paczynski & Stanek 1998), the Large Magellanic Cloud (Salaris et al. 2003) and other stellar systems.

Interesting stellar evolution phase and general astrophysical application make the red giants, and especially the RGC stars subject of numerous surveys. McWilliam (1990) obtained T_{eff} for 671 stars from broad-band photometry, $\log g$ via isochrone fitting as well as the local thermodynamical equilibrium (LTE) abundances from high resolution spectra. Zhao et al. (2001) delivered atmospheric parameters, iron abundances, α -element enhancements, and masses for 39 Red Clump giants selected from the Hipparcos catalogue. Famaey et al. (2005) provided the CORAVEL radial velocities for a sample of about 6 600 K-type giants. Detailed spectroscopic studies of various subsamples of the galactic Red Clump giants were presented in Mishenina et al. (2006), Bizyaev et al. (2006, 2010), Hekker & Meléndez (2007), Liu et al. (2007), Luck & Heiter (2007), Takeda et al. (2008), Puzares et al. (2010).

Gontcharov (2008) summarized kinematical properties and galactic distribution of 97 348 RGC stars based on Tycho-2 proper motions and Tycho-2 and 2MASS photometry. Valentini & Munari (2010) studied 277 RGC stars and presented accurate multi-epoch radial velocities, atmospheric parameters, distances and space velocities (U, V, W). Moreover, Tautvaišienė et al. (2010) in a recent paper presented $^{12}\text{C}/^{13}\text{C}$ abundance ratio determinations in a sample of 34 Galactic clump giants as well as abundances of nitrogen, carbon and oxygen.

Meanwhile a new insight of giants, including clump giants, became available through CoRoT (Baglin et al. 2006) and Kepler (Gilliland et al. 2010) precise photometry. The solar-like oscillations in red giants were first identified in ground-based RV observations (Hatzes & Cochran 1994; Merline 1999). De Ridder et al. (2009) reported the presence of radial and non-radial oscillations in over 300 giants observed with CoRoT. These oscillations were used in massive masses and radii determinations for giants (Kallinger et al. 2010; Bedding et al. 2010; Hekker et al. 2011).

This paper is organized as follows. In Sect. 2, we describe the sample and the observational material. The procedure of Fe lines equivalent widths measurements and its precision are presented in Sect. 3. The outline of the method applied in our spectroscopic analysis is given in Sect. 4 while in the following Sect. 5 we present several tests to evaluate reliability of the method and estimate uncertainties. Section 6 contains summary of the determined atmospheric parameters for our stars. These parameters are used in Sect. 7 to estimate stellar integrated parameters: luminosities, masses, radii, ages. Section 8 presents the method and results of our RV determinations. The comparison of our results with other published data, whenever available, is presented in Sect. 9. Section 10 contains discussion of atmospheric parameters and conclusions are presented in Sect. 11.

2. Targets selection and observations

The sample presented here, 348 stars, originally the SIM-EPIcS¹ reference candidates, selected as presumably RGC stars basing on their existing photometry and reduced proper motions (Gelino et al. 2005; Law et al. 2006) constitute the so-called RGC subsample of the PTPS.

They are relatively bright field stars, with V between 4.5 and 11 mag but in the SIMBAD² database spectral types and/or lu-

¹ Space Interferometry Mission (SIM) key project: Extra-solar Planet Interferometric Survey (EPIcS)
<http://planetquest.jpl.nasa.gov/SIM>

² The SIMBAD astronomical database is operated at CDS, Strasbourg, France.

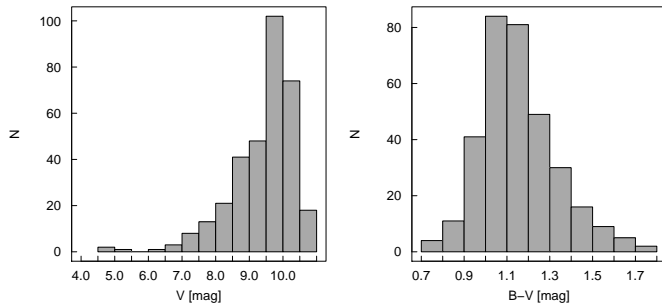


Fig. 1. Histograms of the apparent magnitudes in V band (left panel) and (B–V) (right panel) for the 348 Red Clump giants observed within the PTPS.

minosity class estimates are available only for a few (4 are classified as dwarfs and 22 as giants). The basic photometric data for the sample stars come from the 2MASS Point Source catalogue (Cutri et al. 2003) and the Tycho-2 catalogue (Høg & Murić 2000) compiled by Gelino et al. (2005). For several stars missing data were gathered from Kharchenko & Roeser (2009). The distributions of visual magnitudes and B–V color indices are presented in Fig. 1. Vast majority, 92% of stars, are fainter than $V = 8$ mag with (B–V) between 0.7 to 1.8 magnitudes (1.1 mag on average).

Our sample is composed of much fainter stars than included in most of the other RGC surveys (Famaey et al. 2005; Mishenina et al. 2006; Hekker & Meléndez 2007; Takeda et al. 2008; Valentini & Munari 2010) and can be compared to the more numerous sample of Bizyaev et al. (2006, 2010). The list of stars, their identification and basic observational parameters are presented in Table 1.

Our high quality, high resolution optical spectra were collected since 2004 with the HET (Ramsey et al. 1998) located in the McDonald Observatory. The telescope was equipped with the High Resolution Spectrograph (HRS) fed with a 2 arcsec fiber, working in the $R = 60\,000$ resolution (Tull 1998). The observations were performed in the queue scheduled mode (Shetrone et al. 2007). The spectra consisted of 46 echelle orders recorded on the „blue” CCD chip (407 – 592 nm) and 24 orders on the „red” one (602 – 784 nm). The signal to noise ratio was typically better than 200 – 250 per resolution element. The basic data reduction (flat fielding, extraction of the spectrum, wavelength calibration, normalization to continuum) were performed using standard IRAF³ tasks and scripts. The wavelength calibration was based on Th-Ar lamp spectrum identification presented in Mader & Shetrone (2002).

3. Equivalent widths of Fe lines

Since equivalent widths (EWs) of hundreds of iron lines for every object were needed we used the DAOSPEC⁴ (Stetson & Pancino 2008) to measure the EWs in an automatic manner. However, to validate reliability of the results and estimate uncertainties in EWs we measured spectra of 29 stars

³ IRAF is distributed by the National Optical Astronomy Observatories, which are operated by the Association of Universities for Research in Astronomy, Inc., under cooperative agreement with the National Science Foundation.

⁴ <http://www2.cadc-ccda.hia-ihc.nrc-cnrc.gc.ca/community/STETSON/daospec.html> <http://www.bo.astro.it/~pancino/projects/daospec.html>

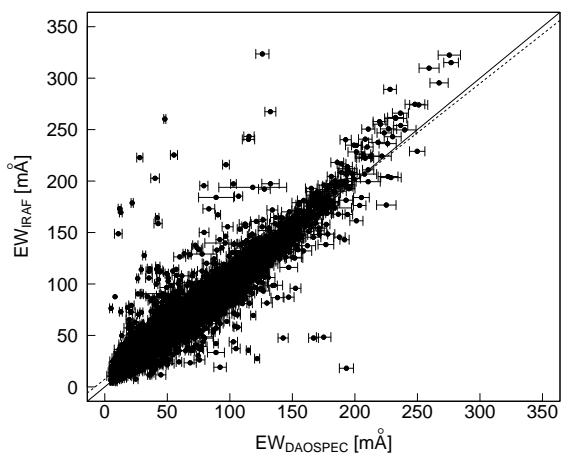


Fig. 2. A comparison of the automatic (DAOSPEC) and handmade (IRAF) EWs measurements of 5 695 Fe lines for 29 stars. The solid line presents the one to one relation, the dashed one is the best linear fit to the data. The individual uncertainties of the DAOSPEC EWs measurements are presented.

manually with the IRAF (Gaussian fitting) as well. In Fig. 2 the comparison of the IRAF (manual) and the DAOSPEC (automatic) measurements is presented. We found that the best agreement between the measurements is reached for lines with the EWs lower than 200 mÅ. Lines with larger EWs revealed some discrepancy towards higher manual EWs values. In general, the linear fit to all measurements is nearly a one to one relation. For 5 632 lines with the $\text{EW} \leq 200$ mÅ we found $\text{EW}_{\text{IRAF}} = (0.937 \pm 0.005)\text{EW}_{\text{DAOSPEC}} + (8.46 \pm 0.35)$ and the Pearson correlation coefficient of $R = 0.939$. The mean difference between the IRAF and the DAOSPEC measurements was 5.3 mÅ with a scatter of 12.8 mÅ. The mean uncertainty in the DAOSPEC EWs was 2.13 mÅ. We proceeded with the automatic measurements in the further analysis.

To apply the procedure described in the following section we measured the EWs of neutral (Fe I) and ionized (Fe II) iron absorption lines for which precise atomic data, i.e. laboratory wavelenghts, lower excitation potentials (χ) and oscillator strength (gf) were available from Takeda et al. (2005a,b). All these atomic data were compiled from the line-lists of Grevesse & Sauval (1999); Meylan et al. (1993) and Kurucz et al. (1984). Due to differences in the spectral coverage and the CCD chip cosmetics we were able to identify up to 296 lines (269 Fe I and 27 Fe II lines) from the initial sample of ~ 330 iron lines from Takeda et al. (2005a) in the HET/HRS spectra. After rejecting blends, very weak and saturated lines we used the EWs of 190 Fe I and 15 Fe II lines per star on average. Only unblended lines with the EWs ranging from 5 mÅ to 200 mÅ were included in the final spectroscopic analysis.

4. An outline of the analysis method

The iron EWs were analyzed with the TGVIT (Takeda et al. 2002a, 2005a), which is a part of the SPTOOL⁵ package. This numerical algorithm is a modified version of an earlier code and is based on the atmospheric models computed by Kurucz (1993a,b). The TGVIT uses an iterative procedure to achieve more cohesive parameter fits and in the version available to us

⁵ <http://optik2.mtk.nao.ac.jp/~takeda/sptool>

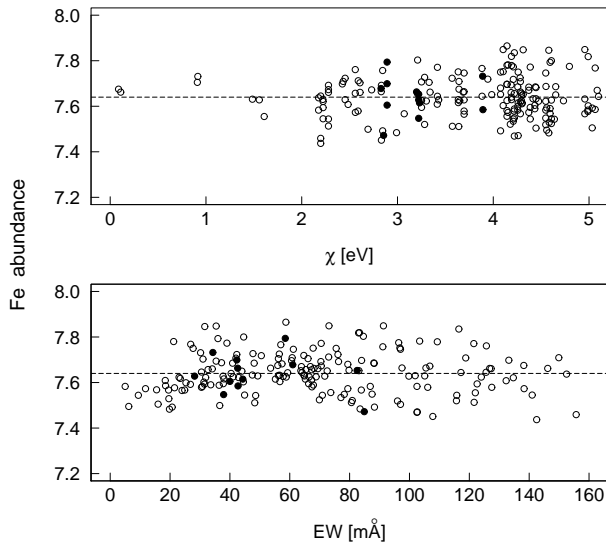


Fig. 3. An illustration of the TGVIT analysis of TYC 3018-00996-1: Fe abundance vs. χ (top panel) relation and Fe abundance vs. EW (bottom panel) relation. The open and filled circles stand for 176 Fe I and 12 Fe II lines respectively. The mean Fe abundance is showed on each panel as a dashed line.

was suitable for lower effective temperatures ($T_{\text{eff}} \geq 4250$ K) than the original version (Takeda et al. 2002a), so we could apply it to the late-type stars in our sample. More details concerning the iteration procedures, data calculations and formulation of the numerical problems are presented in Takeda et al. (2002a,b, 2005a,b).

This purely spectroscopic method is based on analysis of Fe I and Fe II lines and relies on three conditions resulting from the assumption of the local thermodynamical equilibrium (LTE) that have to be satisfied:

1. The abundances derived from Fe I lines may not show any dependence on the lower excitation potential χ (excitation equilibrium);
2. The averaged abundances from Fe I and Fe II lines must be equal (ionization equilibrium);
3. The abundances derived from Fe I lines may not show any dependence on the equivalent widths EWs (matching the curve of growth shape).

We used the TGVIT to calculate T_{eff} , $\log g$, v_t and $[\text{Fe}/\text{H}]$, defined in the standard manner as $[\text{Fe}/\text{H}] = \log(N_{\text{Fe}}/N_{\text{H}}) - \log(N_{\text{Fe}}/N_{\text{H}})_\odot$, with the solar value of 7.50 Kurucz (1993a); Holweger et al. (1991).

Because of relatively low T_{eff} of our stars the number of available Fe II lines was not sufficiently large (less than 10% of Fe I lines) and consequently we neglected the dispersion of Fe II abundances while estimating the minimization function D^2 (TGVIT defines the dispersion D^2 as a function of three arguments: T_{eff} , $\log g$, v_t that is minimized to obtain proper Fe abundance). For the coefficients included in D^2 we assumed the values of: $c_1 = 0$, $c_2 = 1$, $c_3 = 0$ (we refer the reader to Takeda et al. (2002a) for details).

In the vast majority of cases all three above-mentioned conditions were fulfilled what was checked for every star by visual evaluation of relations between Fe abundances and χ or EWs like those presented in Fig. 3. The assumptions were justified if no relation between Fe abundance and these two parameters was present. Another conditions evaluated for every star were

the equivalence of mean Fe abundances for Fe I and Fe II lines and the scatter around average abundance. In turn of visual inspection the Fe lines showing apparent deviations from the mean Fe abundances were rejected. In the following step the parameter were redetermined and the procedure was repeated, if necessary, until coherent solutions for all parameters were reached. The rejected lines were typically unrecognized blends or lines with EWs larger than 150 mÅ with the excitation potential of less than 0.5 eV.

The Fe abundance depends on both T_{eff} and $\log g$. The coupling is so strong that in the iterative approach of Takeda et al. (2002a) T_{eff} and $\log g$ are actually simultaneously fitted and treated as „one variable” (v_t being the other). This coupling may, in principle, lead to degeneracy of purely spectroscopic parameters as higher effective temperature may be compensated by the gravitational acceleration. However, in our sample, composed of stars with effective temperatures similar to the Sun or lower we do not expect this effect to introduce significant uncertainties. We refer the reader to Takeda et al. (2002a) for a detailed discussion of this problem as well as for an extensive discussion on the behavior of the D^2 function, along with its related components, around the converged solutions.

5. Verification of the adopted approach

Before running the TGVIT for our program stars we performed a series of test using various input data. First of all we tested our installation of the TGVIT by running it with the data for the Sun and τ Cet (HD 10700) distributed together with the code. These EWs were obtained from high dispersion spectra obtained at the Okayama Astrophysical Observatory with the 188 cm telescope (Takeda et al. 2005a). Our results are compared with those of Takeda et al. (2005a) in Table 2. The results are practically identical which proves that our installation works well.

In a following step we determined atmospheric parameters (i) for several stars, for which similar determinations were available form Katz et al. (1998) using Echelle spectra available from the ELODIE Library (Soubiran et al. 1998) and (ii) for a few well-known stars with planets, for which recent atmospheric parameters determinations are available in Butler et al. (2006), using our own HET/HRS spectra. The purpose of these tests was to estimate reliability of the adopted method and to search for systematic effects.

Another important reason for that analysis was to assess reliability of uncertainties delivered by the TGVIT as these are determined from the quality of fits for T_{eff} , $\log g$ and microturbulence velocity and should be considered as intrinsic. Only the uncertainties in $[\text{Fe}/\text{H}]$ are based on actual scatter between individual determinations for all lines in use and are expected to be realistic.

5.1. Tests with ELODIE data

We analyzed with the TGVIT spectra of randomly selected 13 stars downloaded from the ELODIE Library (Soubiran et al. 1998)⁶ at the Observatoire de Haute-Provence. Both giants and dwarfs with spectral types of G0-K3 were selected to cover similar parameter space to our sample.

These spectra were obtained with lower than ours resolution of $R = 42\,000$ (Katz et al. 1998). The spectral wavelength range

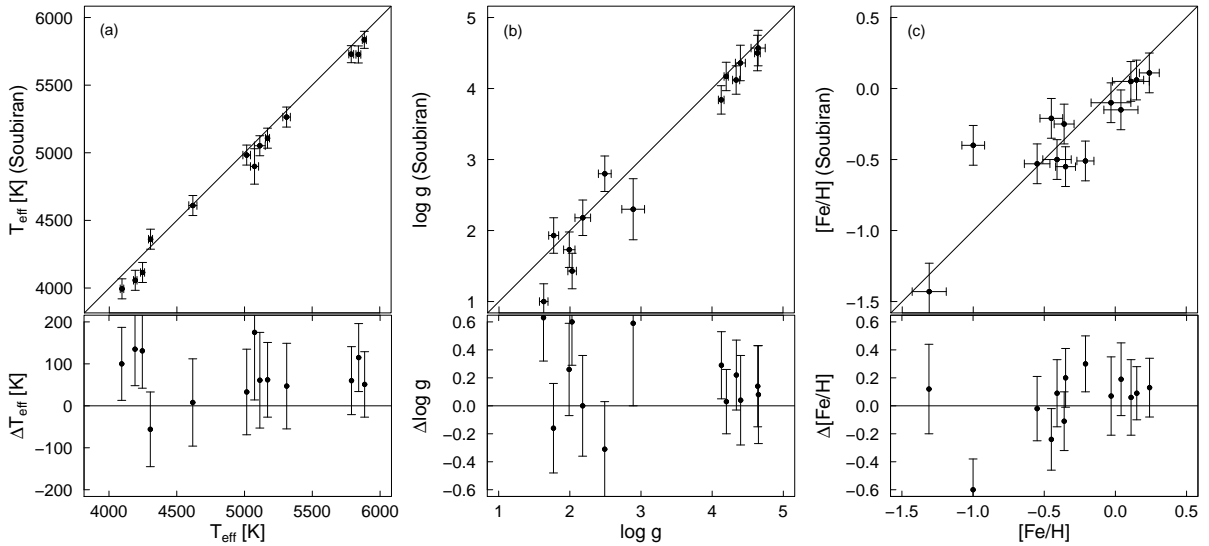
⁶ Library of the ELODIE spectra of F5 to K7 stars is available only in electronic form via <http://vizier.cfa.harvard.edu/viz-bin/VizieR?-source=J/A+AS/133/221>

Table 2. Atmospheric parameters of the Sun and τ Cet determined by Takeda et al. (2005a) and our results.

Name	Sp. Type	Takeda et al.				our results			
		T_{eff} [K]	$\log g$ [cm s ⁻²]	v_t [km s ⁻¹]	[Fe/H]	T_{eff} [K]	$\log g$ [cm s ⁻²]	v_t [km s ⁻¹]	[Fe/H]
Sun	G2V	5785 ± 8	4.44 ± 0.02	0.96 ± 0.06	0.01 ± 0.04	5785 ± 8	4.44 ± 0.02	0.96 ± 0.06	0.02 ± 0.04
τ Cet (HD 10700)	G8V	5420 ± 0	4.68 ± 0.00	0.66 ± 0.10	-0.43 ± 0.06	5420 ± 0	4.68 ± 0.00	0.65 ± 0.10	-0.43 ± 0.06

Table 3. Atmospheric parameters determined by Soubiran et al. (1998) and our results for 13 stars observed with ELODIE.

Name	Sp. Type	Soubiran et al.			our results		
		T_{eff} [K]	$\log g$ [cm s ⁻²]	[Fe/H]	T_{eff} [K]	$\log g$ [cm s ⁻²]	[Fe/H]
HD 10380	K3III	4057 ± 74	1.43 ± 0.25	-0.25 ± 0.14	4192 ± 13	2.03 ± 0.06	-0.36 ± 0.07
HD 10700	G8V	5264 ± 74	4.36 ± 0.25	-0.50 ± 0.14	5311 ± 28	4.40 ± 0.07	-0.41 ± 0.10
HD 22049	K2V	5052 ± 74	4.57 ± 0.25	-0.15 ± 0.14	5113 ± 40	4.65 ± 0.10	0.04 ± 0.12
HD 30834	K3III	4115 ± 74	1.73 ± 0.25	-0.21 ± 0.14	4246 ± 15	1.99 ± 0.08	-0.45 ± 0.08
HD 34411	G0V	5835 ± 63	4.17 ± 0.20	0.06 ± 0.14	5886 ± 15	4.20 ± 0.03	0.15 ± 0.05
HD 39003	K0III	4610 ± 74	2.18 ± 0.25	-0.10 ± 0.14	4618 ± 30	2.18 ± 0.11	-0.03 ± 0.14
HD 39853	K3	3994 ± 74	1.00 ± 0.25	-0.40 ± 0.14	4094 ± 13	1.63 ± 0.06	-1.00 ± 0.08
HD 113226	G8III	4983 ± 74	2.80 ± 0.25	0.05 ± 0.14	5016 ± 28	2.49 ± 0.09	0.11 ± 0.13
HD 124897	K2III	4361 ± 74	1.93 ± 0.25	-0.53 ± 0.14	4305 ± 15	1.77 ± 0.07	-0.55 ± 0.09
HD 132142	K1V	5108 ± 74	4.50 ± 0.25	-0.55 ± 0.14	5170 ± 15	4.64 ± 0.04	-0.35 ± 0.07
HD 175305	G5III	4899 ± 131	2.30 ± 0.43	-1.43 ± 0.20	5074 ± 30	2.89 ± 0.16	-1.31 ± 0.12
HD 204613	G0III	5727 ± 63	3.84 ± 0.20	-0.51 ± 0.14	5842 ± 18	4.13 ± 0.04	-0.21 ± 0.06
HD 217014	G5V	5729 ± 63	4.12 ± 0.20	0.11 ± 0.14	5789 ± 18	4.34 ± 0.05	0.24 ± 0.07

**Fig. 4.** A comparison of the atmospheric parameters for 13 stars observed with the ELODIE. In the following panels the relations (top) and differences (bottom) between our results and those obtained by Soubiran et al. (1998) for T_{eff} (a), $\log g$ (b) and [Fe/H] (c) are presented. The solid lines represent one to one relations.

covered was 390 – 680 nm in 67 Echelle orders. Typical signal to noise ratio was 100 – 150 per pixel. The spectra were reduced, i.e. straightened, wavelength calibrated, cleaned from cosmic ray hits, bad pixels and telluric lines. Because of the narrower spectral range we were able to measure 150 Fe I and 15 Fe II lines per star on average for the further analysis.

The results obtained with the TGVIT for these 13 stars are presented and compared with results of Soubiran et al. (1998) in Table 3 and Fig. 4.

The mean intrinsic uncertainties of our determinations are $\sigma T_{\text{eff}} = 21$ K, $\sigma \log g = 0.07$ and $\sigma [\text{Fe}/\text{H}] = 0.09$, respec-

tively. According to Katz et al. (1998), the average uncertainties based on the internal accuracy assumed for the stars with signal to noise ratio around 100 are $\sigma T_{\text{eff}} = 86$ K, $\sigma \log g = 0.28$ and $\sigma [\text{Fe}/\text{H}] = 0.16$. We note that the mean intrinsic uncertainties in T_{eff} and $\log g$ as given by the TGVIT are about 4 times smaller than uncertainties estimated by Katz et al. (1998) while in the case of [Fe/H] they are comparable. An overall agreement of the results is clear from Fig. 4.

We calculated the mean differences and scatter (rms) between our results and those of Soubiran et al. (1998) (excluding HD 175305 for which uncertainties in Soubiran et al. (1998)

are much larger than typical) and obtained: $\Delta T_{\text{eff}} = 63$ K, $\Delta \log g = 0.15$, $\Delta [\text{Fe}/\text{H}] = 0.02$, $\sigma_D T_{\text{eff}} = 54$ K, $\sigma_D \log g = 0.27$ and $\sigma_D [\text{Fe}/\text{H}] = 0.25$.

Since we used exactly the same spectra as Soubiran et al. (1998) the only sources of the differences in the results and the estimated uncertainties are the applied numerical procedures, the selection of lines and the EW measurements. We note that our intrinsic uncertainties in T_{eff} , $\log g$ are 2.6 – 3.8 times smaller than the resulting scatter in the results. We also note that our results for T_{eff} are systematically 63 K (3 σ) larger and our results for $\log g$ are systematically 0.15 dex (2.1 σ) larger while the $[\text{Fe}/\text{H}]$ results do not show any systematical effects as compared with Soubiran et al. (1998). The scatter in all results, comparable to uncertainties as determined from Katz et al. (1998), and especially in $[\text{Fe}/\text{H}]$, larger than the average uncertainty as estimated by Katz et al. (1998), suggests that our results are more precise than those of Soubiran et al. (1998).

5.2. Tests with Butler et al. (2006) data

We performed another test of quality and reliability of our results using our own HET/HRS spectra of 8 known hosts of planetary systems: HD 10697, HD 38529, HD 72659, HD 74156, HD 75732, HD 88133, HD 118203 and HD 209458, previously analyzed by other authors. The sample contains mainly dwarfs and sub-giants with spectral types ranging from F8 to K0. Our results were compared to the existing determinations collected in Butler et al. (2006), who included the nearby stars and exoplanets data from the Lick, the Keck and the Anglo-Australian Observatory planet searches. The results of our analysis for the 8 planet-hosting stars are summarized in Table 4, where also the atmospheric parameters from Butler et al. (2006) are presented (see also Fig. 5). The mean intrinsic uncertainties for the atmospheric parameters obtained by us and presented in Table 4 are $\sigma T_{\text{eff}} = 15$ K, $\sigma \log g = 0.04$ and $\sigma [\text{Fe}/\text{H}] = 0.06$ while the uncertainties presented by Butler et al. (2006) are: $\sigma T_{\text{eff}} = 55$ K, $\sigma \log g = 0.06$ and $\sigma [\text{Fe}/\text{H}] = 0.03$. The mean intrinsic uncertainties in T_{eff} as given by the TGVIT are 3.6 times smaller than uncertainties estimated given in Butler et al. (2006) while our estimated uncertainties in the $\log g$ and the $[\text{Fe}/\text{H}]$ are comparable.

After rejecting HD 118203, for which the uncertainty in T_{eff} as given in Butler et al. (2006) is 3 times larger than average, we calculated the mean differences and scatter (rms) between our results and those collected in Butler et al. (2006). We obtained: $\Delta T_{\text{eff}} = -31$ K, $\Delta \log g = -0.02$, $\Delta [\text{Fe}/\text{H}] = -0.08$ and $\sigma_D T_{\text{eff}} = 49$ K, $\sigma_D \log g = 0.12$ and $\sigma_D [\text{Fe}/\text{H}] = 0.05$.

Our intrinsic uncertainties in T_{eff} and $\log g$ are 3.3 and 3 times smaller, respectively, than the resulting scatter in the results. The scatter in $[\text{Fe}/\text{H}]$ is similar to our uncertainty estimate.

We note that our results for T_{eff} and $[\text{Fe}/\text{H}]$ are systematically smaller by 31 K (2 σ) and 0.08 dex (1.3 σ), respectively, while the results for $\log g$ do not show any measurable systematical effects as compared with Butler et al. (2006). The scatter among all results, comparable to uncertainties as determined from Butler et al. (2006) and ours, and especially in $[\text{Fe}/\text{H}]$, where it is smaller than our estimate, suggests that the results presented in Butler et al. (2006) are of similar quality or more accurate than ours.

To conclude our tests we note that in general the T_{eff} , $\log g$ and $[\text{Fe}/\text{H}]$ obtained with the TGVIT and those selected from Soubiran et al. (1998) or Butler et al. (2006) agree with each other. The uncertainties in the metallicities, estimated in the TGVIT from the actual Fe abundance distribution as the standard deviation of the mean, are realistic. Our $[\text{Fe}/\text{H}]$ determinations

agree with those of Soubiran et al. (1998) but are systematically 1.3 σ lower than those presented in Butler et al. (2006).

The intrinsic TGVIT uncertainties of T_{eff} are most certainly underestimated. The comparison with Soubiran et al. (1998) results suggests that we should enlarge our σT_{eff} estimates by a factor of 2.6. Similar analysis of scatter between our and Butler et al. (2006) data suggests that our uncertainties are underestimated by a factor of 3.3. If to apply such corrected $\sigma_C T_{\text{eff}} = 3.3 \sigma T_{\text{eff}}$ estimate our results agree with those of Soubiran et al. (1998) or Butler et al. (2006) within 1 σ_C . Similar analysis of scatter leads to a conclusion that our $\sigma \log g$ estimates should be increased by a factor of 3. With such uncertainty estimate our $\log g$ determinations agree with those of Soubiran et al. (1998) or Butler et al. (2006) well within 1 $\sigma_C \log g = 3.0 \sigma \log g$ as well. Since the microturbulence velocity uncertainty is estimated in the same manner as for T_{eff} and $\log g$ we expect that these uncertainties are also underestimated by a factor of 3.

6. Atmospheric parameters

The results of our determinations of the atmospheric parameters for 348 GK giant stars are presented in Table 5 (columns 2–5). In all cases the values of T_{eff} , $\log g$, v_t and $[\text{Fe}/\text{H}]$ are presented together with their intrinsic uncertainties. For 332 objects we obtained consistent solutions for each of stellar parameters in (typically) 10 iterations of the procedure described in Sect. 4.

The spectroscopic analysis revealed that 5 of our presumably giants are actually dwarfs (TYC 0435-01209-1, TYC 0683-01063-1, TYC 1496-01002-1, TYC 3012-00273-1 and TYC 4444-00200-1) with $\log g \geq 4.0$. On the other hand, 4 objects (TYC 2818-00449-1, TYC 2818-00504-1, TYC 2823-01028-1 and TYC 2823-01398-1) recognized in the SIMBAD as dwarfs are actually K-type giants.

The values of T_{eff} , $\log g$, v_t and $[\text{Fe}/\text{H}]$ for 332 star were found to stay generally within the range of the TGVIT model grids. Analysis of 24 stars resulted with effective temperatures below 4250 K with other parameters within the TGVIT range of applicability, however. As the Kurucz (1993a) models included in the TGVIT reach down to 4000 K we consider these determinations as realistic but associated with larger uncertainties as it will be illustrated in Sect. 6.1. For 16 stars the resulting atmospheric parameters were either incoherent or outside the range of applicability of the TGVIT. For these stars a simplified analysis was performed, as described in Sect. 6.2, and they will be discussed separately.

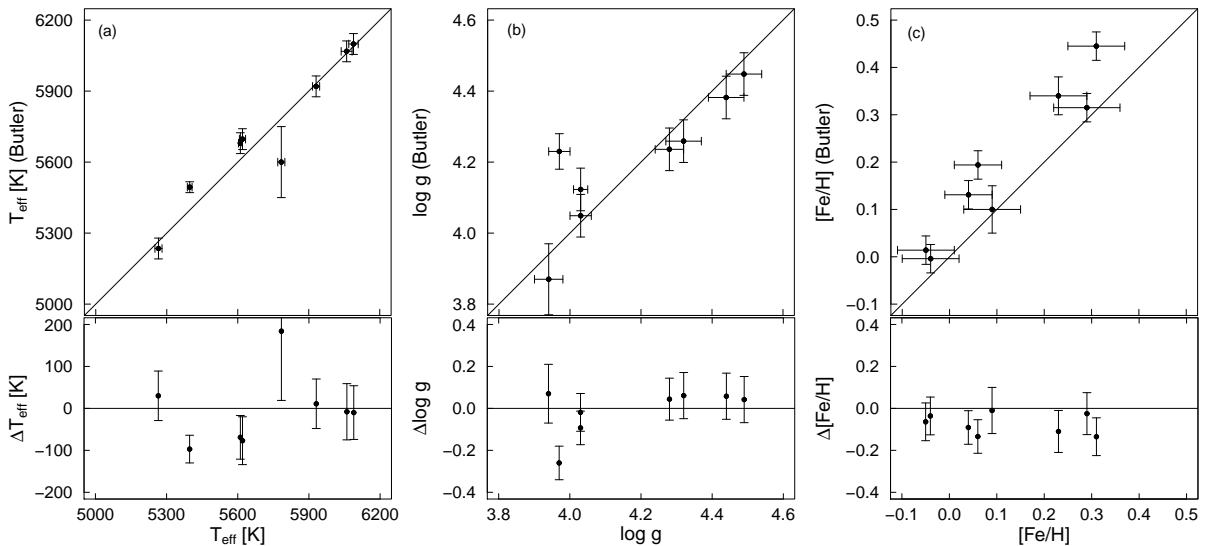
The obtained T_{eff} ranges between 4055 K and 6239 K with a median value at 4736 K. The distribution of T_{eff} is presented in Fig. 6a. Virtually all our stars have T_{eff} between 4000 K and 5200 K (with vast majority, ~ 200 of them, between 4600 K and 5000 K) making them mostly G8-K2 stars. The 5 dwarfs are among the hottest stars in our sample with T_{eff} between 4906 K and 6239 K. The intrinsic uncertainty distribution in T_{eff} is presented in Fig. 6e.

The derived $\log g$ for our sample stars ranges between 1.39 and 4.78 with the median of 2.66. The distribution of $\log g$ is presented in Fig. 6b. The majority of our stars (251 of them) have $\log g$ of 2.0 – 3.0 making them generally giants. Small fractions of 19 bright giants with $\log g \leq 2.0$ and 3 subgiants with $3.7 \leq \log g \leq 4.0$ are present in our sample as well. The intrinsic uncertainty distribution in $\log g$ is presented in Fig. 6f.

The resulting microturbulence velocity, v_t , reaches values from 0.57 km s^{-1} to 2.49 km s^{-1} and has the median value of 1.4 km s^{-1} . Most of our stars have v_t between 1.2 km s^{-1} and

Table 4. Atmospheric parameters taken from Butler et al. (2006) and our results for 8 planet-hosting stars.

Name	Sp. Type	Butler et al.			our results		
		T_{eff} [K]	$\log g$ [cm s ⁻²]	[Fe/H]	T_{eff} [K]	$\log g$ [cm s ⁻²]	[Fe/H]
HD 10697	G5IV	5680 ± 44	4.12 ± 0.06	0.19 ± 0.03	5611 ± 8	4.03 ± 0.02	0.06 ± 0.05
HD 38529	G4V	5697 ± 44	4.05 ± 0.06	0.45 ± 0.03	5620 ± 13	4.03 ± 0.03	0.31 ± 0.06
HD 72659	G0	5920 ± 44	4.24 ± 0.06	-0.01 ± 0.03	5931 ± 15	4.28 ± 0.04	-0.04 ± 0.06
HD 74156	G0	6068 ± 44	4.26 ± 0.06	0.13 ± 0.03	6060 ± 23	4.32 ± 0.05	0.04 ± 0.05
HD 75732	G8V	5235 ± 44	4.45 ± 0.06	0.32 ± 0.03	5265 ± 15	4.49 ± 0.05	0.29 ± 0.07
HD 88133	G5	5494 ± 23	4.23 ± 0.05	0.34 ± 0.03	5397 ± 10	3.97 ± 0.03	0.23 ± 0.06
HD 118203	K0	5600 ± 150	3.87 ± 0.10	0.10 ± 0.03	5784 ± 15	3.94 ± 0.04	0.09 ± 0.06
HD 209458	F8	6099 ± 44	4.38 ± 0.06	0.01 ± 0.03	6089 ± 20	4.44 ± 0.05	-0.05 ± 0.06

**Fig. 5.** A comparison of the atmospheric parameters for 8 known planet-hosting stars. Both relations (top) and differences (bottom) between our results and those of Butler et al. (2006) of T_{eff} (a), $\log g$ (b) and [Fe/H] (c) are presented. The one to one relations are presented as solid lines.

1.6 km s⁻¹ (Fig. 6c). The value of v_t for 5 dwarfs in our sample is scattered over the range 0.57 – 1.68 km s⁻¹. The intrinsic uncertainty distribution of v_t is presented in Fig. 6g.

The metallicity of stars in our sample, [Fe/H], stays within -1.0 to +0.45 range with the median value of -0.15. Fig. 6d presents the distribution and shows that our stars are generally less metal abundant than the Sun, most of them have the [Fe/H] in the range of -0.5 to 0.0. The intrinsic uncertainty distribution in [Fe/H] is presented in Fig. 6h.

Fig. 7 presents a few relations between purely spectroscopic atmospheric parameters presented in Table 5. They illustrate a general resemblance of our sample to those studied by others (cf. for example Takeda et al. 2008). In Fig. 7a one can notice a clear dependence of $\log g$ on T_{eff} . The $\log g$ tends to be higher for hotter stars. For stars with $T_{\text{eff}} \gtrsim 5000$ K the dispersion in surface gravity increases with effective temperature as well. Noticeable relations exist between v_t and both $\log g$ and T_{eff} (Fig. 7b and d). The v_t decreases with both $\log g$ and T_{eff} . In general [Fe/H] values seem to be significantly lower for low $\log g$ stars (Fig. 7e) in our sample, while they reveal uniform distributions in T_{eff} (Fig. 7c) and v_t (Fig. 7f).

6.1. Uncertainty estimates

The mean intrinsic uncertainties of our determinations were found to be: $\sigma T_{\text{eff}} = 13$ K, $\sigma \log g = 0.05$, $\sigma v_t = 0.08$ km s⁻¹ and $\sigma [\text{Fe}/\text{H}] = 0.07$. As already discussed in Sect. 5 all these uncertainties, except [Fe/H], are numerical uncertainties resulting from the iterative procedures of the TGVIT and the real uncertainties are factor of 3 larger (since in a comparison with a larger reference sample our intrinsic uncertainty scaling may change we present our intrinsic uncertainties instead of the scaled ones). In the case of [Fe/H] the numerical uncertainties are the standard deviation of the mean Fe I and Fe II abundances, hence realistic. The intrinsic uncertainties distributions are presented in Fig. 6 (panels e-h). There exists no correlation between the intrinsic uncertainties and the obtained parameter values for any of the atmospheric parameters. The scatter of the intrinsic uncertainties is also uniformly distributed over the respective parameters values but it is worth to note that for the stars with T_{eff} below 4250 K the intrinsic uncertainties are higher, especially in $\log g$ and [Fe/H]. In Fig. 8 the intrinsic uncertainties of T_{eff} , $\log g$ and [Fe/H] as a function of T_{eff} are presented.

Several stars from the sample demonstrate uncertainties of atmospheric parameters at least two times larger than the mean values. In the case of [Fe/H] we noted intrinsic uncertainties

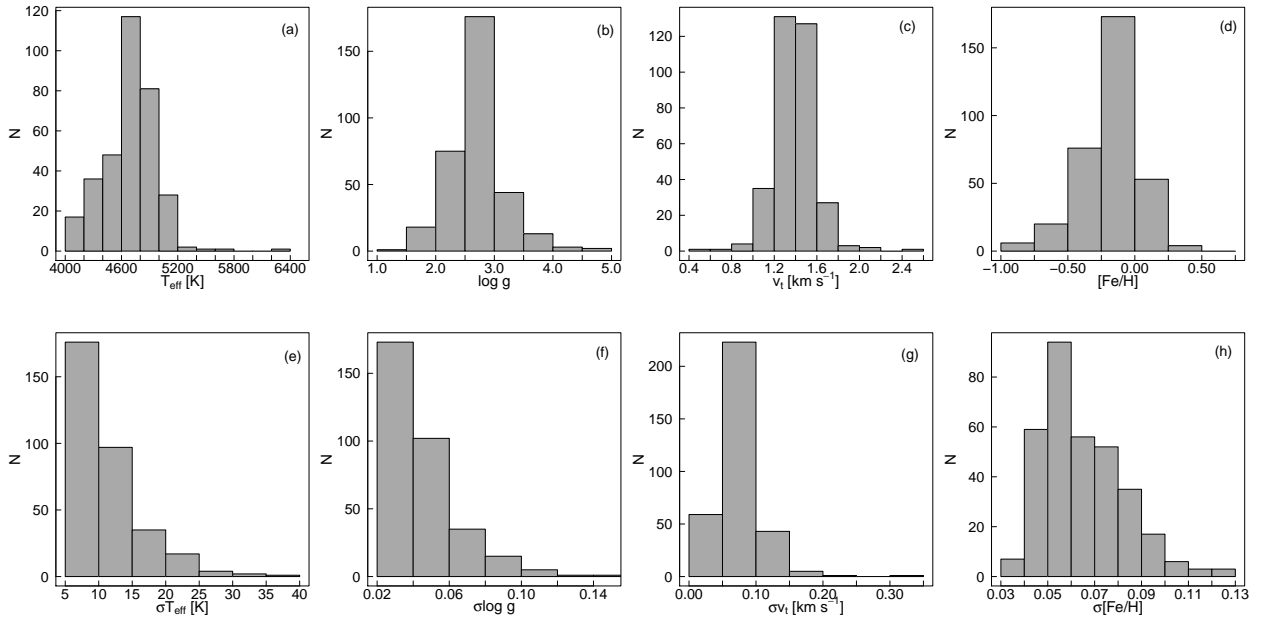


Fig. 6. Distributions of atmospheric parameters for the 332 stars with the complete spectroscopic analysis: T_{eff} , $\log g$, v_t and $[\text{Fe}/\text{H}]$ (panels a-d) and their intrinsic uncertainties (panels e-h) are presented.

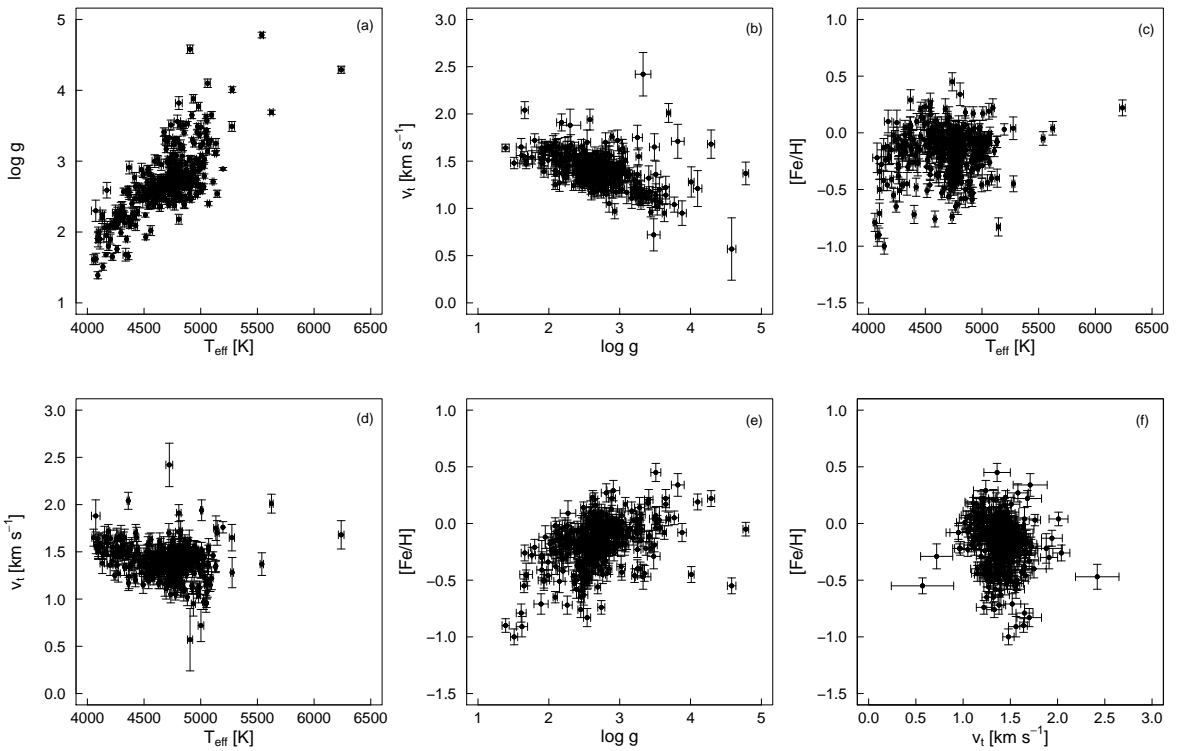


Fig. 7. Relations between T_{eff} , $\log g$, v_t and $[\text{Fe}/\text{H}]$ for the 332 stars with the complete spectroscopic analysis.

larger than 0.12 for six stars (TYC 0870-00241-1, TYC 1425-01506-1, TYC 3012-01520-1, TYC 3304-00408-1, TYC 4006-00980-1 and TYC 4428-01582-1). These result from the highest scatter of Fe abundances with respect to the excitation potential and EWs in the whole sample.

Five objects (TYC 0096-00005-1, TYC 1425-01506-1, TYC 3011-00791-1, TYC 3304-00408-1 and TYC 3930-01790-1) have significantly larger T_{eff} intrinsic uncertainties (≥ 30 K). In

the case of $\log g$ larger than typical intrinsic uncertainty (> 0.1) was obtained for nine stars (TYC 0096-00005-1, TYC 0276-00507-1, TYC 0870-00241-1, TYC 1425-01506-1, TYC 3012-01520-1, TYC 3304-00405-1, TYC 3304-00408-1, TYC 3930-01790-1 and TYC 4006-00980-1). The precision in v_t is the worst (i.e. $\geq 0.15 \text{ km s}^{-1}$) for eight objects (TYC 0683-01063-1, TYC 0870-00084-1, TYC 1425-01506-1, TYC 1496-01002-

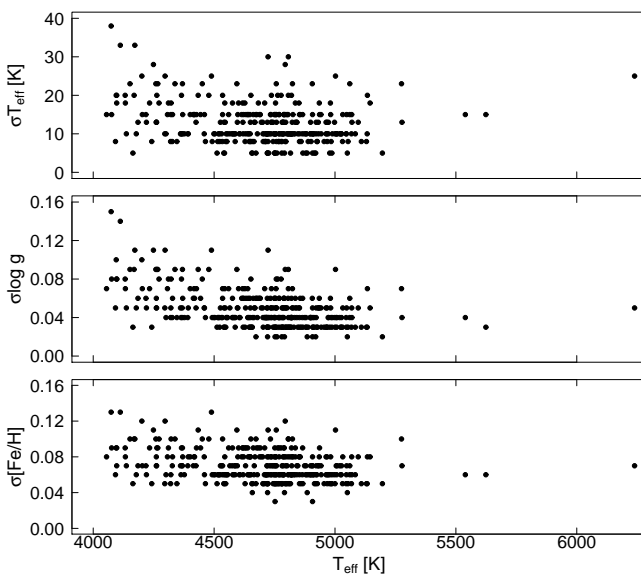


Fig. 8. Relations between the intrinsic uncertainties of σT_{eff} (top panel), $\sigma \log g$ (middle panel) and $\sigma [\text{Fe}/\text{H}]$ (bottom panel) vs. T_{eff} for 332 PTPS stars.

1, TYC 3011-00791-1, TYC 3012-00273-1, TYC 3930-01790-1 and TYC 4444-00200-1).

The reason for such uncertainty increase is not always clear. For some stars it may be associated with low effective temperature, close to the TGVIT model grids limit of $T_{\text{eff}} = 4250$ K (TYC 0096-0005-1, TYC 1425-01506-1, TYC 3304-00405-1, TYC 3304-00408-1, TYC 0276-00507-1, TYC 3012-01520-1). In several other cases relatively the low signal to noise ratio of our spectra might be the reason (TYC 3011-00791-1, TYC 4006-00980-1, TYC 0870-00084-1, TYC 1496-01002-1, TYC 3012-00273-1, TYC 4444-00200-1, TYC 4428-01582-1).

It is also possible that the larger than expected uncertainties may be due to an unresolved stellar companion. This is the case of TYC 0870-00241-1, a star with excellent quality spectra, and all atmospheric parameters well within the TGVIT range, that after several epochs of the PTPS RV monitoring appeared to have a stellar-mass companion (Niedzielski et al. - in prep.).

6.2. Stars with incomplete data

Sixteen stars of our sample have the atmospheric parameters difficult to derive using Takeda et al. (2005a) method. For these stars the solutions found with the TGVIT were either inconsistent or unrealistic. To include at least partly such stars in our analysis we adopted T_{eff} , $\log g$ and initial luminosity estimates from Adamów et al. (in prep.) for all of them. Effective temperatures were calculated from the empirical calibration of Ramírez & Meléndez (2005) based on the Tycho and the 2MASS photometry. Rough estimates of $\log g$ were obtained using the results of Bilir et al. (2006) and Gelino et al. (2005). For all these stars the average value of $[\text{Fe}/\text{H}]$ obtained for the 332 stars with complete spectroscopic analysis, $[\text{Fe}/\text{H}] = -0.15$, was assumed (bottom part of Table 5).

This approach revealed that three stars were indeed too cool for the approach of Takeda et al. (2005a,b). The remaining 13 did not show any different characteristic in comparison with 332 stars with complete spectroscopic analysis and the reasons why they were not applicable to the TGVIT remain to be clarified.

Due to much larger uncertainty of the adopted atmospheric parameters for these stars they will be either discussed separately or ignored in the following sections.

7. Luminosities, masses, ages and radii

For 271 stars from our sample no Hipparcos parallaxes are available and for another 4 (TYC 0017-01084-1, TYC 3663-00622-1, TYC 4006-00019-1 and TYC 3304-00090-1) the Hipparcos parallaxes π are unreliable ($\sigma_\pi \geq \pi$) therefore only estimates of masses and radii based on spectrophotometric parallaxes derived here are actually possible in most cases. For such estimates the bolometric luminosities are required in addition to our $\log g$, T_{eff} and metallicities. We calculated the intrinsic color index $(B-V)_0$ and the bolometric corrections BC_V for our stars from Alonso et al. (1999) empirical calibration. Using available photometry and assuming the standard interstellar reddening with $R = 3.1$ (Rieke & Lebofsky 1985) we estimated luminosities for 57 stars with usable parallaxes. For 275 objects with unknown or unreliable Hipparcos parallaxes we initially assumed M_V from Straizys & Kuriliene (1981) empirical calibration and estimated luminosities on that basis.

Propagation of uncertainty was applied to estimate the luminosity uncertainty. The adopted luminosities, together with their uncertainty estimates are presented in Table 5 (column 11). For the 57 stars with reliable parallaxes the values obtained here were adopted (note that the last column in Table 1 identifies the stars with the Hipparcos parallaxes). For the remaining 275 stars luminosities were constrained better via fitting to evolutionary tracks as described in the following section.

7.1. Stellar masses and luminosities

The stellar masses M/M_\odot , radii R/R_\odot and the estimates of ages were obtained by comparing the positions of stars in the $[\log L/L_\odot, \log g, \log T_{\text{eff}}]$ space with the theoretical evolutionary tracks of Girardi et al. (2000) and Salasnich et al. (2000) for a given metallicity (Fig. 10). We used all available existing tracks corresponding to eight metallicity values: $[Y = 0.23, Z = 0.0004]$, $[Y = 0.23, Z = 0.001]$, $[Y = 0.24, Z = 0.004]$, $[Y = 0.25, Z = 0.008]$, $[Y = 0.273, Z = 0.019]$ (the solar composition), $[Y = 0.30, Z = 0.03]$, $[Y = 0.32, Z = 0.04]$ and $[Y = 0.39, Z = 0.07]$. To derive M/M_\odot for every star the tracks for the nearest metallicity were applied. Then the maximum-likelihood function defined as:

$$\chi^2 = \sum_{i=1}^n \left(\frac{q_i^{\text{obs}} - q_i^{\text{mod}}}{\sigma_i} \right)^2, \quad (1)$$

where q_i^{obs} , q_i^{mod} and σ_i denote observed and modeled parameters and their uncertainties respectively, was minimized over the model parameter space. In our case the number of parameters n was set to 3 as $\log L/L_\odot$, $\log g$ and $\log T_{\text{eff}}$ were used. The area over which the parameter space was explored was defined as $\pm 10 \sigma$ (intrinsic) in $\log g$ and $\log T_{\text{eff}}$ and $\pm 3 \sigma$ in $\log L/L_\odot$. The resulting run of the χ^2 over the model parameters was found to be typically relatively flat, therefore the final stellar mass was calculated as a mean value over an extended area of $\chi^2 \leq 3 \chi^2_{\text{min}}$. That procedure resulted in consistent stellar masses determination and realistic estimates of the uncertainties.

The resulting masses range from $0.6 M/M_\odot$ to $3.4 M/M_\odot$ (see Fig. 9b for a histogram). The majority of stars in our sample have masses below $2 M_\odot$. We identified, however, a significant

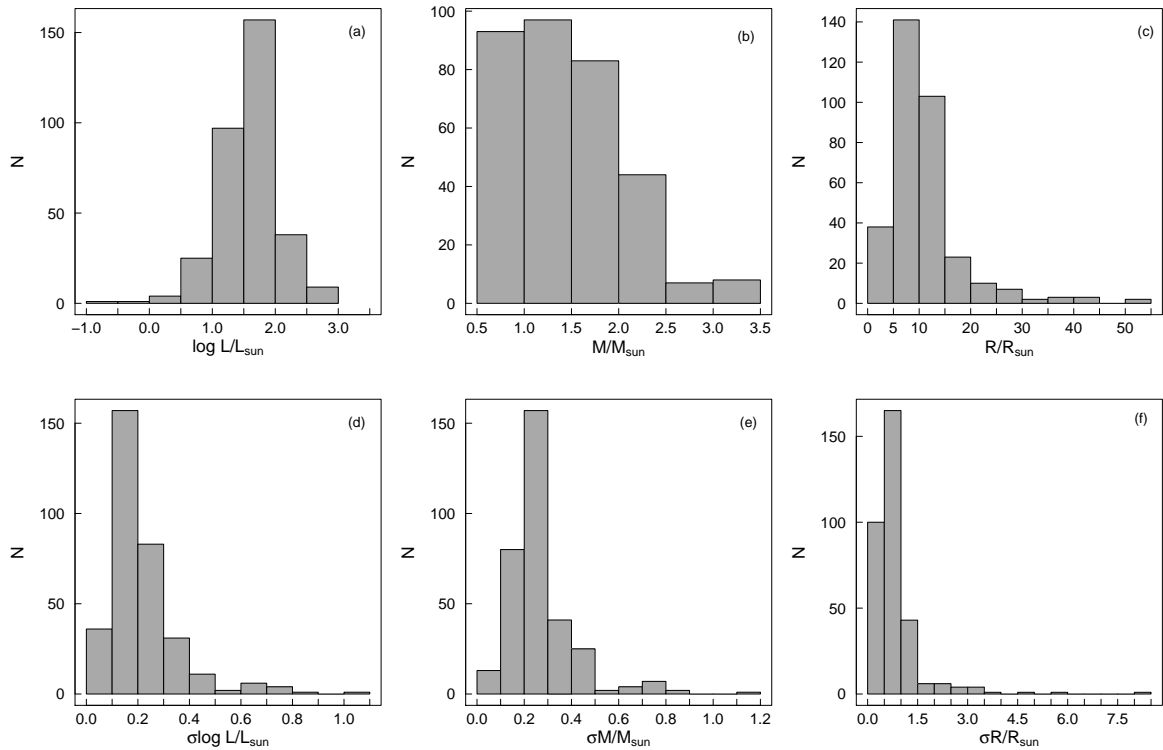


Fig. 9. Distributions of luminosities, masses and radii (panels a-c) as well as their uncertainties (panels d-f) for 332 stars with complete spectroscopic analysis.

number (63 or $\sim 19\%$) of stars which fall in the intermediate-mass range $2 M_{\odot} \leq M \leq 7 M_{\odot}$. Table 5 (column 12) presents the final adopted masses.

The uncertainty of stellar mass obtained by comparison with the selected here theoretical evolutionary tracks (Girardi et al. 2000; Salasnich et al. 2000) depends on the accuracy of determination of the position of a star in the $[\log L/L_{\odot}, \log g, \log T_{\text{eff}}]$ space. The effective temperatures and gravities are relatively well determined, the largest source of uncertainty is the parallax, i.e. luminosity. In the case of stars, for which the parallax π was precise enough, the metallicity model choice may introduce additional uncertainty since we used the existing evolutionary tracks.

We found that for an average red giant with known parallax the mass may be estimated within $0.2 M_{\odot}$ in the best cases, while the mean uncertainty for the whole sample is $\sigma M/M_{\odot} = 0.3$. The uncertainties may become even larger, $\sim 1 M_{\odot}$, for very confused evolutionary tracks regions at lower effective temperatures ($\log T_{\text{eff}} \leq 3.65$).

For most of our stars no reliable parallaxes were available therefore luminosity $\log L/L_{\odot}$ was constrained better than the initial estimate by adopting the luminosity from the fits to the evolutionary tracks, corresponding to the determined $\log g$, $\log T_{\text{eff}}$ and the stellar mass. In Table 5 (column 11) such luminosity estimate is presented for 275 stars. The $\log L/L_{\odot}$ ranges from -0.68 to 2.86 with a peak at 1.6 (Fig. 9a). The mean uncertainty in $\log L/L_{\odot}$ was found to be 0.19 in the best cases, but the average value for the whole sample is $\sigma \log L/L_{\odot} = 0.23$.

The H-R diagram for 332 PTPS stars with the complete spectroscopic analysis is presented in Fig. 10.

7.2. Age estimates

As a large number of presented stars have roughly solar masses, a small uncertainty in mass leads to a significant uncertainties in the resulting age. On the contrary for the intermediate-mass stars the precision in mass is worse but the estimated ages are more robust. Ages of majority of our program stars are therefore uncertain. The estimated stellar ages are presented in Table 5 (column 14). For many stars only a wide range of age is given reflecting the complex nature of RGC region and the difficulties in age determination for single field objects. Nevertheless, we found that a typical star from our sample is $3 - 5$ Gyr old (mean uncertainty in age is $1.1 - 1.5$ Gyr).

7.3. Stellar radii

The stellar radii were estimated from either spectroscopic $\log g$ and the adopted stellar mass or spectroscopic T_{eff} and the adopted luminosity. In every case one parameter obtained from the spectroscopic analysis and one from the model fitting was used according to the equations:

$$R/R_{\odot}(g, M) = \frac{\sqrt{GM_{\odot}(\frac{M}{g})}}{R_{\odot}}, \quad (2)$$

or:

$$R/R_{\odot}(T_{\text{eff}}, L) = \sqrt{\frac{L}{L_{\odot}} \left(\frac{T_{\text{eff}\odot}}{T_{\text{eff}}} \right)^2}, \quad (3)$$

where G is the gravitational constant and M_{\odot} , R_{\odot} , L_{\odot} and $T_{\text{eff}\odot}$ are the solar values of mass, radius, luminosity and effective temperature.

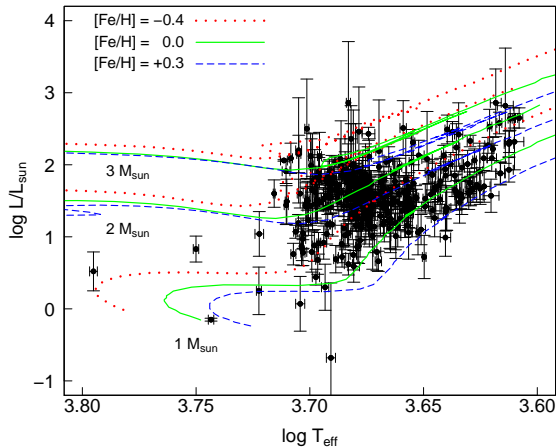


Fig. 10. The H-R diagram for 332 PTPS stars with the complete spectroscopic analysis. The theoretical evolutionary tracks (Girardi et al. 2000) are presented for stellar masses of $1 - 3 M_{\odot}$ and several metallicities. The dotted, solid and dashed lines correspond to $[Fe/H] = -0.4, 0.0, 0.3$, respectively.

The maximum uncertainty was estimated in both approaches by application of the logarithmic derivative method. In Fig. 11 a comparison of radii derived using both methods is presented. Although for several stars the radii differ significantly, the general agreement between both R/R_{\odot} estimates is good. Mean absolute difference between radii determined from the Eqs. 2 and 3 is $\Delta R = 0.7 R_{\odot}$. The largest deviations exist for the most extended stars (cf. Fig. 11). They are most probably a consequence of inaccuracy of the luminosity estimates for those luminous stars without parallax and departure from the LTE conditions in stars with the most extended outer regions. Due to better consistency with the evolutionary status the radii obtained from Eq. 3 with their uncertainties are given in Table 5 (column 13).

The radii of stars in our sample range from $0.6 R_{\odot}$ to $52.1 R_{\odot}$ (Fig. 9c) with majority of about $9 - 11 R_{\odot}$. The mean uncertainty in the derived stellar radii was found to be $0.8 R/R_{\odot}$ (Fig. 9f).

7.4. Stars with incomplete data

For the sixteen stars with incomplete atmospheric data discussed in Sect. 6.2 and presented in the bottom part of the Table 5 we applied essentially the same procedure to obtain luminosities, masses, ages and radii. However, as only rough estimates of $\log g$ and assumed $[Fe/H]$ were available the resulting masses, ages and radii are very uncertain. Therefore, we excluded these 16 stars from our discussion presented in Sect. 10.

8. Radial velocities

For obtaining absolute radial velocities a cross-correlation analysis with an artificial template was applied. To construct the cross-correlation functions (CCFs) the normalized stellar spectra were correlated with a numerical mask consisting of 1 and 0 value points (Nowak & Niedzielski 2008). The non-zero points corresponded to the positions of 300 non-blended, isolated stellar absorption lines at zero velocity. In our RV measurements only the first 17 orders of the „blue” spectra, free from telluric lines, were used. The CCF was computed step by step for each velocity point without merging the orders. For every order the algorithm selected only lines suitable for a given wavelength range.

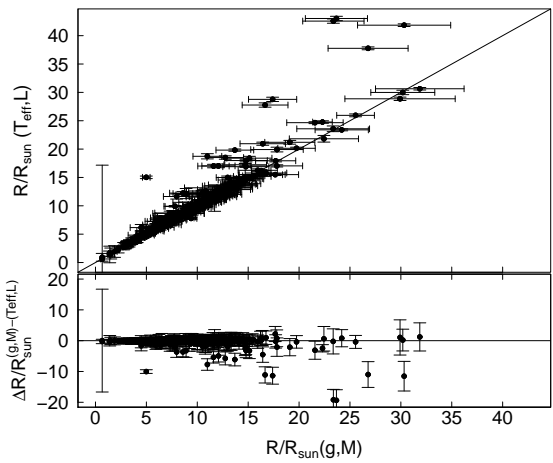


Fig. 11. Comparison of radii obtained from two sets of stellar parameters: $\log g$, M/M_{\odot} and T_{eff} , $\log L/L_{\odot}$ for 332 stars. The solid line corresponds to one to one relation.

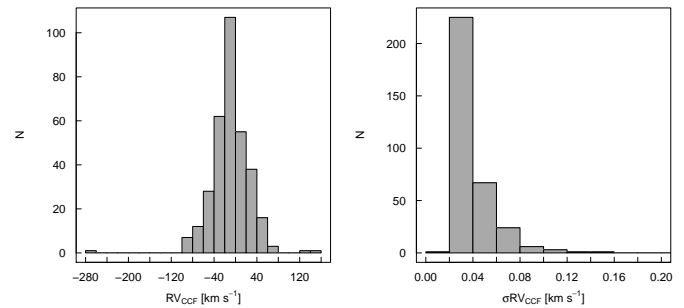


Fig. 12. A histograms of the RVs obtained from the cross-correlation function (left panel) and their uncertainties (right panel) for 347 stars.

The CCFs from all orders were finally added to construct the final CCF for the whole spectrum. The final radial velocities were measured by fitting a Gaussian function to the CCF for the whole spectrum. The RVs uncertainties were computed as $\text{rms}/\sqrt{17}$ of the 17 RVs obtained from fitting a Gaussian to the CCF for each order separately. The mean standard uncertainty obtained this way was $\sigma_{RV_{CCF}} = 0.041 \text{ km s}^{-1}$. In Fig. 12 the distribution of resulting RVs and their uncertainties is presented. The absolute precision of presented RV is lower than the $\sigma_{RV_{CCF}}$. The HRS is neither thermally nor pressure stabilized therefore the wavelength scale of our spectra is affected by these factors and the real uncertainties are likely to be of the order of 1 km s^{-1} .

In Table 5 (columns 6-8) the RVs transformed to the barycenter of the Solar System with the algorithm of Stumpff (1980) for all stars in our sample (except for TYC 3304-00479-1 due to the lack of suitable spectra) are presented together with the epochs of observation (MJD).

9. Comparison with literature data

The vast majority of our stars were studied here for the first time and no comparison with literature data is possible. Nevertheless, several individual objects were included in other surveys and we can compare our results with those of other authors, obtained with various methods.

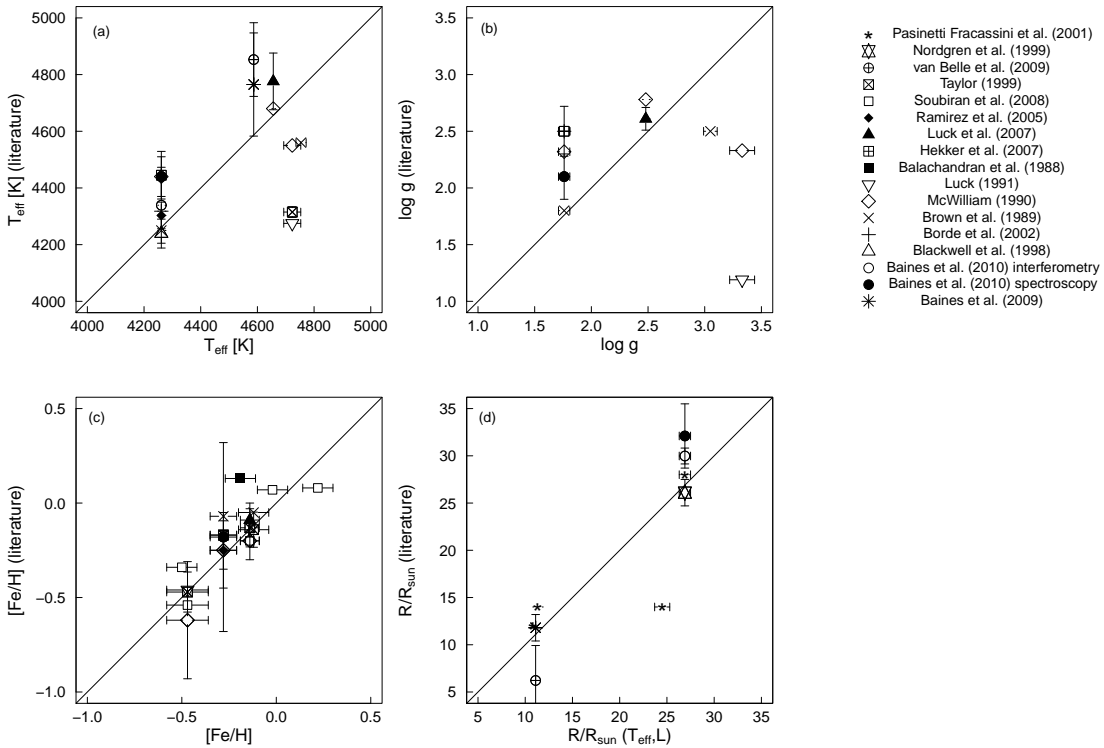


Fig. 15. A comparison of various parameters for stars with the literature data. The uncertainties are presented if available. The solid lines denote the one to one relations.

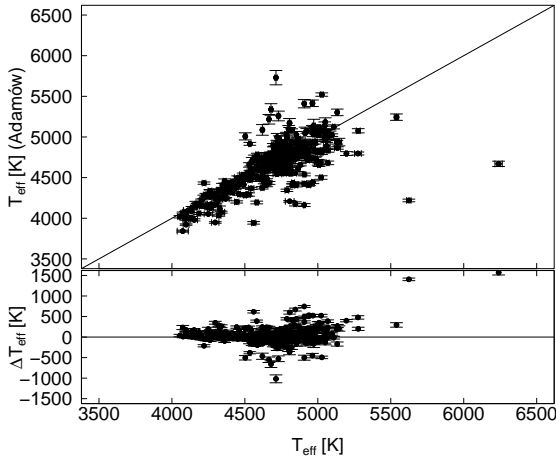


Fig. 13. A comparison of T_{eff} of the 332 PTPS stars obtained in this study and taken from Adamów et al. (in prep.). Both relation (top) and differences (bottom) are presented. The uncertainties of both determinations are shown. The solid line corresponds to one to one relation.

The spectroscopic determinations of T_{eff} were compared with effective temperatures derived by Adamów et al. (in prep.) from the empirical calibration of Ramírez & Meléndez (2005) and the Tycho and the 2MASS photometry, where all our stars were included. The comparison of results for 332 stars is shown in Fig. 13. No significant systematic shift is present in the data, but the scatter, of 224 K on average, increases towards higher effective temperatures. The mean difference between our and Adamów et al. (in prep.) temperatures is $\Delta T_{\text{eff}} = 48$ K and

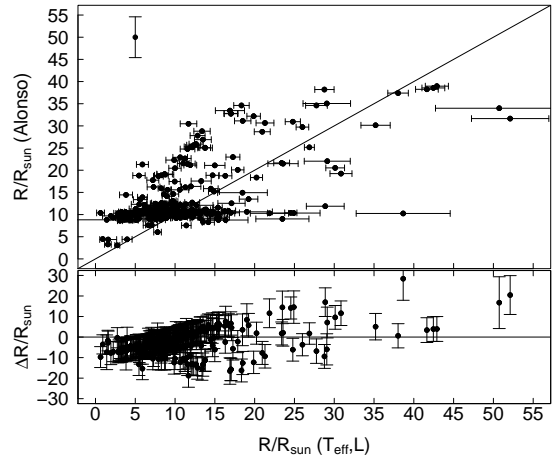


Fig. 14. A comparison of the R/R_{\odot} for the 332 PTPS stars derived here and calculated from the empirical calibration of Alonso et al. (2000). Both relation (top) and differences (bottom) are presented. The uncertainties in our determinations are shown for every target whereas Alonso et al. (2000) a typical uncertainty for $10 R_{\odot}$ star is denoted in the upper left corner. The solid line presents the one to one relation.

only for 4 objects the difference is significantly larger (> 740 K). These stars are: TYC 0683-01063-1, TYC 3319-00170-1, TYC 3930-00665-1 and TYC 3993-01850-1. All of them are significantly reddened by the interstellar extinction what probably affected the photometric T_{eff} .

Our adopted values of stellar radii for 332 stars were compared with estimates obtained from the empirical calibration of

Table 10. The mean differences and the standard deviations between stellar parameters presented in this work and derived by other authors.

Reference	Number of stars	$\Delta T_{\text{eff}} \pm \sigma$ [K]	$\Delta \log g \pm \sigma$ [cm s^{-2}]	$\Delta [\text{Fe}/\text{H}] \pm \sigma$	$\Delta R \pm \sigma$ [R_{\odot}]	$\Delta RV \pm \sigma$ [km s^{-1}]	Remarks
Adamów et al. (in prep.)	332	48 \pm 224	—	—	—	—	(†)
Alonso et al. (2000)	332	—	—	—	-2.2 \pm 5.8	—	(†)
Baines et al. (2009)	1	-178	—	—	-0.7	—	—
Baines et al. (2010) spectroscopy	1	-179	-0.34	-0.10	-5.2	—	—
Baines et al. (2010) interferometry	1	-78	—	—	-3.1	—	—
Balachandran et al. (1988)	1	—	—	-0.32	—	—	—
Bartkevičius & Sperauskas (1999)	1	—	—	—	—	0.113	—
Blackwell & Lynas-Gray (1998)	1	22	—	—	—	—	—
Bordé et al. (2002)	1	-57	-0.74	—	—	—	—
Brown et al. (1989)	2	103 \pm 129	0.26 \pm 0.42	-0.14 \pm 0.10	—	—	(†)
de Medeiros & Mayor (1999)	4	—	—	—	—	0.178 \pm 0.169	(†,*)
Duflot et al. (1995)	5	—	—	—	—	-0.405 \pm 1.810	(†,*)
Famaey et al. (2005)	19	—	—	—	—	0.163 \pm 0.834	(†,*)
Gontcharov (2006)	21	—	—	—	—	0.422 \pm 1.475	(†,*)
Hekker & Meléndez (2007)	1	-184	-0.74	-0.11	—	—	—
Luck (1991)	1	448	2.14	-0.01	—	—	—
Luck & Heiter (2007)	1	-120	-0.13	-0.05	—	—	—
McWilliam (1990)	3	-10 \pm 176	0.05 \pm 0.84	0.06 \pm 0.09	—	—	(†)
Nidever et al. (2002)	1	—	—	—	—	-0.647	—
Nordgren et al. (1999)	1	—	—	—	0.8	—	—
Pasinetti Fracassini et al. (2001)	4	—	—	—	1.4 \pm 6.1	—	(†)
Ramírez & Meléndez (2005)	1	-42	—	-0.03	—	—	—
Soubiran et al. (2008)	5	—	—	0.00 \pm 0.12	—	—	(†)
Taylor (1999)	4	408	—	-0.02 \pm 0.06	—	—	(†)
van Belle & von Braun (2009)	1	-266	—	—	4.9	—	—

Notes. (†) The value after the plus-minus sign is standard deviation (if number of stars to compare is >1). (*) The difference and scatter value obtained with the exception of discrepant stars, see Section 9.1 and Fig. 16 for details.

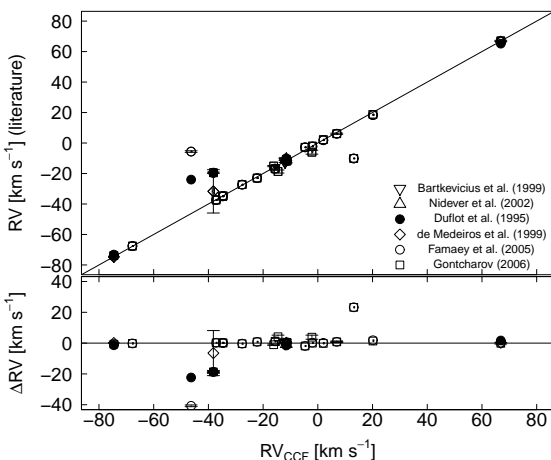


Fig. 16. The radial velocities derived from our cross-correlation analysis compared with those available in the literature. Relation (top) and differences (bottom) between the RV results are shown. The RVs uncertainties are presented if available. The solid line presents the one to one relation.

Alonso et al. (2000), based on the angular diameters obtained from the Infra-Red Flux Method and distances computed from the Hipparcos parallaxes. In most cases the results of R/R_{\odot} were fairly close to each other and comparable within the estimated uncertainties. It is worth mentioning that uncertainties in radii as estimated from Alonso et al. (2000) calibration are large and only a typical uncertainty for a $10 R_{\odot}$ star is presented in Fig. 14. The mean difference between our and calibrated radii is

$\Delta(R/R_{\odot}) = -2.2$ with a scatter of $5.8 R_{\odot}$. It is interesting to note that for the stars with smaller radii our estimates give systematically lower values, while for the stars with larger radii our estimates are systematically larger which is most probably caused by the departure from the LTE.

In Fig. 15 we present a collective comparison of our parameters for several stars with the data available in the literature. The results obtained by other authors are, in general, in agreement with our determinations of T_{eff} , $\log g$, $[\text{Fe}/\text{H}]$ and R/R_{\odot} . In spite of a very low number of stars in common, i.e. 5 for T_{eff} , 4 for $\log g$, 8 for $[\text{Fe}/\text{H}]$ and 5 for R/R_{\odot} , the agreement is obvious, especially in the case of metallicity. From Fig. 15 it appears, however, that the scatter between the determinations of various authors is large what makes the comparison more difficult.

In Fig. 16 the RVs obtained here using the CCF technique are compared with literature data for all stars, for which such determinations were available. In all but 3 cases our radial velocities agree with those of other authors. Large discrepancies exist in the cases of: TYC 3012-02518-1, TYC 3930-01790-1 and TYC 3304-00090-1. The first two stars are members of binary systems (Abt 1981; Meisel 1968) where the latter is in addition chromospherically active (e.g. Strassmeier 1994). The reason for absolute RV discrepancy for TYC 3304-00090-1 is unclear.

The mean differences between the respective parameters are summarized in Table 10. We found that on average our determinations agree with all presented literature results within $\Delta T_{\text{eff}} = -6$ K, $\Delta \log g = 0.07$, $\Delta [\text{Fe}/\text{H}] = -0.07$, $\Delta R/R_{\odot} = -0.6$ and $\Delta RV = -0.029 \text{ km s}^{-1}$ (with exception of the 3 discrepant stars). The mean scatter of these comparisons represented by the standard deviation is equal to 179 K, 0.76 dex, 0.10 dex, $3.8 R_{\odot}$ and 0.841 km s^{-1} for T_{eff} , $\log g$, $[\text{Fe}/\text{H}]$ and R and RV , respec-

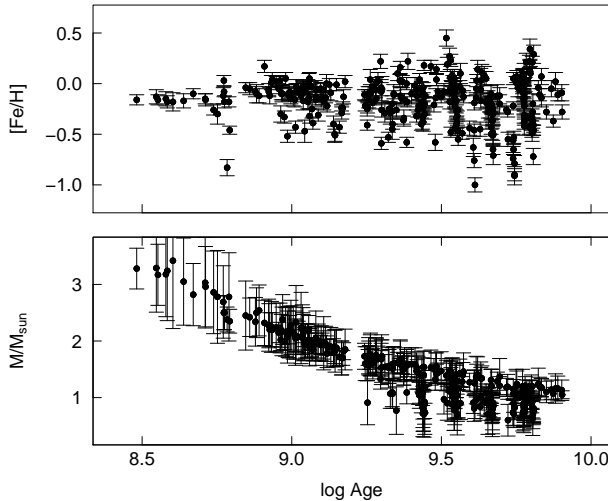


Fig. 18. Relations between $[Fe/H]$ and $\log Age$ (top panel) as well as M/M_{\odot} and $\log Age$ (bottom panel) for the 332 stars with the complete spectroscopic analysis. The uncertainties in $[Fe/H]$ and M/M_{\odot} are only presented. The lower limit of $\log Age$ is presented if in Table 5 (column 14) the age range is given.

tively. No systematic effects were found. Our results agree with those of other authors within the estimated uncertainties.

10. Discussion

Several relations between the integral and the atmospheric parameters are depicted in Fig. 17. From the mass-luminosity relation (Fig. 17a) we infer that relatively high-mass stars tend to be brighter but in the case of solar-mass objects we see a large dispersion in $\log L/L_{\odot}$. A clear correlation exists between $\log L/L_{\odot}$ and $\log R/R_{\odot}$ (Fig. 17b) reflecting the well-known relation $L \sim R^2 T_{\text{eff}}^4$. In Fig. 17c a strong $\log R/R_{\odot}$ dependence on $\log g$, resulting from Eq. 2, is visible. One can also see that the hotter stars in our sample tend to be of higher mass (Fig. 17d), except for the dwarfs which reveal similar masses for a wide range of effective temperatures (~ 1300 K). These effects are to much extend a result of our sample definition well illustrated in $\log L/L_{\odot}$ vs. $\log T_{\text{eff}}$ relation (Fig. 10). In turn, masses of our sample stars show quite uniform distribution versus $\log g$ and $[Fe/H]$ (Fig. 17e and f).

In Fig. 17g we see that our stars are quite uniformly distributed over the metallicity vs. radius plane. Fig. 17h is similar to the mass-luminosity relation (Fig. 17a), probably due to the fact that the stellar radii presented in Fig. 17b result from the derived luminosities.

The age-metallicity relation for 332 PTPS stars is shown in Fig. 18 (top panel). As we stated already in Sect. 7.2 the stellar ages are uncertain and in many cases ambiguously determined. The lower limit of $\log Age$ is presented if in Table 5 (column 14) the age range is given. However, the well-known tendency resulting from the Galactic evolution is maintained. In Fig. 18 (bottom panel) the relation between stellar age and mass is presented (the Pearson correlation coefficient is $R = -0.937$). For the stars with masses larger than the solar a quadratic fit can be determined: $M/M_{\odot} = (1.07 \pm 0.07)(\log Age)^2 - (21.42 \pm 1.30)(\log Age) + (107.93 \pm 6.04)$. Based in Fig. 18 we find that the giants in our sample present a wide range of evolutionary stages. Relatively older stars (≥ 3.2 Gyr) have simultaneously

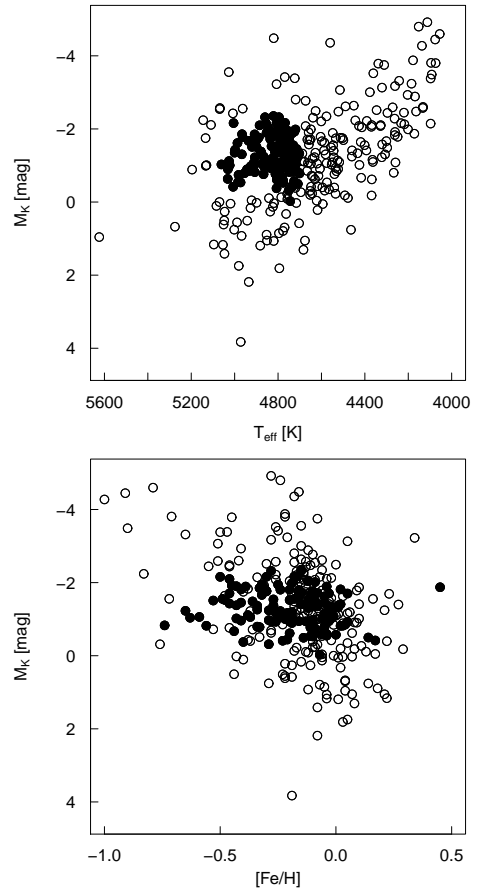


Fig. 19. Relations between M_K and T_{eff} (top panel) as well as M_K and $[Fe/H]$ (bottom panel) for 327 giants. The RGC stars are presented as solid circles while the rest of stars are shown as open circles.

lower masses ($\sim 1 M_{\odot}$) and reveal higher spread in metallicity (0.26). The more massive giants ($> 1.5 M_{\odot}$), with lower spread in metallicity (0.16), are younger (< 3.2 Gyr).

From Fig. 10 one can see that our sample is composed mainly of regular giants evolving along the RGB and giants from the RGC. Only very few stars appeared to be dwarfs. We applied the definitions of RGC as proposed in Jimenez et al. (1998) and Tautvaisiene & Puzeras (2009), i.e. $4700 \text{ K} \leq T_{\text{eff}} \leq 5100 \text{ K}$ and $1.5 \leq \log L/L_{\odot} \leq 1.8$ to our data and due to the large uncertainty in our luminosities we extended the $\log L/L_{\odot}$ range by 0.2 to $[1.3 - 2.0]$. As a result we found 126 stars to fulfill the criteria for the Clump Giants. These stars constitute only about 38% of our sample. The mean absolute magnitudes of these stars in four bands: $M_V = (0.985 \pm 0.499)$ mag, $M_I = (-0.700 \pm 0.502)$ mag, $M_H = (-1.178 \pm 0.502)$ mag and $M_K = (-1.282 \pm 0.508)$ mag confirm that they are the Clump Giants. In Fig. 19 we can see our RGC stars together with the rest of the sample in M_K vs. T_{eff} and M_K vs. $[Fe/H]$ plots. The scatter (defined as the standard deviation) in the absolute magnitudes is large due to the lack of parallaxes and it is not possible to search for relations with either metallicity or temperature. Given the observational uncertainties in luminosity and our sample definition we cannot state that the observed relative frequency of RGC stars reflects the true one.

The stellar masses obtained here by fitting observed stellar parameters to selected evolutionary tracks are model dependent.

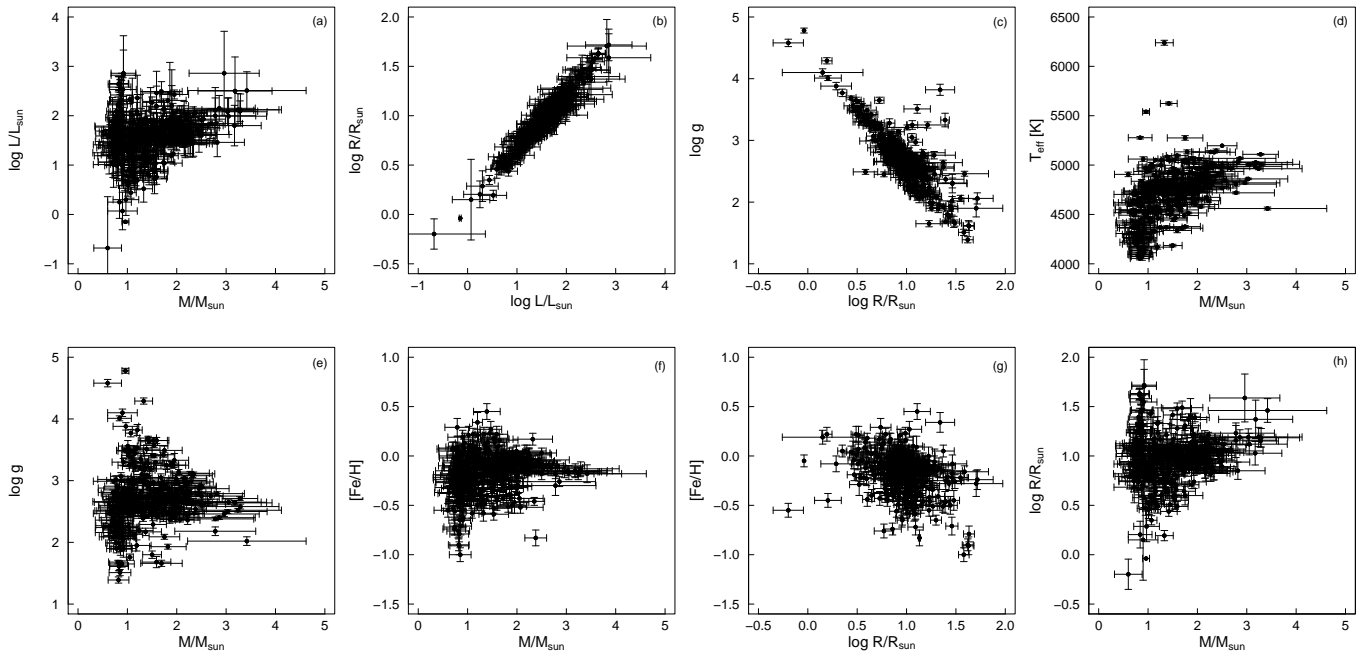


Fig. 17. Some relations between parameters for the 332 stars with the complete spectroscopic analysis. In the following panels the relations between $\log L/L_\odot$, M/M_\odot , $\log R/R_\odot$ and the atmospheric parameters are presented.

Since the mass-loss was ignored they also should be considered as upper limits.

11. Conclusions

We presented the atmospheric parameters (T_{eff} , $\log g$, v_t and $[\text{Fe}/\text{H}]$), luminosities, masses, radii, ages and the absolute radial velocities for 348 stars from the RGC sample of the PTPS. For vast majority of them these are the first determinations.

For 332 stars the complete spectroscopic analysis resulted in precise T_{eff} , $\log g$, v_t and metallicities. The estimated intrinsic uncertainties in derived parameters are: $\sigma T_{\text{eff}} = 13 \text{ K}$, $\sigma \log g = 0.05$, $\sigma v_t = 0.08 \text{ km s}^{-1}$, $\sigma [\text{Fe}/\text{H}] = 0.07$ (the uncertainties in effective temperatures, gravities and microturbulence velocities as discussed in Sect. 5 are underestimated by a factor of 3). In case of 16 stars, for which either incomplete data were available or our spectroscopic approach failed, effective temperatures and $\log g$ were estimated from the existing photometric data.

In turn of our analysis 5 stars from the present sample appeared to be dwarfs and 343 giants, of which 126 are located in the Red Clump. Our RGC sample was found to be composed of stars with T_{eff} between 4055 K and 6239 K with the median value at 4736 K (with vast majority, ~ 200 of them, between 4600 K and 5000 K), generally G8-K2 stars. The determined $\log g$ ranges between 1.39 and 4.78 with the median of 2.66 (majority of our stars, 251 of them, have $\log g$ of 2.0 – 3.0) making them generally giants. A small fraction of 19 bright giants with $\log g \leq 2.0$ and 3 subgiants with $3.7 \leq \log g \leq 4.0$ is present as well. The microturbulence velocity, v_t , for stars from this sample ranges from 0.57 km s^{-1} to 2.49 km s^{-1} and has the median at 1.4 km s^{-1} . The metallicity, $[\text{Fe}/\text{H}]$, of stars in our RGC sample stays within -1.0 to $+0.45$ range with the median of -0.15 , our stars are generally less metal abundant than the Sun, and most of them have $[\text{Fe}/\text{H}]$ in the range of -0.5 – 0.0 .

For all 348 stars luminosities, masses, radii and ages were estimated using the presented atmospheric parameters, archive

photometric data and the Hipparcos parallaxes when available. The $\log L/L_\odot$ range from -0.68 to 2.86 with the maximum peak at 1.6. The resulting masses range from $0.6 M/M_\odot$ to $3.4 M/M_\odot$ with the majority of stars having masses below $2 M_\odot$. We identified, however, 63 (or $\sim 19\%$) stars which fall in the intermediate-mass range $2 M_\odot \leq M \leq 7 M_\odot$. The determined radii range from $0.6 R_\odot$ to $52.1 R_\odot$. Most of our stars have radii of about 9 – $11 R_\odot$. We found that typically stars from our sample are 3 – 5 Gyr old and have mean uncertainties in age of around 1.1 – 1.5 Gyr. Average uncertainties in derived parameters are $\sigma \log L/L_\odot = 0.23$, $\sigma M = 0.3 M_\odot$, $\sigma R = 0.8 R_\odot$.

We find the precision in derived stellar parameters acceptable for the main purpose of our project, i.e. massive planet search. The precision of atmospheric parameters allows for future more sophisticated analysis of individual stars. However, since the lack of the Hipparcos parallaxes was identified as the main source of the uncertainty in luminosities, masses, radii and ages for most of our stars from the presented sample we expect that the GAIA (Lindegren et al. 1994; Perryman et al. 1997; Bailer-Jones 2002) will allow to constrain their intrinsic parameters better.

Acknowledgements. We thank Dr. Yoichi Takeda as well as Dr. Peter Stetson and Dr. Elena Pancino for making their codes available for us. We thank the HET resident astronomers and telescope operators for their continuous support. We also thank anonymous referee for comments and suggestions that helped us to improve the manuscript. PZ, AN, MA and GN were supported in part by the Polish Ministry of Science and Higher Education grants N N203 510938 and N N203 386237. AW was supported by the NASA grant NNX09AB36G. The Hobby-Eberly Telescope (HET) is a joint project of the University of Texas at Austin, the Pennsylvania State University, Stanford University, Ludwig-Maximilians-Universität München, and Georg-August-Universität Göttingen. The HET is named in honor of its principal benefactors, William P. Hobby and Robert E. Eberly. The Center for Exoplanets and Habitable Worlds is supported by the Pennsylvania State University, the Eberly College of Science, and the Pennsylvania Space Grant Consortium. This research has made extensive use of the SIMBAD database, operated at CDS (Strasbourg, France) and NASA's Astrophysics Data System Bibliographic Services.

References

- Abt, H. A. 1981, *ApJS*, 45, 437
- Alonso, A., Arribas, S., & Martínez-Roger, C. 1999, *A&AS*, 140, 261
- Alonso, A., Salaris, M., Arribas, S., Martínez-Roger, C., & Asensio Ramos, A. 2000, *A&A*, 355, 1060
- Baglin, A., Auvergne, M., Barge, P., et al. 2006, in *ESA Special Publication*, Vol. 1306, *The CoRoT Mission Pre-Launch Status - Stellar Seismology and Planet Finding*, ed. M. Fridlund, A. Baglin, J. Lochard, & L. Connors (European Space Agency), 33
- Bailer-Jones, C. A. L. 2002, *Ap&SS*, 280, 21
- Baines, E. K., Döllinger, M. P., Cusano, F., et al. 2010, *ApJ*, 710, 1365
- Baines, E. K., McAlister, H. A., ten Brummelaar, T. A., et al. 2009, *ApJ*, 701, 154
- Balachandran, S., Lambert, D. L., & Stauffer, J. R. 1988, *ApJ*, 333, 267
- Bartkevičius, A. & Sperauskas, J. 1999, *Baltic Astronomy*, 8, 325
- Bedding, T. R., Huber, D., Stello, D., et al. 2010, *ApJ*, 713, L176
- Bilir, S., Karaali, S., Güver, T., Karataş, Y., & Ak, S. G. 2006, *Astronomische Nachrichten*, 327, 72
- Bizyaev, D., Smith, V. V., Arenas, J., et al. 2006, *AJ*, 131, 1784
- Bizyaev, D., Smith, V. V., & Cunha, K. 2010, *AJ*, 140, 1911
- Blackwell, D. E. & Lynas-Gray, A. E. 1998, *A&AS*, 129, 505
- Bordé, P., Coudé du Foresto, V., Chagnon, G., & Perrin, G. 2002, *A&A*, 393, 183
- Brown, J. A., Sneden, C., Lambert, D. L., & Dutchover, Jr., E. 1989, *ApJS*, 71, 293
- Butler, R. P., Marcy, G. W., Williams, E., et al. 1996, *PASP*, 108, 500
- Butler, R. P., Wright, J. T., Marcy, G. W., et al. 2006, *ApJ*, 646, 505
- Cannon, R. D. 1970, *MNRAS*, 150, 111
- Carney, B. W., Latham, D. W., Stefanik, R. P., Laird, J. B., & Morse, J. A. 2003, *AJ*, 125, 293
- Chauvin, G., Lagrange, A.-M., Dumas, C., et al. 2004, *A&A*, 425, L29
- Cochran, W. D. & Hatzes, A. P. 1993, in *ASP Conference Series*, Vol. 36, *Planets Around Pulsars*, ed. J. A. Phillips, S. E. Thorsett, & S. R. Kulkarni (San Francisco: ASP), 267–273
- Cumming, A., Butler, R. P., Marcy, G. W., et al. 2008, *PASP*, 120, 531
- Cutri, R. M., Skrutskie, M. F., van Dyk, S., et al. 2003, *VizieR Online Data Catalog*, 2246
- de Medeiros, J. R. & Mayor, M. 1999, *A&AS*, 139, 433
- De Ridder, J., Barban, C., Baudin, F., et al. 2009, *Nature*, 459, 398
- Duflot, M., Figan, P., & Meyssonnier, N. 1995, *A&AS*, 114, 269
- Famaey, B., Jorissen, A., Luri, X., et al. 2005, *A&A*, 430, 165
- Faulkner, D. J. & Cannon, R. D. 1973, *ApJ*, 180, 435
- Frink, S., Mitchell, D. S., Quirrenbach, A., et al. 2002, *ApJ*, 576, 478
- Gelino, C. R., Shao, M., Tanner, A. M., & Niedzielski, A. 2005, in *LPI Contribution*, Vol. 1286, *Protostars and Planets V*, ed. B. Reipurth, D. Jewitt & K. Keil (Houston: Lunar and Planetary Institute), 8602
- Gettel, S., Wolszczan, A., Niedzielski, A., et al. 2012a, *ApJ*, submitted
- Gettel, S., Wolszczan, A., Niedzielski, A., et al. 2012b, *ApJ*, 745, 28
- Gilliland, R. L., Brown, T. M., Christensen-Dalsgaard, J., et al. 2010, *PASP*, 122, 131
- Girardi, L. 1999, *MNRAS*, 308, 818
- Girardi, L., Bressan, A., Bertelli, G., & Chiosi, C. 2000, *A&AS*, 141, 371
- Gontcharov, G. A. 2006, *Astronomy Letters*, 32, 759
- Gontcharov, G. A. 2008, *Astronomy Letters*, 34, 785
- Gonzalez, G., Brownlee, D., & Ward, P. 2001, *Icarus*, 152, 185
- Gowanlock, M. G., Patton, D. R., & McConnell, S. M. 2011, *Astrobiology*, 11, 855
- Gregory, P. C. & Fischer, D. A. 2010, *MNRAS*, 403, 731
- Grevesse, N. & Sauval, A. J. 1999, *A&A*, 347, 348
- Hatzes, A. P. & Cochran, W. D. 1993, *ApJ*, 413, 339
- Hatzes, A. P. & Cochran, W. D. 1994, *ApJ*, 432, 763
- Hatzes, A. P., Guenther, E. W., Endl, M., et al. 2005, *A&A*, 437, 743
- Haywood, M. 2009, *ApJ*, 698, L1
- Hébrard, G., Désert, J.-M., Díaz, R. F., et al. 2010, *A&A*, 516, A95
- Hekker, S., Gilliland, R. L., Elsworth, Y., et al. 2011, *MNRAS*, 414, 2594
- Hekker, S. & Meléndez, J. 2007, *A&A*, 475, 1003
- Hekker, S., Reffert, S., Quirrenbach, A., et al. 2006, *A&A*, 454, 943
- Hidas, M. G., Tsapras, Y., Mislis, D., et al. 2010, *MNRAS*, 406, 1146
- Høg, E. & Murdin, P. 2000, *Tycho Star Catalogs: The 2.5 Million Brightest Stars* (Bristol: IOP)
- Holweger, H., Bard, A., Kock, M., & Kock, A. 1991, *A&A*, 249, 545
- Jimenez, R., Flynn, C., & Kotoneva, E. 1998, *MNRAS*, 299, 515
- Johnson, J. A., Fischer, D. A., Marcy, G. W., et al. 2007, *ApJ*, 665, 785
- Kallinger, T., Mosser, B., Hekker, S., et al. 2010, *A&A*, 522, A1
- Katz, D., Soubiran, C., Cayrel, R., Adda, M., & Cautain, R. 1998, *A&A*, 338, 151
- Kharchenko, N. V. & Roeser, S. 2009, *VizieR Online Data Catalog*, 1280
- Kurucz, R. 1993a, *ATLAS9 Stellar Atmosphere Programs and 2 km/s grid*. Kurucz CD-ROM No. 13. Cambridge, Mass.: Smithsonian Astrophysical Observatory
- Kurucz, R. 1993b, *SYNTHE Spectrum Synthesis Programs and Line Data*. Kurucz CD-ROM No. 18. Cambridge, Mass.: Smithsonian Astrophysical Observatory
- Kurucz, R. L., Furenlid, I., Brault, J., & Testerman, L. 1984, *Solar flux atlas from 296 to 1300 nm* (New Mexico: National Solar Observatory)
- Law, N. M., Tanner, A., Kulkarni, S., Shao, M., & Gelino, C. 2006, in *BAAS*, Vol. 38, 1227
- Lee, B.-C., Mkrtchian, D. E., Han, I., Kim, K.-M., & Park, M.-G. 2011, *A&A*, 529, A134
- Lindgren, L., Perryman, M. A., Bastian, U., et al. 1994, in *Proc. SPIE*, Vol. 2200, 599–608
- Lineweaver, C. H., Fenner, Y., & Gibson, B. K. 2004, *Science*, 303, 59
- Lissauer, J. J., Fabrycky, D. C., Ford, E. B., et al. 2011, *Nature*, 470, 53
- Liu, Y. J., Zhao, G., Shi, J. R., Pietrzynski, G., & Gieren, W. 2007, *MNRAS*, 382, 553
- Lovis, C. & Mayor, M. 2007, *A&A*, 472, 657
- Luck, R. E. 1991, *ApJS*, 75, 579
- Luck, R. E. & Heiter, U. 2007, *AJ*, 133, 2464
- Mader, J. & Shetrone, M. D. 2002, in *HET Technical Document No. 300* (University of Texas, McDonald Observatory)
- Marcy, G. W. & Butler, R. P. 1996, *ApJ*, 464, L147
- Marois, C., Macintosh, B., Barman, T., et al. 2008, *Science*, 322, 1348
- Mayor, M., Bonfils, X., Forveille, T., et al. 2009, *A&A*, 507, 487
- Mayor, M. & Queloz, D. 1995, *Nature*, 378, 355
- McCabe, M. & Lucas, H. 2010, *International Journal of Astrobiology*, 9, 217
- McWilliam, A. 1990, *ApJS*, 74, 1075
- Meisel, D. D. 1968, *AJ*, 73, 350
- Merline, W. J. 1999, in *ASP Conference Series*, Vol. 185, *Precise Stellar Radial Velocities*, ed. J. B. Hearnshaw & C. D. Scarfe (San Francisco: ASP), 187
- Meylan, T., Furenlid, I., Wiggs, M. S., & Kurucz, R. L. 1993, *ApJS*, 85, 163
- Mishenina, T. V., Bienaymé, O., Gorbaneva, T. I., et al. 2006, *A&A*, 456, 1109
- Nidever, D. L., Marcy, G. W., Butler, R. P., Fischer, D. A., & Vogt, S. S. 2002, *ApJS*, 141, 503
- Niedzielski, A., Goździewski, K., Wolszczan, A., et al. 2009a, *ApJ*, 693, 276
- Niedzielski, A., Konacki, M., Wolszczan, A., et al. 2007, *ApJ*, 669, 1354
- Niedzielski, A., Nowak, G., Adamów, M., & Wolszczan, A. 2009b, *ApJ*, 707, 768
- Niedzielski, A. & Wolszczan, A. 2008, in *IAU Symposium*, Vol. 249, *Exoplanets: Detection, Formation and Dynamics*, ed. Y.-S. Sun, S. Ferraz-Mello, & J.-L. Zhou (Cambridge: CUP), 43–47
- Nordgren, T. E., Germain, M. E., Benson, J. A., et al. 1999, *AJ*, 118, 3032
- Nowak, G. & Niedzielski, A. 2008, in *ASP Conference Series*, Vol. 398, *Extreme Solar Systems*, ed. D. Fischer, F. A. Rasio, S. E. Thorsett, & A. Wolszczan (San Francisco: ASP), 173
- Paczynski, B. & Stanek, K. Z. 1998, *ApJ*, 494, L219
- Pasinetti Fracassini, L. E., Pastori, L., Covino, S., & Pozzi, A. 2001, *A&A*, 367, 521
- Perryman, M. A. C. & ESA, eds. 1997, *ESA Special Publication*, Vol. 1200, *The HIPPARCOS and TYCHO catalogues. Astrometric and photometric star catalogues derived from the ESA HIPPARCOS Space Astrometry Mission* (European Space Agency)
- Perryman, M. A. C., Lindegren, L., & Turon, C. 1997, in *ESA Special Publication*, Vol. 402, *Hipparcos - Venice '97*, ed. R. M. Bonnet, E. Högl, P. L. Bernacca, L. Emiliani, A. Blaauw, C. Turon, J. Kovalevsky, L. Lindegren, H. Hassan, M. Bouffard, B. Strim, D. Heger, M. A. C. Perryman, & L. Woltjer (European Space Agency), 743–748
- Puzeras, E., Tautvaišienė, G., Cohen, J. G., et al. 2010, *MNRAS*, 408, 1225
- Queloz, D., Henry, G. W., Sivan, J. P., et al. 2001, *A&A*, 379, 279
- Ramírez, I. & Meléndez, J. 2005, *ApJ*, 626, 446
- Ramsey, L. W., Adams, M. T., Barnes, T. G., et al. 1998, in *Proc. SPIE*, Vol. 3352, 34–42
- Rieke, G. H. & Lebofsky, M. J. 1985, *ApJ*, 288, 618
- Salaris, M., Percival, S., & Girardi, L. 2003, *MNRAS*, 345, 1030
- Salasnich, B., Girardi, L., Weiss, A., & Chiosi, C. 2000, *A&A*, 361, 1023
- Sato, B., Ando, H., Kambe, E., et al. 2003, *ApJ*, 597, L157
- Setiawan, J., Hatzes, A. P., von der Lühe, O., et al. 2003a, *A&A*, 398, L19
- Setiawan, J., Pasquini, L., da Silva, L., von der Lühe, O., & Hatzes, A. 2003b, *A&A*, 397, 1151
- Shetrone, M., Cornell, M. E., Fowler, J. R., et al. 2007, *PASP*, 119, 556
- Soubiran, C., Bienaymé, O., Mishenina, T. V., & Kovtyukh, V. V. 2008, *A&A*, 480, 91
- Soubiran, C., Katz, D., & Cayrel, R. 1998, *A&AS*, 133, 221
- Stetson, P. B. & Pancino, E. 2008, *PASP*, 120, 1332
- Straizys, V. & Kuriliene, G. 1981, *Ap&SS*, 80, 353
- Strassmeier, K. G. 1994, *A&AS*, 103, 413

- Stumpff, P. 1980, A&AS, 41, 1
 Takeda, Y., Ohkubo, M., & Sadakane, K. 2002a, PASJ, 54, 451
 Takeda, Y., Ohkubo, M., Sato, B., Kambe, E., & Sadakane, K. 2005a, PASJ, 57,
 27
 Takeda, Y., Sato, B., Kambe, E., et al. 2005b, PASJ, 57, 109
 Takeda, Y., Sato, B., Kambe, E., Sadakane, K., & Ohkubo, M. 2002b, PASJ, 54,
 1041
 Takeda, Y., Sato, B., & Murata, D. 2008, PASJ, 60, 781
 Tautvaišiene, G. & Puzeras, E. 2009, in IAU Symposium, Vol. 254, The Galaxy
 Disk in Cosmological Context, ed. J. Andersen, J. Bland-Hawthorn, &
 B. Nordström (Cambridge: CUP), 75P
 Tautvaišienė, G., Edvardsson, B., Puzeras, E., Barisevičius, G., & Ilyin, I. 2010,
 MNRAS, 409, 1213
 Taylor, B. J. 1999, A&AS, 134, 523
 Tull, R. G. 1998, in Proc. SPIE, Vol. 3355, 387–398
 Valentini, M. & Munari, U. 2010, A&A, 522, A79
 van Belle, G. T. & von Braun, K. 2009, ApJ, 694, 1085
 Wolszczan, A. & Frail, D. A. 1992, Nature, 355, 145
 Zhao, G., Qiu, H. M., & Mao, S. 2001, ApJ, 551, L85

Table 1. Basic catalogue data for the sample stars.

No.	TYC	Names HD	BD	Spectral Type	V [mag]	(B–V) [mag]	π [mas]	Ref.
1	TYC 0014 00693 1	–	BD+04 126	G5	9.25	0.961 ± 0.044	–	T
2	TYC 0014 00731 1	HD 4446	BD+04 118	G5	8.99	1.026 ± 0.035	2.00 ± 1.34	H
3	TYC 0014 00752 1	–	BD+04 119	K0	9.75	1.146 ± 0.070	–	T
4	TYC 0014 00769 1	–	BD+04 107	K0	10.11	1.326 ± 0.125	–	T
5	TYC 0014 00882 1	–	BD+04 112	K2	9.96	1.307 ± 0.096	–	T
6	TYC 0017 00572 1	–	BD+04 122	K2	8.97	1.132 ± 0.040	2.34 ± 1.33	H
7	TYC 0017 00668 1	–	–	–	10.46	0.749 ± 0.119	–	T
8	TYC 0017 00900 1	–	BD+05 107	K0	9.67	1.036 ± 0.065	–	T
9	TYC 0017 01084 1	HD 4760	BD+05 109	K2	7.51	1.428 ± 0.019	0.58 ± 0.98	H
10	TYC 0017 01136 1	–	BD+04 111	K0	9.53	1.037 ± 0.047	–	T
11	TYC 0017 01292 1	–	BD+04 114	K0	9.28	0.947 ± 0.042	–	T
12	TYC 0017 01299 1	HD 4366	BD+04 113	K0	8.83	1.172 ± 0.031	–	T
13	TYC 0018 00446 1	–	BD+04 132	K2	10.37	0.978 ± 0.101	–	T
14	TYC 0096 00005 1	–	BD+06 758	K5	9.84	1.450 ± 0.166	–	T
15	TYC 0096 00109 1	–	BD+06 750A	K0	9.77	0.982 ± 0.068	–	T
16	TYC 0096 00163 1	–	–	–	10.49	1.014 ± 0.166	–	T
17	TYC 0096 00301 1	–	–	–	9.89	1.136 ± 0.105	–	T
18	TYC 0096 00371 1	–	BD+06 755	K2	10.18	1.363 ± 0.158	–	T
19	TYC 0096 00378 1	–	–	–	10.41	0.875 ± 0.113	–	T
20	TYC 0096 00417 1	–	–	–	9.84	1.056 ± 0.156	–	T
21	TYC 0096 00418 1	–	–	–	10.62	1.209 ± 0.131	–	K
22	TYC 0096 00659 1	HD 30897	BD+05 751	K0	8.28	1.263 ± 0.020	3.43 ± 1.33	H
23	TYC 0096 00708 1	–	–	–	10.17	1.254 ± 0.146	–	T
24	TYC 0096 00732 1	–	BD+06 750B	K	10.11	0.903 ± 0.088	–	T
25	TYC 0096 00778 1	–	BD+06 754	K0	9.59	1.038 ± 0.067	–	T
26	TYC 0096 00887 1	–	–	–	10.50	1.464 ± 0.290	–	T
27	TYC 0272 00909 1	–	–	–	10.76	1.040 ± 0.262	–	T
28	TYC 0273 00125 1	–	BD+01 2626	–	9.95	1.201 ± 0.070	–	T
29	TYC 0273 00150 1	–	–	–	10.21	1.042 ± 0.105	–	T
30	TYC 0273 00224 1	HD 103485	BD+02 2493	K5	8.28	1.562 ± 0.025	–	T
31	TYC 0273 00279 1	–	BD+02 2492	K0	10.04	0.990 ± 0.063	–	T
32	TYC 0273 00451 1	–	–	–	10.86	1.113 ± 0.382	–	T
33	TYC 0273 00669 1	HD 102842	BD+01 2619	K0	9.53	1.100 ± 0.071	–	T
34	TYC 0276 00507 1	–	BD+03 2562	K2	9.58	1.271 ± 0.086	–	T
35	TYC 0400 00329 1	–	–	–	10.40	1.111 ± 0.095	–	T
36	TYC 0401 01176 1	–	–	–	10.24	1.076 ± 0.091	–	T
37	TYC 0401 01874 1	–	BD+01 3439	K0	10.23	1.344 ± 0.140	–	T
38	TYC 0401 02049 1	HD 157855	BD+01 3432	K5	9.31	1.303 ± 0.044	3.78 ± 1.46	H
39	TYC 0401 02075 1	–	–	–	10.11	1.341 ± 0.107	–	T
40	TYC 0405 00236 1	–	BD+02 3328	K	9.62	1.194 ± 0.059	–	T
41	TYC 0405 00405 1	–	BD+02 3317	G5	9.89	1.101 ± 0.065	–	T
42	TYC 0405 00414 1	–	–	–	9.85	1.123 ± 0.059	–	T
43	TYC 0405 00510 1	–	BD+03 3401	K0	9.92	1.161 ± 0.064	–	T
44	TYC 0405 00581 1	–	BD+02 3322	K0	10.03	1.330 ± 0.106	–	T
45	TYC 0405 01114 1	–	BD+02 3313	K2	9.49	1.306 ± 0.055	–	T
46	TYC 0405 01633 1	HD 157936	BD+02 3314	G5	8.50	1.201 ± 0.021	4.83 ± 1.97	H
47	TYC 0405 01634 1	–	–	–	10.25	1.124 ± 0.094	–	T
48	TYC 0405 01855 1	HD 158253	BD+02 3321	K2	9.14	1.595 ± 0.059	–	T
49	TYC 0418 00640 1	–	–	–	10.73	1.199 ± 0.216	–	T
50	TYC 0418 00912 1	–	BD+02 3332	K2	10.37	1.168 ± 0.119	–	T
51	TYC 0430 00356 1	–	BD+01 3567	K2	10.15	1.227 ± 0.135	–	T
52	TYC 0430 02902 1	HD 165592	BD+01 3593	K0	8.94	1.043 ± 0.035	–	T
53	TYC 0434 00031 1	–	BD+02 3465	K2	10.14	1.108 ± 0.151	–	T
54	TYC 0434 00551 1	–	–	–	10.15	1.097 ± 0.123	–	T
55	TYC 0434 00632 1	HD 164734	BD+03 3572	G5	8.10	0.930 ± 0.017	4.79 ± 1.34	H
56	TYC 0434 00756 1	–	BD+03 3584	–	9.94	1.082 ± 0.086	–	T
57	TYC 0434 01143 1	–	–	–	10.28	1.030 ± 0.121	–	T
58	TYC 0434 01505 1	–	BD+03 3590	K0III	9.78	1.192 ± 0.093	–	T
59	TYC 0434 03595 1	HD 165574	BD+02 3489	K0	8.87	1.367 ± 0.065	2.26 ± 1.40	H
60	TYC 0434 03897 1	–	–	–	10.18	1.225 ± 0.147	–	T
61	TYC 0434 04234 1	HD 165742	BD+02 3493	K5	6.51	1.481 ± 0.012	4.07 ± 0.89	H
62	TYC 0434 04538 1	–	–	–	10.26	1.223 ± 0.192	–	T
63	TYC 0434 04779 1	HD 165419	BD+01 3585	K2	7.20	1.318 ± 0.015	–	T
64	TYC 0435 01209 1	–	BD+03 3603	K0III	9.55	0.880 ± 0.071	–	T
65	TYC 0435 03332 1	–	BD+02 3497	K0	9.04	1.100 ± 0.040	–	T
66	TYC 0435 03989 1	–	BD+02 3505	K0	9.43	1.155 ± 0.059	–	T

Table 1. continued.

No.	TYC	Names HD	BD	Spectral Type	V [mag]	(B–V) [mag]	π [mas]	Ref.
67	TYC 0683 00667 1	–	BD+07 735	–	9.31	0.914 ± 0.045	–	T
68	TYC 0683 00789 1	–	BD+07 721	K0	9.44	1.135 ± 0.059	–	T
69	TYC 0683 01063 1	–	–	–	10.06	1.280 ± 0.116	–	T
70	TYC 0683 01190 1	–	BD+07 736	K0	9.07	1.154 ± 0.040	–	T
71	TYC 0684 00553 1	–	–	–	10.31	1.052 ± 0.115	–	T
72	TYC 0684 00744 1	–	BD+07 742	K5	9.62	1.357 ± 0.090	–	T
73	TYC 0684 01276 1	–	–	–	10.61	1.589 ± 0.400	–	T
74	TYC 0863 00082 1	–	BD+15 2372	G5	9.75	0.897 ± 0.060	–	T
75	TYC 0863 00230 1	–	BD+15 2371	K0	9.35	1.115 ± 0.052	–	T
76	TYC 0870 00084 1	–	–	KOIII	10.22	0.925 ± 0.193	–	T
77	TYC 0870 00114 1	HD 102272	BD+14 2434	K2	8.69	1.020 ± 0.015	2.76 ± 1.11	H
78	TYC 0870 00130 1	–	BD+15 2387	K0	9.12	0.922 ± 0.032	2.23 ± 1.54	H
79	TYC 0870 00204 1	–	BD+15 2375	–	10.28	1.061 ± 0.134	–	T
80	TYC 0870 00207 1	–	BD+15 2386	G0	9.65	1.259 ± 0.080	–	T
81	TYC 0870 00241 1	HD 102103	BD+15 2374	K0	6.51	1.165 ± 0.009	4.80 ± 0.87	H
82	TYC 0870 00255 1	–	BD+15 2390	G5	10.17	1.009 ± 0.095	–	T
83	TYC 0870 00314 1	–	–	K2	10.06	1.051 ± 0.141	–	T
84	TYC 0870 00937 1	–	BD+15 2385	K0	9.82	1.100 ± 0.068	–	T
85	TYC 0955 00126 1	–	–	–	10.78	1.769 ± 0.364	–	Tc
86	TYC 0956 00028 1	–	BD+14 2970	K0	10.06	1.698 ± 0.241	–	T
87	TYC 1058 00120 1	HD 188105	BD+07 4275	K0	7.63	1.185 ± 0.014	4.75 ± 1.21	H
88	TYC 1058 00205 1	HD 188369	BD+08 4263	K2	8.75	1.197 ± 0.029	1.84 ± 1.35	H
89	TYC 1058 00635 1	HD 188004	BD+08 4249	K0	8.98	1.080 ± 0.033	–	T
90	TYC 1058 00979 1	–	BD+08 4223	K2	10.10	1.253 ± 0.076	–	T
91	TYC 1058 01279 1	HD 188237	BD+08 4259	K0	8.00	1.098 ± 0.018	–	T
92	TYC 1058 01329 1	–	BD+08 4256	K0	9.83	1.108 ± 0.064	–	T
93	TYC 1058 01537 1	HD 187377	BD+08 4228	G5	9.41	1.061 ± 0.040	–	T
94	TYC 1058 01931 1	–	–	–	9.72	1.029 ± 0.091	–	T
95	TYC 1058 02389 1	HD 188124	BD+08 4252	K2	8.95	1.150 ± 0.047	–	T
96	TYC 1058 02865 1	HD 188214	BD+08 4258	K2	8.48	1.113 ± 0.029	–	T
97	TYC 1058 02919 1	–	–	–	10.27	1.033 ± 0.134	–	T
98	TYC 1058 02972 1	HD 187094	BD+07 4230	G5	9.39	1.238 ± 0.034	–	T
99	TYC 1058 03032 1	HD 187526	BD+08 4230	K2	10.20	0.822 ± 0.086	–	T
100	TYC 1058 03402 1	–	BD+08 4232	–	9.85	1.012 ± 0.052	–	K
101	TYC 1208 00063 1	–	–	–	9.53	1.031 ± 0.063	–	T
102	TYC 1208 00261 1	HD 10364	BD+19 277	K2	8.04	1.170 ± 0.026	4.84 ± 1.20	H
103	TYC 1208 00623 1	–	BD+18 219	K5	9.25	1.488 ± 0.077	–	T
104	TYC 1208 00699 1	–	–	–	10.17	1.147 ± 0.128	–	T
105	TYC 1211 00015 1	–	–	–	10.49	0.854 ± 0.115	–	T
106	TYC 1211 00016 1	–	–	–	10.37	1.050 ± 0.104	–	T
107	TYC 1211 00103 1	–	–	–	9.92	1.078 ± 0.089	–	T
108	TYC 1211 00153 1	–	–	–	10.43	0.938 ± 0.084	–	K
109	TYC 1211 00335 1	–	BD+19 271	K2	9.88	1.249 ± 0.078	–	T
110	TYC 1211 00406 1	–	–	–	9.93	1.075 ± 0.067	–	T
111	TYC 1211 00449 1	–	–	–	10.73	1.030 ± 0.156	–	T
112	TYC 1211 00603 1	–	BD+20 274	–	9.36	1.358 ± 0.067	–	T
113	TYC 1211 00677 1	–	–	–	9.86	1.180 ± 0.095	–	T
114	TYC 1422 00100 1	–	BD+20 2454	K2	10.42	1.170 ± 0.172	–	T
115	TYC 1422 00614 1	–	–	–	10.21	0.950 ± 0.085	–	T
116	TYC 1422 00790 1	–	BD+20 2457	K2	9.72	1.180 ± 0.064	–	T
117	TYC 1422 01044 1	–	–	–	9.77	1.300 ± 0.082	–	T
118	TYC 1423 00013 1	–	–	–	9.74	1.661 ± 0.157	–	T
119	TYC 1423 00156 1	–	–	–	10.50	1.259 ± 0.186	–	T
120	TYC 1423 00165 1	–	BD+20 2464	–	10.61	1.017 ± 0.111	–	K
121	TYC 1423 00248 1	–	–	–	10.00	1.285 ± 0.121	–	T
122	TYC 1423 00270 1	–	BD+20 2473	K0	10.55	0.910 ± 0.143	–	T
123	TYC 1423 00364 1	–	–	–	10.36	1.414 ± 0.227	–	T
124	TYC 1423 00457 1	HD 89930	BD+19 2335	G5	7.12	0.983 ± 0.011	3.73 ± 0.83	H
125	TYC 1425 01506 1	HD 89196	BD+20 2460	K2	8.04	1.551 ± 0.028	2.68 ± 0.97	H
126	TYC 1426 00662 1	–	BD+21 2173	K0	9.54	1.047 ± 0.049	–	T
127	TYC 1426 00810 1	HD 89772	BD+20 2475	K	8.95	1.239 ± 0.045	–	T
128	TYC 1426 01004 1	–	–	–	10.24	0.932 ± 0.092	–	T
129	TYC 1426 01209 1	HD 89471	BD+21 2175	K0	7.73	1.308 ± 0.021	2.18 ± 0.94	H
130	TYC 1496 00050 1	–	–	–	10.20	0.795 ± 0.131	–	T
131	TYC 1496 00290 1	–	–	–	9.91	1.204 ± 0.105	–	T
132	TYC 1496 00572 1	HD 143257	BD+16 2855	K2	7.73	1.470 ± 0.020	3.34 ± 1.03	H

Table 1. continued.

No.	TYC	Names HD	BD	Spectral Type	V [mag]	(B–V) [mag]	π [mas]	Ref.
133	TYC 1496 00637 1	HD 143064	BD+16 2851	K5	8.52	1.290 ± 0.039	3.90 ± 1.24	H
134	TYC 1496 00840 1	—	BD+16 2852	K0	9.67	0.907 ± 0.060	—	T
135	TYC 1496 00961 1	—	—	—	10.10	0.929 ± 0.172	—	T
136	TYC 1496 01002 1	—	—	—	10.41	0.990 ± 0.261	—	T
137	TYC 1496 01656 1	—	—	—	10.45	1.601 ± 0.266	—	Tc
138	TYC 1496 01841 1	HD 142245	BD+15 2925	K0	7.46	1.036 ± 0.016	9.40 ± 0.94	H
139	TYC 1503 01050 1	—	BD+15 2940	K0	9.01	1.006 ± 0.036	1.71 ± 1.33	H
140	TYC 2818 00449 1	—	BD+39 373	K3V	9.17	1.016 ± 0.058	4.17 ± 1.23	H
141	TYC 2818 00504 1	—	BD+40 334	K5V	8.46	1.281 ± 0.002	2.76 ± 1.12	H
142	TYC 2818 00733 1	—	BD+40 317	K0	8.37	1.244 ± 0.021	2.60 ± 0.99	H
143	TYC 2818 00874 1	—	BD+40 338	—	9.92	1.048 ± 0.083	—	T
144	TYC 2818 01153 1	—	BD+40 321	K2	8.96	1.370 ± 0.045	—	T
145	TYC 2818 02188 1	HD 9712	BD+40 328	K1III	6.39	1.122 ± 0.007	8.41 ± 0.77	H
146	TYC 2822 00208 1	—	—	—	10.30	1.080 ± 0.104	—	T
147	TYC 2822 00410 1	HD 9416	BD+41 300	G5III	8.57	0.934 ± 0.019	2.61 ± 1.09	H
148	TYC 2822 00812 1	—	BD+40 303	K0	9.55	1.222 ± 0.057	—	T
149	TYC 2822 01573 1	—	BD+41 306	G0	9.18	0.967 ± 0.033	—	T
150	TYC 2822 01643 1	HD 9519	BD+41 304	K2	7.90	1.332 ± 0.019	—	T
151	TYC 2822 02010 1	—	—	—	10.42	1.168 ± 0.129	—	T
152	TYC 2823 01028 1	—	BD+40 351	K2V	8.88	1.031 ± 0.028	4.92 ± 1.18	H
153	TYC 2823 01398 1	—	BD+40 348	K2V	9.49	1.050 ± 0.047	—	T
154	TYC 2823 01786 1	HD 10455	BD+40 352	K0	8.14	1.072 ± 0.016	—	T
155	TYC 3011 00547 1	—	BD+44 2037	K0	9.20	1.114 ± 0.043	—	T
156	TYC 3011 00791 1	HD 95127	BD+44 2038	K0	8.15	1.311 ± 0.019	2.34 ± 1.04	H
157	TYC 3012 00126 1	—	BD+44 2059	G5	9.57	1.030 ± 0.063	—	T
158	TYC 3012 00145 1	HD 96992	BD+44 2063	K0	8.57	1.023 ± 0.023	2.60 ± 1.07	H
159	TYC 3012 00273 1	—	BD+44 2057	G5	9.52	0.761 ± 0.047	—	T
160	TYC 3012 00285 1	—	BD+44 2047	K5	9.58	1.256 ± 0.057	—	T
161	TYC 3012 00470 1	—	—	—	9.81	0.962 ± 0.052	—	T
162	TYC 3012 00667 1	HD 96127	BD+45 1892	K2	7.43	1.503 ± 0.014	1.85 ± 0.89	H
163	TYC 3012 00676 1	—	BD+44 2041	K0	9.29	1.045 ± 0.042	—	T
164	TYC 3012 01263 1	—	—	—	10.01	1.104 ± 0.066	—	T
165	TYC 3012 01504 1	—	BD+43 2070	K0	8.92	1.003 ± 0.027	7.27 ± 1.19	H
166	TYC 3012 01520 1	—	BD+43 2080	K5	9.21	1.302 ± 0.041	—	T
167	TYC 3012 02518 1	HD 95296	BD+43 2069	K0	6.69	1.114 ± 0.008	4.74 ± 0.77	H
168	TYC 3012 02527 1	—	BD+44 2046	K2	9.16	1.025 ± 0.047	—	T
169	TYC 3018 00288 1	—	BD+41 2310	G9III	10.05	1.070 ± 0.062	—	T
170	TYC 3018 00336 1	—	BD+41 2304	K2III	9.05	1.243 ± 0.042	—	T
171	TYC 3018 00350 1	HD 108872	BD+41 2298	K1III	8.63	1.070 ± 0.015	4.98 ± 1.26	H
172	TYC 3018 00704 1	HD 109461	BD+41 2305	G8III	8.79	0.890 ± 0.015	1.83 ± 1.19	H
173	TYC 3018 00708 1	HD 110065	BD+41 2313	K0III	8.21	0.940 ± 0.013	10.07 ± 1.06	H
174	TYC 3018 00996 1	HD 109681	BD+41 2308	K2III	7.58	1.125 ± 0.010	7.86 ± 0.95	H
175	TYC 3018 01050 1	HD 109740	BD+41 2309	K1III	8.81	1.160 ± 0.015	3.78 ± 1.36	H
176	TYC 3020 01183 1	—	BD+42 2322	K2III	9.75	1.213 ± 0.013	5.60 ± 1.61	H
177	TYC 3020 02438 1	—	BD+42 2320	G8III	10.49	1.035 ± 0.261	—	T
178	TYC 3105 00152 1	—	—	K1III	9.90	1.141 ± 0.084	—	T
179	TYC 3105 00228 1	—	BD+39 3457	K0	10.36	0.958 ± 0.086	—	T
180	TYC 3105 00535 1	—	BD+38 3228	K5	9.71	1.253 ± 0.071	—	T
181	TYC 3105 00683 1	—	BD+38 3201	—	9.54	1.046 ± 0.064	—	T
182	TYC 3105 00692 1	—	—	K0III	9.73	1.191 ± 0.169	—	T
183	TYC 3105 00873 1	—	—	—	10.39	1.144 ± 0.156	—	T
184	TYC 3105 01095 1	—	BD+37 3182	K0	9.80	0.889 ± 0.063	—	T
185	TYC 3105 01137 1	—	BD+38 3205	K2	8.99	1.201 ± 0.038	—	T
186	TYC 3105 01851 1	—	BD+37 3198	K0	9.80	0.951 ± 0.053	—	T
187	TYC 3105 01862 1	—	—	—	9.78	1.002 ± 0.051	—	T
188	TYC 3105 02077 1	—	BD+38 3235	K0III	9.74	1.273 ± 0.214	—	T
189	TYC 3109 00661 1	—	BD+39 3464	K0	10.38	0.856 ± 0.074	—	T
190	TYC 3109 01946 1	—	—	—	10.71	0.775 ± 0.101	—	T
191	TYC 3109 02342 1	—	BD+39 3480	K0	9.17	0.948 ± 0.034	—	T
192	TYC 3118 00440 1	—	BD+39 3493	G0	9.84	1.139 ± 0.065	—	T
193	TYC 3118 02068 1	—	BD+38 3258	K2	10.42	1.089 ± 0.121	—	T
194	TYC 3122 02192 1	—	—	—	10.64	1.022 ± 0.141	—	T
195	TYC 3226 00556 1	HD 215443	BD+43 4293	K0	9.20	0.956 ± 0.020	—	T
196	TYC 3226 00696 1	—	BD+43 4303	—	9.82	1.380 ± 0.056	—	T
197	TYC 3226 00993 1	HD 215472	BD+43 4295	K0	9.63	1.076 ± 0.032	—	T
198	TYC 3226 00997 1	HD 215335	BD+43 4288	K0	7.22	1.178 ± 0.007	6.56 ± 0.81	H

Table 1. continued.

No.	TYC	Names		Spectral	V	(B–V)	π	Ref.
		HD	BD	Type	[mag]	[mag]	[mas]	
199	TYC 3226 01219 1	HD 216016	BD+43 4310	K0	9.62	1.150 ± 0.032	—	T
200	TYC 3226 01373 1	HD 215576	BD+43 4299	—	9.21	1.176 ± 0.025	—	T
201	TYC 3226 01589 1	—	—	—	9.97	1.122 ± 0.053	—	T
202	TYC 3226 01858 1	HD 216161	BD+42 4506	K0	9.63	1.220 ± 0.051	—	T
203	TYC 3226 02051 1	HD 215346	BD+43 4289	K5	8.42	1.354 ± 0.015	—	T
204	TYC 3226 02100 1	HD 215897	BD+42 4501	G5	9.56	1.148 ± 0.044	—	T
205	TYC 3226 02285 1	HD 214868	BD+43 4266	K3III	4.50	1.318 ± 0.003	10.81 ± 0.56	H
206	TYC 3227 00068 1	HD 216307	BD+42 4517	K0	9.62	1.143 ± 0.043	—	T
207	TYC 3227 00213 1	HD 216257	BD+44 4251	K0	7.95	1.375 ± 0.011	5.66 ± 1.00	H
208	TYC 3227 00413 1	HD 216536	BD+43 4329	K0	9.22	1.208 ± 0.031	—	T
209	TYC 3300 00133 1	—	—	—	9.49	1.171 ± 0.044	—	T
210	TYC 3300 01380 1	—	BD+47 678	K0	8.79	1.033 ± 0.022	—	T
211	TYC 3300 01645 1	—	BD+47 682	K0	9.56	1.474 ± 0.071	—	T
212	TYC 3300 01952 1	—	BD+48 749	K0	8.86	1.176 ± 0.034	—	T
213	TYC 3304 00088 1	—	—	—	9.70	0.968 ± 0.048	—	T
214	TYC 3304 00090 1	—	BD+48 740	K2	8.69	1.252 ± 0.032	0.11 ± 1.32	H
215	TYC 3304 00101 1	HD 17092	BD+49 767	K0III	7.73	1.247 ± 0.014	—	T
216	TYC 3304 00110 1	—	BD+48 725	K2	10.10	1.273 ± 0.097	—	T
217	TYC 3304 00323 1	—	BD+48 738	K0	9.14	1.246 ± 0.046	—	T
218	TYC 3304 00405 1	—	BD+49 775	K2	9.91	1.587 ± 0.126	—	T
219	TYC 3304 00408 1	HD 17028	BD+48 750	K0	8.27	1.513 ± 0.028	1.31 ± 1.10	H
220	TYC 3304 00553 1	—	—	—	9.21	1.702 ± 0.090	—	T
221	TYC 3304 01910 1	—	BD+49 772	K2	9.20	1.429 ± 0.043	—	T
222	TYC 3314 01371 1	—	—	—	9.96	1.211 ± 0.106	—	T
223	TYC 3318 00789 1	—	BD+49 835	K0	9.52	1.126 ± 0.053	—	T
224	TYC 3318 01302 1	—	BD+49 852	K0	9.71	1.355 ± 0.134	—	T
225	TYC 3318 01333 1	—	—	—	9.85	1.231 ± 0.072	—	T
226	TYC 3318 01427 1	—	—	—	9.94	1.361 ± 0.123	—	T
227	TYC 3318 01487 1	—	BD+49 859	K0	9.65	1.048 ± 0.135	—	T
228	TYC 3318 01515 1	—	BD+49 828	K0	9.41	1.160 ± 0.053	—	T
229	TYC 3318 01538 1	HD 18927	BD+49 838	K0	8.34	1.147 ± 0.024	—	T
230	TYC 3319 00170 1	—	—	—	10.79	1.038 ± 0.111	—	K
231	TYC 3319 00172 1	—	BD+49 872	K0	9.24	1.513 ± 0.077	—	T
232	TYC 3319 00366 1	HD 19636	BD+48 859	K2	9.00	1.146 ± 0.040	—	T
233	TYC 3319 00892 1	HD 20076	BD+48 873	K0	8.31	1.182 ± 0.023	—	T
234	TYC 3430 00053 1	—	—	—	10.21	0.978 ± 0.084	—	T
235	TYC 3430 00480 1	—	BD+52 1375	K0	9.79	1.017 ± 0.060	—	T
236	TYC 3430 00683 1	—	—	—	10.78	0.911 ± 0.158	—	T
237	TYC 3430 00747 1	HD 233601	BD+53 1310	K5	9.52	1.615 ± 0.114	—	T
238	TYC 3431 00680 1	—	—	—	9.66	0.890 ± 0.042	—	T
239	TYC 3621 00326 1	HD 215909	BD+44 4234	K2	8.31	1.435 ± 0.017	3.91 ± 1.05	H
240	TYC 3621 00445 1	—	BD+44 4237	K2	10.11	1.214 ± 0.068	—	T
241	TYC 3621 00792 1	HD 215150	BD+44 4203	K2	9.60	1.091 ± 0.039	—	T
242	TYC 3663 00024 1	—	—	—	10.44	1.407 ± 0.134	—	T
243	TYC 3663 00578 1	—	—	—	10.67	1.180 ± 0.156	—	T
244	TYC 3663 00622 1	HD 236545	BD+56 135	K0	8.98	1.121 ± 0.021	0.75 ± 1.29	H
245	TYC 3663 00654 1	—	—	—	10.28	1.268 ± 0.106	—	T
246	TYC 3663 00789 1	HD 236525	BD+56 127	K2	8.87	1.107 ± 0.018	—	T
247	TYC 3663 01007 1	HD 236559	BD+56 140	K5	8.97	1.228 ± 0.025	—	T
248	TYC 3663 01040 1	HD 236565	BD+56 142	K2	8.58	1.136 ± 0.016	2.97 ± 1.14	H
249	TYC 3663 01463 1	—	BD+55 182	—	9.40	1.010 ± 0.033	—	T
250	TYC 3663 01888 1	—	—	—	10.35	1.427 ± 0.143	—	T
251	TYC 3663 01966 1	—	—	—	9.72	0.988 ± 0.040	—	T
252	TYC 3663 01992 1	—	—	—	9.93	0.916 ± 0.043	—	T
253	TYC 3663 02054 1	—	—	—	9.90	1.213 ± 0.059	—	T
254	TYC 3663 02059 1	—	—	—	9.76	1.117 ± 0.044	—	T
255	TYC 3663 02434 1	HD 236543	BD+56 134	K2	8.96	1.165 ± 0.020	2.24 ± 1.30	H
256	TYC 3667 00262 1	HD 236563	BD+57 163	K2	9.77	1.164 ± 0.044	—	T
257	TYC 3667 00512 1	HD 236530	BD+57 146	K2	9.21	1.121 ± 0.035	—	T
258	TYC 3667 00550 1	—	—	—	10.09	0.933 ± 0.053	—	T
259	TYC 3667 01178 1	HD 3933	BD+57 130	K0	8.00	0.893 ± 0.011	1.45 ± 1.07	H
260	TYC 3667 01280 1	—	—	—	9.81	1.020 ± 0.037	—	T
261	TYC 3667 01442 1	—	—	—	10.38	1.033 ± 0.085	—	T
262	TYC 3667 01636 1	—	BD+57 144	G8III	8.86	1.020 ± 0.019	1.67 ± 1.29	H
263	TYC 3667 01656 1	HD 236562	BD+57 162	K2	9.52	1.265 ± 0.038	—	T
264	TYC 3676 02387 1	—	—	—	9.51	1.109 ± 0.032	—	T

Table 1. continued.

No.	TYC	Names	Spectral	V	(B–V)	π	Ref.
		HD	Type	[mag]	[mag]	[mas]	
		BD					
265	TYC 3805 00193 1	HD 233604	BD+54 1280	K5	10.32	1.007 ± 0.115	— T
266	TYC 3805 00709 1	HD 77819	BD+53 1309	G5	7.55	0.928 ± 0.012	5.29 ± 0.96 H
267	TYC 3805 01162 1	—	—	—	10.11	1.343 ± 0.135	— T
268	TYC 3806 00244 1	—	—	—	10.06	0.889 ± 0.063	— T
269	TYC 3806 00861 1	—	—	—	10.36	1.065 ± 0.078	— T
270	TYC 3806 01026 1	—	—	—	10.58	1.091 ± 0.132	— T
271	TYC 3806 01071 1	HD 233612	BD+53 1318	K7	9.69	1.362 ± 0.076	— T
272	TYC 3806 01289 1	HD 233615	BD+53 1324	M0	9.91	1.284 ± 0.082	— T
273	TYC 3917 01107 1	HD 238914	BD+59 1909	K7	8.77	1.015 ± 0.023	1.13 ± 0.73 H
274	TYC 3917 01228 1	—	—	—	10.25	1.023 ± 0.085	— T
275	TYC 3930 00143 1	HD 238928	BD+59 1916	K2	9.63	1.414 ± 0.073	— T
276	TYC 3930 00383 1	—	—	—	9.99	1.256 ± 0.081	— T
277	TYC 3930 00519 1	—	BD+59 1920	—	9.64	1.346 ± 0.064	— T
278	TYC 3930 00524 1	HD 174259	BD+59 1921	K0	7.19	0.953 ± 0.010	5.55 ± 0.51 H
279	TYC 3930 00551 1	—	—	—	10.69	0.962 ± 0.105	— T
280	TYC 3930 00665 1	—	—	—	9.96	1.365 ± 0.101	— T
281	TYC 3930 00681 1	—	—	—	10.27	1.135 ± 0.088	— T
282	TYC 3930 00783 1	HD 174062	BD+59 1918	K2	8.45	0.956 ± 0.020	— T
283	TYC 3930 00952 1	—	—	—	9.53	1.433 ± 0.061	— T
284	TYC 3930 01302 1	—	—	—	10.61	1.133 ± 0.188	— T
285	TYC 3930 01530 1	—	—	—	10.12	0.959 ± 0.069	— T
286	TYC 3930 01669 1	—	BD+58 1834	K0	9.33	0.938 ± 0.036	— T
287	TYC 3930 01790 1	HD 175306	BD+59 1925	KOII-IIISB	4.63	1.185 ± 0.013	10.12 ± 0.43 H
288	TYC 3993 00227 1	HD 240189	BD+56 2947	K0	9.51	0.902 ± 0.045	— T
289	TYC 3993 01107 1	HD 240188	BD+55 2896	K5	9.18	1.143 ± 0.038	— T
290	TYC 3993 01850 1	—	—	—	9.83	1.137 ± 0.055	— T
291	TYC 4006 00019 1	HD 240237	BD+57 2714	K2	8.19	1.682 ± 0.029	0.67 ± 0.86 H
292	TYC 4006 00340 1	—	—	—	10.57	1.318 ± 0.200	— T
293	TYC 4006 00629 1	HD 219415	BD+55 2926	K	8.94	1.002 ± 0.027	— T
294	TYC 4006 00797 1	HD 240226	BD+55 2918	K5	9.38	1.136 ± 0.043	— T
295	TYC 4006 00832 1	—	BD+56 2967	G5	9.84	1.197 ± 0.070	— T
296	TYC 4006 00980 1	HD 240210	BD+56 2959	K7	8.31	1.597 ± 0.029	— T
297	TYC 4006 01008 1	HD 240224	BD+56 2963	K5	8.69	1.320 ± 0.030	1.15 ± 1.04 H
298	TYC 4006 01039 1	HD 219812	BD+55 2937	K	8.56	1.052 ± 0.020	— T
299	TYC 4006 01055 1	—	—	—	10.10	1.229 ± 0.098	— T
300	TYC 4211 00364 1	—	BD+67 1020	K0	8.97	1.042 ± 0.032	— T
301	TYC 4211 00383 1	—	BD+67 1028	K0	9.77	1.123 ± 0.069	— T
302	TYC 4211 00438 1	—	BD+67 1024	K0	9.82	1.197 ± 0.073	— T
303	TYC 4215 01352 1	—	BD+60 1847	K2	8.98	1.431 ± 0.042	— T
304	TYC 4215 02018 1	—	—	—	9.89	0.991 ± 0.051	— T
305	TYC 4215 02349 1	—	BD+59 1923	K0	9.51	1.097 ± 0.047	— T
306	TYC 4421 01222 1	—	BD+68 933	K0	8.74	1.115 ± 0.028	— T
307	TYC 4421 01437 1	—	BD+68 937	K0	8.43	1.072 ± 0.023	— T
308	TYC 4421 01706 1	—	BD+68 944	K0	8.90	1.082 ± 0.063	— T
309	TYC 4421 01779 1	HD 160723	BD+69 930	K0	7.25	1.037 ± 0.011	— T
310	TYC 4421 01996 1	HD 160450	BD+68 940	K2	7.98	1.054 ± 0.015	3.45 ± 0.67 H
311	TYC 4421 02304 1	—	BD+68 931	K0	8.96	1.240 ± 0.036	— T
312	TYC 4421 02783 1	—	BD+67 1023	K0	9.39	1.104 ± 0.050	— T
313	TYC 4421 02880 1	HD 159966	BD+68 938	KOIII	5.07	1.077 ± 0.004	15.02 ± 0.54 H
314	TYC 4428 00192 1	—	BD+67 1033	K0	9.04	1.069 ± 0.033	— T
315	TYC 4428 00560 1	—	BD+68 958	K0	9.54	1.293 ± 0.062	— T
316	TYC 4428 01506 1	—	BD+68 953	K0	9.29	1.187 ± 0.057	— T
317	TYC 4428 01561 1	—	BD+68 951	K0	9.79	1.167 ± 0.072	— T
318	TYC 4428 01582 1	—	BD+69 935	K2	9.47	1.245 ± 0.071	— T
319	TYC 4444 00200 1	—	BD+68 1063	K0	10.01	1.035 ± 0.065	— T
320	TYC 4444 00717 1	HD 184737	BD+68 1071	K0	7.35	1.153 ± 0.009	5.85 ± 0.52 H
321	TYC 4444 01116 1	—	—	—	9.92	1.417 ± 0.101	— T
322	TYC 4445 00579 1	HD 187178	BD+68 1078	K	8.65	1.060 ± 0.023	2.96 ± 0.73 H
323	TYC 4448 00021 1	HD 184873	BD+69 1052	K0	7.64	0.951 ± 0.015	4.03 ± 0.58 H
324	TYC 4448 00811 1	—	BD+70 1068	K0	9.28	1.149 ± 0.039	— T
325	TYC 4448 01402 1	—	—	—	10.00	1.186 ± 0.086	— T
326	TYC 4448 01430 1	—	—	—	9.84	1.211 ± 0.072	— T
327	TYC 4448 01464 1	—	—	—	9.94	1.301 ± 0.093	— T
328	TYC 4449 00492 1	—	BD+69 1059	K5	9.25	1.114 ± 0.047	— T
329	TYC 4449 01168 1	—	BD+70 1082	K2	8.99	1.139 ± 0.032	— T
330	TYC 4449 01170 1	—	BD+69 1062	K0	9.24	1.030 ± 0.036	— T

Table 1. continued.

No.	TYC	Names HD	BD	Spectral Type	V [mag]	(B–V) [mag]	π [mas]	Ref.
331	TYC 4449 01543 1	–	BD+69 1061	K2	9.11	1.002 ± 0.035	–	T
332	TYC 4449 01785 1	–	–	–	10.02	1.040 ± 0.074	–	T
333	TYC 0405 00684 1	–	BD+02 3308	–	9.85	1.074 ± 0.055	–	T
334	TYC 0405 01700 1	–	–	–	10.18	1.259 ± 0.113	–	T
335	TYC 1062 00017 1	HD 187552	BD+09 4280	–	7.96	1.046 ± 0.015	–	T
336	TYC 1496 00374 1	–	BD+15 2932	K2	10.06	1.321 ± 0.156	0.84 ± 1.78	H
337	TYC 1496 01016 1	–	BD+16 2854	M0	10.49	1.091 ± 0.145	–	Tc
338	TYC 2818 00602 1	–	–	–	9.96	0.794 ± 0.079	–	T
339	TYC 2818 00990 1	–	–	–	10.13	0.950 ± 0.064	–	T
340	TYC 3020 01288 1	–	BD+42 2315	–	9.70	1.175 ± 0.051	–	T
341	TYC 3105 01103 1	–	BD+37 3172	–	9.21	1.184 ± 0.047	–	T
342	TYC 3226 00868 1	HD 215040	BD+43 4270	K5	9.12	1.500 ± 0.040	0.37 ± 1.31	H
343	TYC 3226 01083 1	HD 215325	BD+43 4287	–	9.62	1.294 ± 0.043	–	T
344	TYC 3304 00479 1	HD 16992	BD+49 758	–	8.66	1.158 ± 0.026	–	T
345	TYC 3318 00020 1	–	BD+48 848	–	9.45	1.396 ± 0.069	–	T
346	TYC 3431 00086 1	–	–	–	10.50	1.070 ± 0.128	–	T
347	TYC 3663 00838 1	HD 236555	BD+56 138	G5	9.05	0.860 ± 0.019	1.83 ± 1.31	H
348	TYC 4006 00890 1	–	BD+56 2957	–	9.44	1.439 ± 0.069	–	T

Notes. The following columns present: (1) running number, (2–5) identifications and spectral type from SIMBAD, (6–8) data from Tycho and Hipparcos catalogues (visual magnitude, color index, Hipparcos parallax in microarcseconds), (9) designation of data origin (T, H – The Hipparcos and Tycho Catalogues (Perryman & ESA 1997), K – Kharchenko & Roeser (2009), Tc – Tycho magnitudes transformed into Johnson magnitudes).

Table 5. Derived physical parameters for the PTPS Red Giant Clump sample stars. Intrinsic uncertainties of atmospheric parameters are presented (see Sect. 5 for a discussion).

No.	T_{eff} [K]	$\log g$ [cm s ⁻²]	v_t [km s ⁻¹]	[Fe/H]	RV [km s ⁻¹]	MJD +2400000 [d]	(B-V) ₀ [mag]	M_V [mag]	BC_V [mag]	$\log L/L_\odot$	M [M_\odot]	R [R_\odot]	Age [Gyr]
1	4820 ± 10	2.47 ± 0.04	1.34 ± 0.04	-0.39 ± 0.06	31.133 ± 0.025	54792.237534	0.946	0.82	-0.328	1.91 ± 0.09	1.8 ± 0.2	13.0 ± 0.4	1.2 ± 0.4
2	4785 ± 10	2.58 ± 0.03	1.38 ± 0.08	-0.32 ± 0.06	31.499 ± 0.024	54428.223773	0.972	0.33	-0.342	1.91 ± 0.66	1.5 ± 0.3	13.1 ± 2.3	2.6 ± 1.7
3	4709 ± 08	2.43 ± 0.04	1.43 ± 0.04	-0.34 ± 0.05	-1.671 ± 0.024	54420.247014	1.011	0.80	-0.376	1.73 ± 0.19	1.3 ± 0.3	11.0 ± 0.6	3.5 ± 1.1
4	4540 ± 05	2.35 ± 0.03	1.24 ± 0.05	-0.46 ± 0.05	28.285 ± 0.029	54786.223617	1.096	0.76	-0.462	1.60 ± 0.25	0.8 ± 0.3	10.2 ± 0.8	3.6 - 9.3
5	4368 ± 10	2.19 ± 0.04	1.52 ± 0.07	-0.04 ± 0.07	-29.305 ± 0.092	54046.260480	1.243	-2.50	-0.584	1.85 ± 0.19	1.2 ± 0.3	14.7 ± 0.8	6.7 ± 5.4
6	4548 ± 08	2.51 ± 0.03	1.28 ± 0.05	-0.32 ± 0.05	21.017 ± 0.027	54428.235521	1.106	0.74	-0.458	1.79 ± 0.58	0.7 ± 0.4	12.7 ± 2.1	3.6 - 9.3
7	4757 ± 15	2.69 ± 0.05	1.19 ± 0.06	-0.37 ± 0.06	-12.755 ± 0.021	54812.164960	0.980	0.80	-0.354	1.44 ± 0.07	1.1 ± 0.1	7.7 ± 0.2	7.5 ± 2.5
8	4543 ± 05	2.40 ± 0.03	1.28 ± 0.05	-0.37 ± 0.05	20.670 ± 0.025	54039.133009	1.103	0.76	-0.461	1.46 ± 0.30	0.7 ± 0.3	8.7 ± 0.9	4.7 - 9.3
9	4076 ± 15	1.62 ± 0.08	1.56 ± 0.08	-0.91 ± 0.09	-67.789 ± 0.057	53747.080046	1.385	-2.52	-0.820	2.65 ± 0.14	0.8 ± 0.2	42.5 ± 1.4	5.6 - 7.9
10	4753 ± 10	2.43 ± 0.04	1.50 ± 0.05	-0.41 ± 0.05	-1.305 ± 0.042	54321.371817	0.977	0.80	-0.356	1.87 ± 0.19	1.6 ± 0.3	12.7 ± 0.7	1.8 ± 1.1
11	4981 ± 18	3.77 ± 0.06	1.04 ± 0.08	0.05 ± 0.06	23.056 ± 0.034	53631.407685	0.922	0.91	-0.267	0.44 ± 0.11	1.1 ± 0.1	2.2 ± 0.3	5.5 - 7.9
12	4622 ± 15	3.00 ± 0.06	1.26 ± 0.10	-0.06 ± 0.08	-39.840 ± 0.033	53665.306597	1.092	0.80	-0.415	1.11 ± 0.27	1.0 ± 0.3	5.6 ± 0.7	2.7 - 8.3
13	4750 ± 05	2.68 ± 0.03	1.39 ± 0.05	-0.16 ± 0.05	-1.140 ± 0.025	54852.068466	1.010	0.80	-0.357	1.70 ± 0.26	2.0 ± 0.5	10.5 ± 0.8	1.2 ± 1.0
14	4172 ± 33	2.59 ± 0.11	1.47 ± 0.12	0.10 ± 0.10	45.814 ± 0.061	53779.164913	1.386	0.55	-0.756	1.57 ± 0.23	0.9 ± 0.3	11.7 ± 1.0	3.7 - 8.8
15	5000 ± 10	2.91 ± 0.03	1.27 ± 0.05	-0.08 ± 0.05	29.195 ± 0.023	54788.413790	0.895	0.92	-0.261	1.65 ± 0.19	2.5 ± 0.3	8.9 ± 0.5	0.6 ± 0.6
16	4720 ± 10	2.79 ± 0.05	1.21 ± 0.05	-0.09 ± 0.06	-44.031 ± 0.045	54780.287176	1.035	0.80	-0.371	1.54 ± 0.12	1.7 ± 0.2	8.8 ± 0.4	1.8 ± 0.6
17	4702 ± 10	2.73 ± 0.04	1.37 ± 0.04	0.01 ± 0.05	-2.986 ± 0.027	54065.233744	1.057	0.80	-0.379	1.59 ± 0.20	1.7 ± 0.3	9.4 ± 0.6	1.9 ± 1.7
18	4565 ± 10	2.70 ± 0.05	1.25 ± 0.06	0.05 ± 0.07	13.281 ± 0.033	54788.395162	1.136	0.77	-0.450	1.36 ± 0.13	1.1 ± 0.2	7.7 ± 0.4	4.5 - 8.4
19	4752 ± 05	2.55 ± 0.02	1.43 ± 0.04	-0.46 ± 0.03	46.241 ± 0.028	54778.276071	0.971	0.80	-0.357	1.65 ± 0.03	1.3 ± 0.1	9.9 ± 0.1	3.6 ± 1.1
20	4720 ± 05	2.42 ± 0.03	1.35 ± 0.05	-0.19 ± 0.05	-48.559 ± 0.025	54452.319612	1.023	0.80	-0.371	1.80 ± 0.19	1.4 ± 0.3	11.9 ± 0.7	2.8 ± 1.1
21	4620 ± 10	2.62 ± 0.03	1.40 ± 0.06	-0.16 ± 0.06	-3.906 ± 0.028	54778.292419	1.082	0.80	-0.416	1.64 ± 0.17	1.6 ± 0.3	10.3 ± 0.6	2.4 ± 1.6
22	4737 ± 20	3.51 ± 0.07	1.36 ± 0.14	0.45 ± 0.08	1.090 ± 0.033	53038.199387	1.093	0.43	-0.365	1.87 ± 0.42	1.4 ± 0.3	12.8 ± 1.5	3.3 ± 2.4
23	4984 ± 08	2.87 ± 0.04	1.36 ± 0.05	-0.04 ± 0.05	-12.642 ± 0.028	54782.271262	0.908	0.92	-0.266	1.62 ± 0.36	2.5 ± 0.6	8.7 ± 1.0	0.7 ± 0.5
24	5051 ± 05	3.44 ± 0.02	0.96 ± 0.05	-0.22 ± 0.04	48.990 ± 0.019	54869.175023	0.855	0.95	-0.246	0.84 ± 0.17	1.1 ± 0.2	3.4 ± 0.4	5.5 ± 2.5
25	4736 ± 10	2.85 ± 0.04	1.05 ± 0.09	-0.23 ± 0.06	-7.991 ± 0.030	53778.173009	1.009	0.80	-0.363	1.26 ± 0.36	0.9 ± 0.4	6.3 ± 0.9	1.8 - 9.2
26	4643 ± 10	2.74 ± 0.04	1.19 ± 0.08	-0.09 ± 0.06	41.543 ± 0.074	55136.458918	1.077	0.80	-0.403	1.46 ± 0.19	1.4 ± 0.3	8.3 ± 0.6	3.4 ± 1.1
27	4492 ± 08	2.81 ± 0.04	1.15 ± 0.09	0.08 ± 0.06	29.780 ± 0.035	55241.423929	1.180	0.73	-0.498	1.06 ± 0.31	0.7 ± 0.3	5.6 ± 0.8	5.9 - 8.4
28	4272 ± 18	2.15 ± 0.08	1.27 ± 0.09	-0.51 ± 0.10	73.773 ± 0.050	53033.388131	1.265	-2.50	-0.648	2.01 ± 0.19	0.8 ± 0.2	18.5 ± 1.0	4.7 - 9.3
29	4882 ± 10	3.53 ± 0.03	1.02 ± 0.09	0.01 ± 0.06	-2.587 ± 0.024	54216.128964	0.965	0.86	-0.302	0.69 ± 0.19	1.2 ± 0.3	3.1 ± 0.4	5.6 ± 1.1
30	4097 ± 20	1.93 ± 0.08	1.57 ± 0.12	-0.50 ± 0.09	27.560 ± 0.084	53753.402870	1.395	-2.51	-0.811	2.29 ± 0.18	0.9 ± 0.2	27.8 ± 1.4	4.7 - 9.3
31	4935 ± 18	3.88 ± 0.06	0.95 ± 0.13	-0.08 ± 0.08	7.606 ± 0.024	53025.500347	0.927	0.89	-0.283	0.30 ± 0.32	1.0 ± 0.3	1.9 ± 1.0	3.2 - 7.9
32	4913 ± 10	2.46 ± 0.04	1.39 ± 0.05	-0.59 ± 0.06	26.809 ± 0.021	55240.451111	0.873	0.87	-0.295	1.89 ± 0.18	1.5 ± 0.3	12.2 ± 0.6	2.0 ± 1.5
33	4853 ± 15	2.39 ± 0.05	1.56 ± 0.09	-0.58 ± 0.08	-31.307 ± 0.033	53511.183137	0.905	0.84	-0.317	1.85 ± 0.11	1.3 ± 0.2	11.9 ± 0.4	3.0 ± 1.5
34	4095 ± 20	1.89 ± 0.10	1.52 ± 0.09	-0.71 ± 0.09	50.884 ± 0.062	53073.392043	1.383	-2.51	-0.806	2.32 ± 0.15	0.9 ± 0.2	28.8 ± 1.2	4.7 - 9.3
35	4768 ± 08	2.60 ± 0.03	1.26 ± 0.06	-0.18 ± 0.06	-32.248 ± 0.024	55346.380121	0.998	0.80	-0.349	1.91 ± 0.19	2.5 ± 0.3	13.2 ± 0.7	0.6 ± 0.6
36	4927 ± 08	3.30 ± 0.03	1.12 ± 0.06	-0.15 ± 0.05	-4.958 ± 0.023	54659.255463	0.922	0.89	-0.287	1.04 ± 0.14	1.6 ± 0.2	4.6 ± 0.3	2.3 ± 0.6
37	4865 ± 10	2.64 ± 0.04	1.41 ± 0.06	-0.29 ± 0.06	-41.322 ± 0.026	54616.268293	0.936	0.84	-0.310	1.72 ± 0.19	1.7 ± 0.3	10.2 ± 0.6	1.5 ± 1.1
38	4553 ± 08	2.67 ± 0.04	1.35 ± 0.09	-0.02 ± 0.06	4.906 ± 0.032	54331.157975	1.134	1.67	-0.457	1.41 ± 0.42	1.1 ± 0.1	8.2 ± 1.2	5.9 - 8.4
39	4649 ± 08	2.52 ± 0.03	1.36 ± 0.05	-0.15 ± 0.06	10.850 ± 0.027	55335.410909	1.067	0.80	-0.399	1.82 ± 0.09	2.0 ± 0.2	12.6 ± 0.4	1.3 ± 0.4
40	4714 ± 08	2.43 ± 0.04	1.41 ± 0.06	-0.41 ± 0.06	-1.212 ± 0.024	53179.321464	1.000	0.80	-0.374	1.73 ± 0.19	1.3 ± 0.3	11.0 ± 0.6	3.5 ± 1.1
41	4885 ± 05	2.47 ± 0.02	1.36 ± 0.04	-0.46 ± 0.04	17.256 ± 0.022	55352.362199	0.904	0.86	-0.304	2.04 ± 0.07	2.4 ± 0.2	14.6 ± 0.3	0.6 ± 0.1
42	4719 ± 10	2.80 ± 0.05	1.70 ± 0.10	-0.33 ± 0.07	-83.899 ± 0.054	54259.364745	1.007	0.80	-0.371	1.21 ± 0.35	0.8 ± 0.3	6.0 ± 0.9	2.7 - 9.2
43	4659 ± 08	2.57 ± 0.04	1.29 ± 0.05	-0.13 ± 0.05	9.883 ± 0.025	55324.312928	1.064	0.80	-0.394	1.78 ± 0.08	2.0 ± 0.2	11.9 ± 0.3	1.2 ± 0.4
44	4523 ± 08	2.60 ± 0.03	1.35 ± 0.08	0.09 ± 0.06	-47.249 ± 0.059	55286.421875	1.164	0.75	-0.478	1.45 ± 0.06	1.1 ± 0.1	8.7 ± 0.2	5.9 - 8.4
45	4425 ± 13	2.64 ± 0.05	1.20 ± 0.07	0.10 ± 0.07	-47.601 ± 0.055	54652.180301	1.224	0.69	-0.545	1.37 ± 0.11	1.1 ± 0.1	8.3 ± 0.4	6.3 - 8.7
46	4518 ± 10	2.47 ± 0.04	1.23 ± 0.04	-0.24 ± 0.06	10.267 ± 0.031	54586.351273	1.131	1.70	-0.477	1.41 ± 0.41	0.6 ± 0.3	8.3 ± 1.2	4.7 - 9.3
47	4781 ± 08	2.65 ± 0.03	1.31 ± 0.05	-0.15 ± 0.05	18.341 ± 0.025	55320.343773	0.996	0.80	-0.343	1.76 ± 0.21	2.2 ± 0.4	11.1 ± 0.7	1.0 ± 0.5

Table 5. continued.

No.	T_{eff} [K]	$\log g$ [cm s ⁻²]	v_t [km s ⁻¹]	[Fe/H]	RV [km s ⁻¹]	MJD +2400000 [d]	(B-V) ₀ [mag]	M_V [mag]	BC_V [mag]	$\log L/L_{\odot}$	M [M_{\odot}]	R [R_{\odot}]	Age [Gyr]
48	4185 ± 13	1.80 ± 0.06	1.72 ± 0.07	-0.21 ± 0.07	-37.959 ± 0.058	53899.345226	1.350	-2.50	-0.732	2.27 ± 0.11	1.5 ± 0.2	26.0 ± 0.8	3.0 ± 1.7
49	4242 ± 08	2.09 ± 0.03	1.25 ± 0.05	-0.65 ± 0.05	-58.151 ± 0.060	55346.395069	1.274	-2.50	-0.670	2.06 ± 0.16	0.8 ± 0.2	19.9 ± 0.8	4.7 - 9.3
50	4758 ± 08	2.63 ± 0.03	1.43 ± 0.06	-0.28 ± 0.05	-22.987 ± 0.028	54659.286887	0.991	0.80	-0.354	1.55 ± 0.18	1.2 ± 0.2	8.8 ± 0.5	5.3 ± 4.3
51	4665 ± 08	2.60 ± 0.04	1.38 ± 0.06	-0.05 ± 0.06	-2.783 ± 0.029	54625.277234	1.070	0.80	-0.390	1.76 ± 0.10	1.9 ± 0.2	11.6 ± 0.4	1.2 ± 0.3
52	4922 ± 10	2.68 ± 0.04	1.33 ± 0.07	-0.32 ± 0.07	-17.624 ± 0.027	53831.440538	0.903	0.88	-0.290	1.75 ± 0.19	1.9 ± 0.3	10.3 ± 0.6	1.1 ± 0.7
53	4503 ± 10	2.52 ± 0.04	1.40 ± 0.06	-0.11 ± 0.06	-60.770 ± 0.044	54588.374664	1.152	0.74	-0.488	1.55 ± 0.16	1.2 ± 0.2	9.8 ± 0.5	7.7 ± 5.5
54	4806 ± 10	2.51 ± 0.03	1.41 ± 0.06	-0.24 ± 0.06	4.424 ± 0.027	54661.298293	0.972	0.81	-0.333	1.84 ± 0.05	1.7 ± 0.1	12.0 ± 0.2	1.5 ± 0.3
55	5031 ± 08	2.79 ± 0.03	1.24 ± 0.06	-0.10 ± 0.05	-46.638 ± 0.039	53906.353669	0.878	1.34	-0.251	1.46 ± 0.29	2.8 ± 0.6	7.1 ± 0.7	0.5 ± 0.2
56	4874 ± 10	2.88 ± 0.04	1.26 ± 0.07	-0.03 ± 0.07	13.892 ± 0.031	54650.200475	0.964	0.85	-0.305	1.56 ± 0.18	2.1 ± 0.3	8.5 ± 0.5	1.0 ± 0.4
57	4800 ± 10	2.63 ± 0.03	1.35 ± 0.05	-0.09 ± 0.05	-44.947 ± 0.023	54545.481811	0.994	0.80	-0.335	1.83 ± 0.16	2.3 ± 0.4	11.9 ± 0.6	1.0 ± 0.4
58	4721 ± 05	2.55 ± 0.02	1.49 ± 0.05	-0.26 ± 0.04	18.823 ± 0.116	54345.140972	1.014	0.80	-0.370	1.62 ± 0.11	1.2 ± 0.2	9.7 ± 0.3	5.2 ± 2.6
59	4451 ± 23	2.55 ± 0.08	1.48 ± 0.09	-0.15 ± 0.10	-76.261 ± 0.054	53485.383883	1.181	0.06	-0.522	2.08 ± 0.66	0.9 ± 0.2	18.5 ± 3.1	5.9 - 8.4
60	4730 ± 10	2.66 ± 0.04	1.31 ± 0.05	-0.18 ± 0.07	24.346 ± 0.026	55349.397402	1.019	0.80	-0.366	1.73 ± 0.19	2.0 ± 0.3	10.9 ± 0.6	1.1 ± 1.1
61	4178 ± 10	2.06 ± 0.05	1.59 ± 0.08	-0.22 ± 0.06	-22.196 ± 0.063	53820.472292	1.354	-0.84	-0.739	2.53 ± 0.24	0.9 ± 0.3	35.2 ± 1.8	3.5 - 8.5
62	4679 ± 10	2.49 ± 0.04	1.49 ± 0.05	-0.38 ± 0.06	-52.461 ± 0.044	54650.211105	1.024	0.80	-0.390	1.58 ± 0.15	1.0 ± 0.2	9.4 ± 0.5	3.6 - 9.3
63	4393 ± 10	2.40 ± 0.05	1.38 ± 0.08	-0.06 ± 0.08	14.290 ± 0.040	53868.341227	1.226	0.67	-0.565	1.52 ± 0.20	0.9 ± 0.2	10.0 ± 0.7	6.0 - 8.4
64	5539 ± 15	4.78 ± 0.04	1.37 ± 0.12	-0.05 ± 0.06	-37.274 ± 0.273	54588.359485	0.673	5.05	-0.129	-0.15 ± 0.02	1.0 ± 0.1	0.9 ± 0.1	4.1 ± 7.0
65	4955 ± 08	3.03 ± 0.03	1.43 ± 0.07	-0.05 ± 0.05	-4.778 ± 0.045	53550.226713	0.921	0.90	-0.276	1.48 ± 0.12	2.1 ± 0.2	7.5 ± 0.3	0.9 ± 0.3
66	4973 ± 13	3.00 ± 0.04	1.37 ± 0.08	-0.11 ± 0.06	-16.177 ± 0.034	53546.219248	0.904	0.91	-0.270	1.46 ± 0.27	2.2 ± 0.4	7.2 ± 0.7	1.0 ± 0.6
67	4963 ± 10	2.52 ± 0.03	1.38 ± 0.05	-0.18 ± 0.06	33.379 ± 0.029	54769.464635	0.900	0.91	-0.274	2.12 ± 0.33	3.2 ± 0.9	15.6 ± 1.3	0.4 ± 0.6
68	4747 ± 10	2.56 ± 0.04	1.33 ± 0.06	-0.21 ± 0.06	48.768 ± 0.034	53775.183657	1.005	0.80	-0.358	1.61 ± 0.19	1.2 ± 0.3	9.5 ± 0.6	4.7 ± 1.1
69	6239 ± 25	4.29 ± 0.05	1.68 ± 0.15	0.22 ± 0.07	-8.165 ± 0.069	53432.134271	0.480	3.98	-0.032	0.52 ± 0.27	1.3 ± 0.2	1.6 ± 0.4	2.0 ± 0.2
70	4601 ± 18	2.41 ± 0.07	1.48 ± 0.10	-0.17 ± 0.09	-6.757 ± 0.025	53041.181910	1.092	0.80	-0.427	1.89 ± 0.20	2.0 ± 0.5	13.9 ± 0.8	1.3 ± 1.0
71	4719 ± 10	2.38 ± 0.03	1.53 ± 0.05	-0.18 ± 0.05	33.329 ± 0.033	54458.165012	1.025	0.80	-0.371	2.11 ± 0.25	2.8 ± 0.8	17.0 ± 1.1	0.6 ± 0.5
72	4233 ± 18	2.11 ± 0.07	1.49 ± 0.10	-0.07 ± 0.09	-4.881 ± 0.050	53749.254786	1.326	-2.50	-0.693	1.72 ± 0.24	0.8 ± 0.3	13.5 ± 1.1	3.5 - 8.5
73	4652 ± 08	2.69 ± 0.03	1.43 ± 0.08	0.02 ± 0.06	-57.421 ± 0.032	55114.373756	1.085	0.80	-0.398	1.57 ± 0.09	1.6 ± 0.2	9.4 ± 0.3	2.3 ± 0.8
74	4931 ± 13	2.92 ± 0.05	1.46 ± 0.09	-0.26 ± 0.07	20.095 ± 0.023	53799.224815	0.906	0.89	-0.286	1.41 ± 0.20	1.4 ± 0.3	7.0 ± 0.5	2.6 ± 1.8
75	4749 ± 15	2.86 ± 0.06	1.40 ± 0.10	0.03 ± 0.08	5.634 ± 0.027	53073.403895	1.034	0.80	-0.357	1.46 ± 0.14	1.7 ± 0.2	7.9 ± 0.4	1.9 ± 0.8
76	5002 ± 25	3.48 ± 0.09	0.72 ± 0.17	-0.29 ± 0.11	-25.141 ± 0.033	53071.428513	0.866	0.92	-0.262	0.79 ± 0.28	1.1 ± 0.3	3.3 ± 0.6	2.1 - 8.9
77	4750 ± 10	2.57 ± 0.04	1.45 ± 0.06	-0.49 ± 0.06	-11.987 ± 0.026	54242.203385	0.969	0.74	-0.358	1.75 ± 0.40	1.3 ± 0.1	11.1 ± 1.3	3.7 ± 0.9
78	4998 ± 13	3.21 ± 0.04	1.30 ± 0.07	-0.46 ± 0.06	-31.729 ± 0.020	53031.336701	0.846	0.63	-0.266	1.76 ± 0.67	1.3 ± 0.2	10.1 ± 2.0	4.1 ± 2.6
79	4649 ± 10	2.61 ± 0.04	1.48 ± 0.10	-0.22 ± 0.08	-9.646 ± 0.028	53093.367847	1.059	0.80	-0.399	1.40 ± 0.25	0.8 ± 0.2	7.7 ± 0.7	4.7 - 9.2
80	4401 ± 15	2.26 ± 0.07	1.38 ± 0.07	-0.72 ± 0.08	125.280 ± 0.036	53041.300677	1.160	0.68	-0.549	1.71 ± 0.22	0.7 ± 0.2	12.3 ± 0.9	6.4 - 9.3
81	4489 ± 25	2.45 ± 0.11	1.36 ± 0.10	-0.06 ± 0.13	-6.033 ± 0.035	53476.118802	1.166	-0.08	-0.498	2.13 ± 0.21	1.7 ± 0.3	19.2 ± 1.2	2.0 ± 1.2
82	4824 ± 23	3.23 ± 0.07	1.12 ± 0.08	-0.06 ± 0.10	-25.210 ± 0.029	53023.374485	0.985	0.82	-0.325	1.04 ± 0.14	1.3 ± 0.2	4.7 ± 0.4	4.3 ± 2.3
83	4763 ± 20	3.23 ± 0.08	1.23 ± 0.10	0.02 ± 0.09	20.142 ± 0.030	53034.336719	1.026	0.80	-0.351	0.95 ± 0.23	1.2 ± 0.3	4.4 ± 0.6	7.6 ± 5.5
84	4789 ± 15	2.93 ± 0.06	1.35 ± 0.09	-0.04 ± 0.08	35.433 ± 0.027	53731.429641	1.005	0.80	-0.340	1.40 ± 0.17	1.7 ± 0.3	7.3 ± 0.5	2.0 ± 0.9
85	4972 ± 10	3.49 ± 0.04	1.09 ± 0.08	-0.19 ± 0.06	-34.256 ± 0.030	55254.434566	0.894	0.91	-0.271	0.68 ± 0.20	1.0 ± 0.2	3.0 ± 0.4	4.5 - 6.1
86	4092 ± 08	1.39 ± 0.05	1.64 ± 0.04	-0.90 ± 0.06	-266.022 ± 0.077	54518.443166	1.373	-2.51	-0.804	2.64 ± 0.16	0.8 ± 0.2	41.6 ± 1.4	5.6 - 7.9
87	4598 ± 15	2.51 ± 0.05	1.46 ± 0.08	-0.11 ± 0.08	-50.900 ± 0.038	53902.306534	1.100	0.75	-0.429	1.77 ± 0.28	1.7 ± 0.1	12.1 ± 1.0	1.8 ± 0.4
88	4673 ± 15	2.76 ± 0.06	1.54 ± 0.12	-0.10 ± 0.10	-19.340 ± 0.040	53542.289497	1.060	-0.35	-0.386	2.19 ± 0.71	1.6 ± 0.3	19.0 ± 3.2	2.5 ± 1.6
89	4785 ± 13	2.55 ± 0.05	1.48 ± 0.09	-0.34 ± 0.08	40.319 ± 0.041	53193.230828	0.970	0.80	-0.342	1.75 ± 0.18	1.5 ± 0.3	10.9 ± 0.6	2.4 ± 1.8
90	4594 ± 23	3.00 ± 0.09	1.36 ± 0.11	0.01 ± 0.11	-52.444 ± 0.045	53202.384439	1.115	0.79	-0.432	1.01 ± 0.31	0.9 ± 0.3	5.1 ± 0.8	3.4 - 8.3
91	4755 ± 10	2.53 ± 0.03	1.39 ± 0.05	-0.27 ± 0.06	-1.403 ± 0.024	53918.271227	0.994	0.80	-0.355	1.68 ± 0.19	1.3 ± 0.3	10.2 ± 0.6	3.6 ± 1.1
92	4925 ± 08	2.92 ± 0.03	1.39 ± 0.09	-0.10 ± 0.06	-32.196 ± 0.033	53206.211626	0.930	0.88	-0.287	1.57 ± 0.17	2.2 ± 0.3	8.4 ± 0.5	0.9 ± 0.4
93	4866 ± 15	2.70 ± 0.06	1.51 ± 0.10	-0.29 ± 0.09	41.527 ± 0.039	53513.363061	0.935	0.84	-0.310	1.61 ± 0.13	1.5 ± 0.2	9.0 ± 0.4	2.0 ± 0.9
94	5196 ± 05	2.89 ± 0.02	1.76 ± 0.06	0.03 ± 0.05	-5.223 ± 0.049	53907.287755	0.820	1.04	-0.203	1.60 ± 0.19	2.5 ± 0.3	7.8 ± 0.5	0.6 ± 0.6
95	4691 ± 15	2.75 ± 0.06	1.46 ± 0.09	-0.10 ± 0.09	-22.413 ± 0.036	53538.304282	1.050	0.80	-0.385	1.53 ± 0.19	1.6 ± 0.3	8.8 ± 0.6	2.2 ± 1.1

Table 5. continued.

No.	T_{eff} [K]	$\log g$ [cm s ⁻²]	v_t [km s ⁻¹]	[Fe/H]	RV [km s ⁻¹]	MJD +2400000 [d]	(B-V) ₀ [mag]	M_V [mag]	BC_V [mag]	$\log L/L_{\odot}$	M [M_{\odot}]	R [R_{\odot}]	Age [Gyr]
96	4758 ± 13	3.04 ± 0.05	1.63 ± 0.10	-0.17 ± 0.07	-94.844 ± 0.054	53927.234230	1.005	0.80	-0.354	1.18 ± 0.22	1.4 ± 0.3	5.7 ± 0.6	4.3 ± 3.5
97	4907 ± 10	2.80 ± 0.04	1.48 ± 0.07	-0.25 ± 0.07	10.585 ± 0.033	54581.426817	0.919	0.87	-0.294	1.54 ± 0.21	1.6 ± 0.3	8.2 ± 0.6	2.1 ± 1.7
98	4650 ± 13	2.50 ± 0.05	1.49 ± 0.10	-0.15 ± 0.08	5.231 ± 0.034	53543.277917	1.067	0.80	-0.399	1.83 ± 0.15	2.0 ± 0.3	12.7 ± 0.6	1.3 ± 0.7
99	5133 ± 10	3.12 ± 0.03	1.35 ± 0.06	-0.08 ± 0.05	-16.819 ± 0.034	54608.359595	0.835	0.99	-0.221	1.44 ± 0.27	2.3 ± 0.4	6.6 ± 0.6	0.8 ± 0.5
100	4588 ± 10	2.74 ± 0.04	1.39 ± 0.09	0.10 ± 0.07	-1.743 ± 0.032	54578.453507	1.130	0.79	-0.437	1.49 ± 0.11	1.6 ± 0.2	8.8 ± 0.4	2.3 ± 0.7
101	4719 ± 10	2.62 ± 0.04	1.28 ± 0.08	-0.43 ± 0.07	36.025 ± 0.033	53687.118218	0.994	0.80	-0.372	1.49 ± 0.17	1.1 ± 0.2	8.3 ± 0.5	4.6 - 6.3
102	4641 ± 15	2.75 ± 0.06	1.42 ± 0.09	0.06 ± 0.08	-21.598 ± 0.033	53747.149942	1.096	1.23	-0.405	1.57 ± 0.29	1.4 ± 0.2	9.4 ± 0.9	3.4 ± 1.5
103	4133 ± 18	2.24 ± 0.07	1.55 ± 0.12	-0.13 ± 0.08	-18.753 ± 0.064	54044.337292	1.393	0.52	-0.786	1.88 ± 0.15	0.8 ± 0.2	17.0 ± 0.8	6.0 - 8.5
104	4577 ± 10	2.37 ± 0.04	1.40 ± 0.05	-0.06 ± 0.06	-5.778 ± 0.032	54424.300550	1.117	0.79	-0.442	1.97 ± 0.12	2.1 ± 0.3	15.4 ± 0.5	1.1 ± 0.4
105	5084 ± 10	3.29 ± 0.03	1.15 ± 0.07	-0.40 ± 0.06	36.346 ± 0.027	54785.317894	0.819	0.96	-0.239	1.07 ± 0.09	1.4 ± 0.1	4.4 ± 0.2	2.7 ± 0.7
106	4723 ± 08	2.95 ± 0.04	1.17 ± 0.04	-0.14 ± 0.05	46.803 ± 0.024	54757.383461	1.027	0.80	-0.369	1.27 ± 0.27	1.4 ± 0.4	6.5 ± 0.7	4.1 ± 3.4
107	4658 ± 05	2.66 ± 0.03	1.30 ± 0.04	-0.11 ± 0.04	-16.512 ± 0.035	54678.409491	1.067	0.80	-0.394	1.59 ± 0.19	1.6 ± 0.3	9.6 ± 0.6	2.2 ± 1.1
108	4899 ± 10	2.82 ± 0.04	1.38 ± 0.06	-0.09 ± 0.06	26.750 ± 0.073	54045.338750	0.944	0.86	-0.296	1.65 ± 0.08	2.2 ± 0.2	9.3 ± 0.3	1.0 ± 0.4
109	4261 ± 13	2.20 ± 0.06	1.36 ± 0.09	-0.31 ± 0.08	-49.937 ± 0.128	54046.331736	1.288	0.61	-0.662	1.64 ± 0.20	0.8 ± 0.3	12.1 ± 0.8	6.0 - 8.4
110	4822 ± 10	2.81 ± 0.04	1.38 ± 0.08	-0.02 ± 0.06	9.961 ± 0.023	54040.342679	0.991	0.82	-0.326	1.60 ± 0.19	2.0 ± 0.3	9.1 ± 0.6	1.1 ± 1.1
111	5054 ± 08	3.57 ± 0.03	1.07 ± 0.07	-0.04 ± 0.05	20.790 ± 0.020	54758.391418	0.875	0.95	-0.244	0.87 ± 0.27	1.5 ± 0.3	3.6 ± 0.6	2.7 ± 2.2
112	4296 ± 10	1.99 ± 0.05	1.66 ± 0.05	-0.46 ± 0.05	5.556 ± 0.039	53629.480822	1.253	-2.50	-0.630	1.96 ± 0.18	0.8 ± 0.2	17.3 ± 0.9	6.4 - 9.3
113	4391 ± 10	2.16 ± 0.04	1.57 ± 0.08	-0.26 ± 0.07	6.697 ± 0.042	54346.308657	1.209	-2.50	-0.562	1.77 ± 0.32	0.8 ± 0.4	13.3 ± 1.3	2.2 - 9.3
114	4541 ± 13	2.89 ± 0.05	1.19 ± 0.08	0.22 ± 0.06	37.959 ± 0.041	54579.224902	1.170	0.76	-0.468	1.16 ± 0.09	1.1 ± 0.1	6.2 ± 0.3	6.2 - 8.7
115	4806 ± 15	2.85 ± 0.06	1.47 ± 0.09	-0.20 ± 0.08	37.368 ± 0.027	53034.273131	0.977	0.81	-0.333	1.29 ± 0.11	1.1 ± 0.1	6.4 ± 0.3	4.6 - 6.3
116	4137 ± 10	1.51 ± 0.05	1.48 ± 0.06	-1.00 ± 0.07	143.415 ± 0.099	53752.504774	1.330	-2.50	-0.756	2.58 ± 0.15	0.8 ± 0.2	38.0 ± 1.3	4.1 - 7.9
117	4263 ± 20	2.15 ± 0.09	1.46 ± 0.09	-0.14 ± 0.09	-2.437 ± 0.049	53457.307558	1.301	-2.50	-0.665	1.75 ± 0.20	0.9 ± 0.3	13.8 ± 0.9	3.5 - 8.4
118	4267 ± 23	2.26 ± 0.09	1.51 ± 0.11	-0.11 ± 0.09	23.252 ± 0.050	53449.331615	1.301	0.61	-0.662	1.60 ± 0.22	0.8 ± 0.3	11.6 ± 0.9	6.0 - 8.4
119	4327 ± 08	2.24 ± 0.04	1.34 ± 0.09	-0.17 ± 0.07	8.978 ± 0.057	53041.233999	1.258	0.64	-0.612	1.65 ± 0.21	0.9 ± 0.3	11.9 ± 0.8	3.5 - 8.4
120	4363 ± 10	2.60 ± 0.04	1.17 ± 0.08	0.00 ± 0.06	31.498 ± 0.042	54785.474780	1.250	0.66	-0.588	1.39 ± 0.30	0.8 ± 0.4	8.7 ± 1.0	3.5 - 8.4
121	4365 ± 20	2.57 ± 0.08	1.34 ± 0.11	0.05 ± 0.09	49.467 ± 0.141	54046.488356	1.255	0.66	-0.588	1.40 ± 0.31	0.8 ± 0.4	8.8 ± 1.1	3.5 - 8.4
122	4816 ± 05	2.48 ± 0.03	1.34 ± 0.06	-0.58 ± 0.05	42.873 ± 0.028	54786.474051	0.924	0.82	-0.331	1.69 ± 0.19	1.1 ± 0.2	10.1 ± 0.6	2.4 - 7.8
123	4618 ± 18	2.66 ± 0.07	1.35 ± 0.08	-0.22 ± 0.09	42.361 ± 0.029	53037.462593	1.077	0.80	-0.417	1.25 ± 0.42	0.7 ± 0.4	6.6 ± 1.2	2.8 - 9.3
124	4821 ± 10	2.75 ± 0.04	1.45 ± 0.09	-0.15 ± 0.07	-1.759 ± 0.023	53043.248727	0.976	-0.04	-0.327	2.05 ± 0.24	2.1 ± 0.5	15.2 ± 1.0	1.0 ± 0.8
125	4074 ± 38	2.30 ± 0.15	1.88 ± 0.17	-0.22 ± 0.13	-11.271 ± 0.075	53037.249311	1.429	-0.20	-0.846	2.32 ± 0.39	0.9 ± 0.2	29.1 ± 3.0	6.0 - 8.5
126	4535 ± 15	2.88 ± 0.06	1.35 ± 0.09	-0.10 ± 0.07	14.779 ± 0.037	53024.291377	1.136	0.76	-0.468	1.06 ± 0.37	0.8 ± 0.4	5.5 ± 1.0	2.8 - 8.4
127	4427 ± 15	2.09 ± 0.07	1.70 ± 0.09	-0.26 ± 0.09	9.932 ± 0.038	53031.467911	1.186	-2.50	-0.537	1.86 ± 0.21	0.9 ± 0.2	14.5 ± 0.9	3.6 - 9.3
128	4978 ± 05	2.96 ± 0.03	1.37 ± 0.05	0.03 ± 0.05	1.863 ± 0.026	54517.400122	0.920	0.91	-0.268	1.51 ± 0.28	2.2 ± 0.4	7.7 ± 0.7	0.9 ± 0.5
129	4311 ± 18	2.31 ± 0.08	1.56 ± 0.10	-0.08 ± 0.09	16.613 ± 0.052	53031.486644	1.275	-0.68	-0.627	2.42 ± 0.44	0.9 ± 0.2	29.1 ± 2.9	6.0 - 8.4
130	5145 ± 18	2.54 ± 0.05	1.70 ± 0.13	-0.83 ± 0.08	32.290 ± 0.048	53161.339294	0.747	0.99	-0.230	2.06 ± 0.01	2.4 ± 0.2	13.5 ± 0.1	0.6 ± 0.3
131	4614 ± 15	2.51 ± 0.06	1.36 ± 0.07	-0.36 ± 0.08	-13.981 ± 0.026	53399.503681	1.063	0.80	-0.419	1.45 ± 0.24	0.8 ± 0.2	8.3 ± 0.7	4.7 - 9.3
132	4321 ± 15	2.57 ± 0.05	1.49 ± 0.08	0.05 ± 0.06	-34.790 ± 0.061	53768.496354	1.282	-0.23	-0.622	2.24 ± 0.33	0.8 ± 0.2	23.6 ± 1.9	6.0 - 8.4
133	4544 ± 18	2.81 ± 0.07	1.58 ± 0.11	0.27 ± 0.08	26.699 ± 0.048	53899.315550	1.175	1.12	-0.467	1.64 ± 0.37	1.5 ± 0.2	10.7 ± 1.3	3.4 ± 1.7
134	4818 ± 10	2.52 ± 0.04	1.48 ± 0.07	-0.43 ± 0.06	-51.971 ± 0.036	53543.300608	0.942	0.82	-0.329	1.84 ± 0.06	1.7 ± 0.2	12.0 ± 0.2	1.4 ± 0.3
135	4989 ± 10	3.37 ± 0.04	1.12 ± 0.07	-0.22 ± 0.06	12.857 ± 0.020	54588.228021	0.882	0.92	-0.266	0.88 ± 0.22	1.1 ± 0.2	3.7 ± 0.5	2.7 - 9.0
136	5061 ± 23	4.10 ± 0.06	1.21 ± 0.19	0.19 ± 0.07	-43.320 ± 0.051	54309.204375	0.907	5.98	-0.240	0.07 ± 0.38	0.9 ± 0.3	1.4 ± 3.8	3.3 - 8.1
137	4164 ± 05	1.68 ± 0.03	1.50 ± 0.05	-0.46 ± 0.05	-7.149 ± 0.051	55261.393229	1.347	-2.50	-0.744	2.22 ± 0.16	0.8 ± 0.2	24.8 ± 1.0	6.4 - 9.3
138	4922 ± 13	3.65 ± 0.05	1.14 ± 0.09	0.17 ± 0.06	6.921 ± 0.029	53768.486412	0.968	2.11	-0.287	1.17 ± 0.14	1.5 ± 0.3	5.3 ± 0.3	2.9 ± 1.6
139	4796 ± 13	2.80 ± 0.05	1.50 ± 0.09	-0.28 ± 0.07	38.046 ± 0.029	53416.444028	0.972	0.07	-0.338	2.01 ± 0.75	1.1 ± 0.2	14.7 ± 2.8	7.1 ± 4.2
140	4695 ± 13	3.17 ± 0.05	1.11 ± 0.11	0.11 ± 0.08	10.999 ± 0.024	53754.134688	1.073	2.27	-0.383	1.14 ± 0.36	1.3 ± 0.2	5.6 ± 0.9	4.3 ± 2.4
141	4220 ± 13	1.65 ± 0.05	1.55 ± 0.05	-0.55 ± 0.06	-34.611 ± 0.036	54774.333958	1.299	0.66	-0.691	1.91 ± 0.39	0.9 ± 0.2	16.9 ± 1.8	3.6 - 9.3
142	4522 ± 10	2.53 ± 0.04	1.50 ± 0.07	-0.11 ± 0.06	-31.227 ± 0.039	53682.109884	1.142	0.13	-0.476	2.04 ± 0.39	1.2 ± 0.2	17.1 ± 1.7	6.7 ± 3.5
143	4751 ± 05	2.78 ± 0.03	1.19 ± 0.05	-0.29 ± 0.05	7.728 ± 0.024	54458.224132	0.993	0.80	-0.357	1.26 ± 0.18	0.9 ± 0.2	6.3 ± 0.5	4.6 - 9.2

Table 5. continued.

No.	T_{eff} [K]	$\log g$ [cm s ⁻²]	v_t [km s ⁻¹]	[Fe/H]	RV [km s ⁻¹]	MJD +2400000 [d]	(B-V) ₀ [mag]	M_V [mag]	BC_V [mag]	$\log L/L_\odot$	M [M_\odot]	R [R_\odot]	Age [Gyr]
144	4203 ± 15	1.90 ± 0.07	1.64 ± 0.09	-0.41 ± 0.07	11.901 ± 0.048	53632.486806	1.322	-2.50	-0.710	2.09 ± 0.17	0.8 ± 0.2	21.0 ± 1.0	6.4 - 9.3
145	4754 ± 18	3.05 ± 0.06	1.60 ± 0.09	-0.12 ± 0.08	66.882 ± 0.082	53743.175799	1.013	0.68	-0.355	1.77 ± 0.12	1.7 ± 0.3	11.3 ± 0.5	2.3 ± 1.6
146	4717 ± 10	2.72 ± 0.04	1.34 ± 0.06	0.02 ± 0.06	-14.624 ± 0.028	55129.385538	1.050	0.80	-0.372	1.63 ± 0.21	1.8 ± 0.4	9.8 ± 0.7	1.5 ± 1.2
147	4987 ± 05	2.65 ± 0.03	1.46 ± 0.05	-0.16 ± 0.05	10.761 ± 0.029	53990.489392	0.891	0.52	-0.266	1.80 ± 0.41	3.2 ± 0.5	10.7 ± 1.2	0.4 ± 0.2
148	4604 ± 10	2.46 ± 0.04	1.42 ± 0.06	-0.06 ± 0.06	1.349 ± 0.028	54780.322106	1.102	0.80	-0.426	1.88 ± 0.19	2.0 ± 0.3	13.7 ± 0.8	1.2 ± 1.1
149	5109 ± 08	2.71 ± 0.03	1.46 ± 0.04	-0.16 ± 0.05	-37.126 ± 0.037	53631.484572	0.837	0.98	-0.229	2.09 ± 0.21	3.3 ± 0.4	14.2 ± 0.8	0.3 ± 0.1
150	4307 ± 15	2.36 ± 0.07	1.46 ± 0.09	-0.15 ± 0.08	-21.798 ± 0.046	53746.165787	1.272	0.63	-0.628	1.48 ± 0.29	0.7 ± 0.4	9.9 ± 1.0	4.5 - 8.4
151	4853 ± 08	3.40 ± 0.03	1.11 ± 0.08	0.18 ± 0.05	9.318 ± 0.025	54786.298113	1.003	0.84	-0.313	0.90 ± 0.26	1.5 ± 0.3	4.0 ± 0.6	2.8 ± 2.5
152	4585 ± 10	2.45 ± 0.04	1.33 ± 0.08	-0.76 ± 0.07	-51.044 ± 0.029	53747.177488	1.037	2.34	-0.436	1.14 ± 0.28	0.8 ± 0.2	5.9 ± 0.8	4.1 - 7.9
153	4807 ± 10	2.85 ± 0.04	1.42 ± 0.07	-0.40 ± 0.05	-6.293 ± 0.023	54368.234549	0.951	0.81	-0.334	1.31 ± 0.23	1.1 ± 0.3	6.5 ± 0.6	2.2 - 6.3
154	4833 ± 10	2.85 ± 0.04	1.43 ± 0.06	0.05 ± 0.06	-7.491 ± 0.023	53745.174329	0.995	0.82	-0.321	1.54 ± 0.09	2.0 ± 0.2	8.4 ± 0.3	1.1 ± 0.2
155	4770 ± 10	3.29 ± 0.04	1.13 ± 0.08	0.04 ± 0.06	7.341 ± 0.024	53749.303194	1.025	0.80	-0.348	0.87 ± 0.24	1.1 ± 0.2	4.0 ± 0.6	2.7 - 8.2
156	4807 ± 30	3.82 ± 0.09	1.71 ± 0.18	0.34 ± 0.10	-15.627 ± 0.051	53024.519155	1.046	-0.83	-0.332	2.36 ± 0.46	1.2 ± 0.1	21.9 ± 2.4	6.2 ± 2.0
157	4901 ± 08	2.54 ± 0.04	1.54 ± 0.08	-0.52 ± 0.06	-25.798 ± 0.028	53449.139687	0.888	0.86	-0.299	1.90 ± 0.23	2.1 ± 0.5	12.4 ± 0.8	1.0 ± 0.6
158	4725 ± 10	2.76 ± 0.04	1.39 ± 0.11	-0.45 ± 0.08	-36.782 ± 0.028	53480.296829	0.988	0.54	-0.369	1.83 ± 0.42	0.9 ± 0.2	12.3 ± 1.5	6.3 - 9.2
159	5277 ± 13	4.01 ± 0.04	1.28 ± 0.16	-0.45 ± 0.07	-34.031 ± 0.029	53449.158582	0.737	5.55	-0.191	0.25 ± 0.33	0.8 ± 0.2	1.6 ± 1.1	4.3 - 8.7
160	4369 ± 23	2.91 ± 0.09	1.24 ± 0.13	0.29 ± 0.09	29.732 ± 0.063	53037.285336	1.282	0.66	-0.591	0.99 ± 0.26	0.8 ± 0.2	5.5 ± 0.8	6.4 - 8.8
161	4942 ± 15	3.25 ± 0.05	1.27 ± 0.08	-0.23 ± 0.07	-2.924 ± 0.030	53430.426157	0.904	0.89	-0.282	0.92 ± 0.23	1.0 ± 0.2	3.9 ± 0.5	2.7 - 6.2
162	4152 ± 23	2.06 ± 0.09	1.66 ± 0.11	-0.24 ± 0.10	-37.175 ± 0.071	53025.533461	1.372	-1.64	-0.763	2.86 ± 0.47	0.9 ± 0.2	52.1 ± 4.9	4.5 - 8.5
163	4720 ± 13	2.98 ± 0.06	1.27 ± 0.11	-0.10 ± 0.08	-12.958 ± 0.027	53719.408999	1.034	0.80	-0.371	1.20 ± 0.16	1.3 ± 0.2	6.0 ± 0.4	4.6 ± 2.3
164	4346 ± 08	1.90 ± 0.04	1.48 ± 0.06	-0.30 ± 0.05	-15.466 ± 0.038	54560.109948	1.234	-2.50	-0.595	2.01 ± 0.16	0.9 ± 0.2	17.9 ± 0.8	4.7 - 9.3
165	4796 ± 15	3.30 ± 0.05	1.16 ± 0.09	-0.05 ± 0.08	-2.422 ± 0.025	53893.162031	1.001	3.22	-0.337	0.75 ± 0.21	1.1 ± 0.2	3.4 ± 0.5	7.4 ± 3.5
166	4201 ± 25	2.09 ± 0.10	1.36 ± 0.11	-0.15 ± 0.12	41.307 ± 0.057	53034.302222	1.343	-2.50	-0.719	1.70 ± 0.22	0.8 ± 0.3	13.4 ± 1.0	6.0 - 8.5
167	4627 ± 18	2.56 ± 0.07	1.47 ± 0.08	0.00 ± 0.09	13.124 ± 0.034	53038.261910	1.096	0.01	-0.412	2.06 ± 0.19	1.9 ± 0.2	16.7 ± 0.9	1.3 ± 0.3
168	4851 ± 18	3.51 ± 0.05	1.08 ± 0.10	0.07 ± 0.08	20.326 ± 0.024	53749.318310	0.989	0.84	-0.314	0.72 ± 0.14	1.2 ± 0.2	3.2 ± 0.3	6.8 ± 3.4
169	4596 ± 13	2.65 ± 0.05	1.29 ± 0.08	-0.37 ± 0.07	-38.160 ± 0.027	53094.191227	1.073	0.79	-0.429	1.19 ± 0.37	0.6 ± 0.3	6.2 ± 1.0	6.4 - 9.3
170	4478 ± 20	2.88 ± 0.09	1.28 ± 0.12	0.13 ± 0.10	26.091 ± 0.037	53031.359421	1.195	0.72	-0.508	1.10 ± 0.21	0.9 ± 0.2	5.9 ± 0.6	6.2 - 8.7
171	4648 ± 15	2.66 ± 0.06	1.47 ± 0.09	-0.02 ± 0.08	20.144 ± 0.028	53094.394994	1.083	2.12	-0.400	1.21 ± 0.28	1.6 ± 0.3	6.2 ± 0.8	2.6 ± 1.6
172	4856 ± 15	2.39 ± 0.06	1.47 ± 0.08	-0.50 ± 0.08	-16.139 ± 0.022	53041.335417	0.913	0.10	-0.315	1.99 ± 0.62	1.9 ± 0.3	14.0 ± 2.3	1.4 ± 1.1
173	5096 ± 13	3.65 ± 0.05	1.22 ± 0.12	0.22 ± 0.08	2.006 ± 0.027	53511.266030	0.896	3.09	-0.229	0.76 ± 0.15	1.6 ± 0.2	3.1 ± 0.3	2.4 ± 1.0
174	4709 ± 18	3.28 ± 0.07	1.20 ± 0.10	0.14 ± 0.09	-1.992 ± 0.031	53030.369433	1.070	1.89	-0.376	1.30 ± 0.15	1.4 ± 0.3	6.7 ± 0.4	4.2 ± 3.6
175	4576 ± 18	2.69 ± 0.06	1.48 ± 0.09	-0.14 ± 0.09	-14.555 ± 0.032	53034.360116	1.109	1.54	-0.442	1.46 ± 0.37	1.2 ± 0.2	8.6 ± 1.2	6.8 ± 3.5
176	4464 ± 08	2.49 ± 0.04	1.39 ± 0.07	0.14 ± 0.05	-12.715 ± 0.032	54570.141360	1.205	3.47	-0.518	0.72 ± 0.30	1.6 ± 0.2	3.8 ± 0.8	3.0 ± 1.7
177	4808 ± 10	2.73 ± 0.03	1.43 ± 0.07	-0.19 ± 0.06	-38.236 ± 0.031	54606.277772	0.977	0.81	-0.332	1.53 ± 0.19	1.3 ± 0.3	8.4 ± 0.6	3.5 ± 1.1
178	4673 ± 05	2.45 ± 0.02	1.43 ± 0.05	-0.14 ± 0.05	-52.130 ± 0.032	54608.292847	1.055	0.80	-0.386	1.97 ± 0.07	2.2 ± 0.3	14.8 ± 0.3	1.1 ± 0.4
179	4788 ± 15	2.49 ± 0.06	1.40 ± 0.09	-0.63 ± 0.09	47.293 ± 0.034	53202.369178	0.932	0.80	-0.343	1.58 ± 0.19	0.9 ± 0.2	9.0 ± 0.6	4.0 - 7.8
180	4607 ± 10	2.66 ± 0.04	1.38 ± 0.09	0.08 ± 0.06	-44.205 ± 0.060	54607.289375	1.117	0.80	-0.425	1.52 ± 0.19	1.4 ± 0.3	9.0 ± 0.6	3.4 ± 1.1
181	4785 ± 13	3.08 ± 0.04	1.36 ± 0.09	-0.18 ± 0.07	-35.687 ± 0.039	53544.425469	0.990	0.80	-0.342	1.16 ± 0.08	1.4 ± 0.1	5.5 ± 0.2	3.4 ± 0.9
182	4515 ± 08	1.93 ± 0.04	1.39 ± 0.06	-0.51 ± 0.06	19.892 ± 0.027	54599.288947	1.105	-2.50	-0.477	2.31 ± 0.18	1.8 ± 0.4	23.4 ± 1.0	1.4 ± 1.0
183	4377 ± 10	2.09 ± 0.04	1.52 ± 0.08	-0.15 ± 0.06	-49.615 ± 0.049	54573.387905	1.228	-2.50	-0.574	2.13 ± 0.14	1.8 ± 0.3	20.2 ± 0.8	1.9 ± 1.6
184	4897 ± 10	2.74 ± 0.04	1.35 ± 0.05	-0.03 ± 0.06	-19.361 ± 0.026	54573.365052	0.953	0.86	-0.297	1.75 ± 0.19	2.2 ± 0.3	10.4 ± 0.6	1.1 ± 1.1
185	4619 ± 13	3.02 ± 0.06	1.49 ± 0.09	-0.38 ± 0.09	-57.467 ± 0.050	53549.407760	1.058	0.80	-0.416	1.19 ± 0.41	0.8 ± 0.4	6.2 ± 1.1	2.7 - 9.2
186	4754 ± 10	2.43 ± 0.05	1.34 ± 0.05	-0.25 ± 0.07	-3.914 ± 0.026	53989.217778	0.997	0.80	-0.355	1.87 ± 0.19	1.6 ± 0.3	12.7 ± 0.7	1.8 ± 1.1
187	4860 ± 08	2.50 ± 0.03	1.62 ± 0.06	-0.15 ± 0.05	-3.478 ± 0.026	54640.176227	0.956	0.84	-0.311	2.08 ± 0.28	3.0 ± 0.8	15.5 ± 1.1	0.5 ± 0.5
188	4703 ± 08	2.99 ± 0.03	1.36 ± 0.08	-0.19 ± 0.05	-20.718 ± 0.041	54626.231898	1.033	0.80	-0.379	1.01 ± 0.46	0.7 ± 0.4	4.8 ± 1.1	2.7 - 9.2
189	4819 ± 10	3.20 ± 0.03	1.21 ± 0.06	0.03 ± 0.06	-16.428 ± 0.028	54608.276354	0.999	0.82	-0.327	1.05 ± 0.19	1.4 ± 0.2	4.8 ± 0.5	4.1 ± 3.6
190	4782 ± 10	2.74 ± 0.04	1.23 ± 0.05	-0.41 ± 0.05	-8.128 ± 0.022	55277.438808	0.962	0.80	-0.344	1.41 ± 0.19	1.1 ± 0.3	7.4 ± 0.5	6.3 ± 1.1
191	4738 ± 13	2.65 ± 0.04	1.29 ± 0.08	-0.38 ± 0.07	-1.454 ± 0.029	53485.366823	0.989	0.80	-0.363	1.48 ± 0.17	1.1 ± 0.2	8.2 ± 0.5	2.7 - 6.3

Table 5. continued.

No.	T_{eff} [K]	$\log g$ [cm s ⁻²]	v_t [km s ⁻¹]	[Fe/H]	RV [km s ⁻¹]	MJD +2400000 [d]	(B-V) ₀ [mag]	M_V [mag]	BC_V [mag]	$\log L/L_{\odot}$	M [M_{\odot}]	R [R_{\odot}]	Age [Gyr]
192	4967 ± 13	2.75 ± 0.05	1.41 ± 0.07	-0.12 ± 0.08	14.873 ± 0.028	53906.434902	0.906	0.91	-0.272	1.84 ± 0.30	2.7 ± 0.6	11.3 ± 1.0	0.6 ± 0.5
193	4460 ± 15	2.64 ± 0.05	1.35 ± 0.08	0.21 ± 0.06	28.227 ± 0.041	55132.075984	1.216	0.71	-0.522	1.42 ± 0.06	1.2 ± 0.1	8.6 ± 0.2	6.4 ± 2.4
194	5047 ± 10	3.63 ± 0.03	0.95 ± 0.09	-0.08 ± 0.06	-6.542 ± 0.022	55277.450741	0.874	0.95	-0.246	0.78 ± 0.18	1.4 ± 0.2	3.2 ± 0.4	3.1 ± 1.5
195	5005 ± 10	2.65 ± 0.04	1.45 ± 0.08	-0.17 ± 0.07	8.296 ± 0.029	53609.436424	0.881	0.92	-0.260	1.99 ± 0.37	3.0 ± 0.8	13.2 ± 1.3	0.4 ± 0.4
196	4459 ± 10	2.47 ± 0.05	1.41 ± 0.08	-0.03 ± 0.08	-8.064 ± 0.038	54049.222176	1.188	0.71	-0.519	1.53 ± 0.20	1.0 ± 0.2	9.8 ± 0.7	3.5 - 8.4
197	4797 ± 08	2.78 ± 0.03	1.35 ± 0.06	-0.03 ± 0.05	-15.896 ± 0.029	53954.465949	1.003	0.80	-0.336	1.60 ± 0.14	2.0 ± 0.3	9.2 ± 0.4	1.2 ± 0.4
198	4556 ± 10	2.55 ± 0.04	1.36 ± 0.06	-0.03 ± 0.06	-27.666 ± 0.031	53985.171875	1.132	1.16	-0.455	1.62 ± 0.15	1.4 ± 0.2	10.4 ± 0.5	3.6 ± 2.4
199	4908 ± 10	2.62 ± 0.03	1.49 ± 0.09	-0.33 ± 0.06	-8.811 ± 0.045	53574.306279	0.909	0.87	-0.295	1.83 ± 0.07	2.0 ± 0.1	11.4 ± 0.3	0.9 ± 0.2
200	4751 ± 15	2.86 ± 0.06	1.55 ± 0.11	-0.03 ± 0.09	-23.126 ± 0.034	53575.263796	1.026	0.80	-0.357	1.48 ± 0.09	1.7 ± 0.2	8.1 ± 0.3	1.9 ± 0.6
201	4812 ± 10	2.95 ± 0.03	1.25 ± 0.04	-0.11 ± 0.05	-34.049 ± 0.037	54764.255428	0.985	0.81	-0.330	1.43 ± 0.21	1.7 ± 0.3	7.5 ± 0.6	1.8 ± 1.7
202	4716 ± 10	3.03 ± 0.04	1.20 ± 0.08	0.07 ± 0.06	-17.562 ± 0.062	54046.227008	1.057	0.80	-0.373	1.14 ± 0.18	1.2 ± 0.2	5.6 ± 0.5	5.6 ± 3.5
203	4320 ± 08	2.26 ± 0.04	1.57 ± 0.06	-0.02 ± 0.05	-8.676 ± 0.046	53895.412286	1.275	0.63	-0.621	1.58 ± 0.20	0.8 ± 0.2	11.0 ± 0.7	6.0 - 8.4
204	4867 ± 05	2.97 ± 0.03	1.35 ± 0.06	-0.05 ± 0.05	-15.275 ± 0.036	53570.306389	0.965	0.84	-0.308	1.48 ± 0.19	2.0 ± 0.3	7.7 ± 0.5	1.1 ± 1.1
205	4261 ± 13	1.76 ± 0.05	1.54 ± 0.07	-0.28 ± 0.07	-11.527 ± 0.041	53898.399618	1.291	-0.41	-0.663	2.33 ± 0.08	1.1 ± 0.1	26.9 ± 0.6	8.0 ± 2.1
206	4836 ± 13	2.66 ± 0.05	1.51 ± 0.10	-0.08 ± 0.08	-8.528 ± 0.035	53542.387442	0.977	0.82	-0.321	1.83 ± 0.35	2.3 ± 0.6	11.7 ± 1.2	1.0 ± 0.8
207	4301 ± 10	2.18 ± 0.04	1.49 ± 0.06	-0.19 ± 0.06	-2.923 ± 0.047	53893.432153	1.272	1.39	-0.632	1.59 ± 0.20	0.9 ± 0.2	11.3 ± 0.8	6.0 - 8.4
208	4639 ± 15	2.36 ± 0.07	1.61 ± 0.09	-0.17 ± 0.09	-17.175 ± 0.036	53544.374659	1.071	0.80	-0.405	2.04 ± 0.07	2.2 ± 0.2	16.2 ± 0.4	1.1 ± 0.4
209	5007 ± 10	3.08 ± 0.03	1.51 ± 0.09	0.17 ± 0.06	-14.890 ± 0.031	53723.261835	0.927	0.93	-0.257	1.43 ± 0.27	2.3 ± 0.4	6.9 ± 0.7	0.8 ± 0.4
210	4982 ± 15	3.00 ± 0.05	1.48 ± 0.07	-0.09 ± 0.08	-5.547 ± 0.023	53026.191806	0.902	0.91	-0.267	1.46 ± 0.27	2.1 ± 0.4	7.2 ± 0.7	1.0 ± 0.6
211	4370 ± 15	2.17 ± 0.06	1.55 ± 0.08	-0.12 ± 0.08	-8.099 ± 0.043	53996.300515	1.235	-2.50	-0.580	1.94 ± 0.17	1.4 ± 0.3	16.3 ± 0.8	5.0 ± 3.8
212	4769 ± 15	2.74 ± 0.06	1.45 ± 0.07	-0.05 ± 0.08	-26.284 ± 0.048	53310.395087	1.014	0.80	-0.349	1.65 ± 0.19	2.0 ± 0.3	9.8 ± 0.6	1.2 ± 1.1
213	4963 ± 13	2.68 ± 0.05	1.53 ± 0.08	-0.30 ± 0.08	22.897 ± 0.031	54032.231534	0.885	0.91	-0.275	1.78 ± 0.10	2.0 ± 0.2	10.5 ± 0.4	0.9 ± 0.2
214	4534 ± 08	2.48 ± 0.04	1.58 ± 0.08	-0.13 ± 0.06	-46.321 ± 0.038	53747.205093	1.133	0.75	-0.468	1.69 ± 0.20	1.5 ± 0.3	11.4 ± 0.7	3.7 ± 3.5
215	4587 ± 08	2.56 ± 0.03	1.41 ± 0.06	0.03 ± 0.06	5.486 ± 0.028	54153.094688	1.122	0.79	-0.437	1.69 ± 0.04	1.6 ± 0.1	11.1 ± 0.2	2.3 ± 0.5
216	4218 ± 15	2.09 ± 0.06	1.40 ± 0.06	-0.02 ± 0.07	0.847 ± 0.047	54425.124601	1.341	-2.50	-0.708	1.67 ± 0.22	0.7 ± 0.3	12.8 ± 0.9	6.0 - 8.5
217	4414 ± 15	2.24 ± 0.06	1.41 ± 0.08	-0.20 ± 0.07	-6.306 ± 0.039	53604.374248	1.200	0.68	-0.547	1.69 ± 0.33	0.7 ± 0.4	12.0 ± 1.3	2.8 - 9.3
218	4249 ± 28	2.27 ± 0.11	1.45 ± 0.10	0.09 ± 0.11	-23.567 ± 0.052	53031.169253	1.332	0.60	-0.684	1.67 ± 0.19	0.8 ± 0.2	12.6 ± 0.9	6.0 - 8.4
219	4112 ± 33	1.90 ± 0.14	1.59 ± 0.11	-0.28 ± 0.13	-5.596 ± 0.064	53041.123553	1.398	-1.50	-0.803	2.82 ± 0.80	0.9 ± 0.2	50.7 ± 8.0	4.5 - 8.5
220	4259 ± 23	2.23 ± 0.09	1.64 ± 0.11	-0.05 ± 0.10	-22.126 ± 0.046	53689.372876	1.310	0.60	-0.671	1.63 ± 0.20	0.8 ± 0.3	12.0 ± 0.9	6.0 - 8.4
221	4444 ± 15	2.29 ± 0.06	1.52 ± 0.09	-0.14 ± 0.09	-6.538 ± 0.037	53775.145394	1.186	0.70	-0.527	1.89 ± 0.15	1.5 ± 0.3	14.9 ± 0.7	3.0 ± 2.4
222	5019 ± 10	3.25 ± 0.04	1.36 ± 0.08	-0.06 ± 0.07	-3.927 ± 0.033	53308.437234	0.889	0.94	-0.255	1.23 ± 0.21	1.9 ± 0.2	5.5 ± 0.5	1.3 ± 0.7
223	4781 ± 13	2.82 ± 0.05	1.26 ± 0.08	-0.44 ± 0.07	1.887 ± 0.035	53633.334850	0.959	0.80	-0.345	1.28 ± 0.16	1.0 ± 0.2	6.4 ± 0.4	3.5 - 6.3
224	4560 ± 15	2.02 ± 0.07	1.63 ± 0.07	-0.18 ± 0.09	-19.165 ± 0.068	54045.404468	1.114	-2.50	-0.451	2.51 ± 0.38	3.4 ± 1.2	28.9 ± 2.4	0.4 ± 0.6
225	4776 ± 10	2.97 ± 0.04	1.33 ± 0.06	-0.06 ± 0.06	19.491 ± 0.027	53724.299416	1.009	0.80	-0.346	1.30 ± 0.16	1.5 ± 0.2	6.5 ± 0.4	2.6 ± 1.6
226	4784 ± 10	2.64 ± 0.03	1.33 ± 0.05	-0.09 ± 0.06	6.902 ± 0.024	54417.384259	1.002	0.80	-0.342	1.81 ± 0.21	2.2 ± 0.4	11.7 ± 0.7	1.1 ± 0.5
227	4853 ± 10	2.81 ± 0.04	1.49 ± 0.08	-0.04 ± 0.06	23.388 ± 0.031	53664.457500	0.973	0.84	-0.314	1.62 ± 0.26	2.1 ± 0.5	9.1 ± 0.8	1.1 ± 0.8
228	4943 ± 10	2.85 ± 0.03	1.56 ± 0.06	-0.19 ± 0.06	3.351 ± 0.031	53610.379670	0.909	0.89	-0.281	1.52 ± 0.16	1.6 ± 0.3	7.9 ± 0.4	1.9 ± 1.2
229	4936 ± 15	2.75 ± 0.05	1.43 ± 0.10	-0.10 ± 0.09	4.369 ± 0.026	53688.166505	0.924	0.89	-0.283	1.80 ± 0.14	2.5 ± 0.4	10.9 ± 0.5	0.8 ± 0.4
230	4713 ± 08	2.72 ± 0.04	1.36 ± 0.06	-0.24 ± 0.06	-78.472 ± 0.032	54759.451146	1.021	0.80	-0.374	1.36 ± 0.27	0.9 ± 0.3	7.2 ± 0.7	2.7 - 9.2
231	4338 ± 23	1.68 ± 0.09	1.47 ± 0.05	-0.45 ± 0.10	-13.505 ± 0.038	53041.135457	1.226	-2.50	-0.598	2.46 ± 0.14	1.6 ± 0.3	30.1 ± 1.2	2.2 ± 1.8
232	4826 ± 15	2.69 ± 0.05	1.47 ± 0.11	-0.19 ± 0.08	-17.641 ± 0.023	53041.167992	0.968	0.82	-0.325	1.57 ± 0.19	1.4 ± 0.3	8.7 ± 0.6	2.7 ± 1.1
233	4830 ± 10	2.70 ± 0.03	1.42 ± 0.06	-0.12 ± 0.06	2.707 ± 0.031	54015.481817	0.975	0.82	-0.323	1.76 ± 0.32	2.2 ± 0.6	10.9 ± 1.0	1.1 ± 0.8
234	4899 ± 13	3.03 ± 0.04	1.62 ± 0.11	-0.43 ± 0.07	32.087 ± 0.044	53037.430671	0.900	0.86	-0.299	1.17 ± 0.16	1.1 ± 0.2	5.3 ± 0.4	6.2 ± 4.2
235	4669 ± 13	2.55 ± 0.05	1.29 ± 0.08	-0.49 ± 0.08	-26.270 ± 0.024	53749.236794	1.016	0.80	-0.389	1.46 ± 0.12	0.9 ± 0.1	8.2 ± 0.4	6.4 - 9.2
236	4708 ± 10	2.69 ± 0.04	1.27 ± 0.05	-0.56 ± 0.06	-2.676 ± 0.023	54565.231192	0.985	0.80	-0.377	1.44 ± 0.21	0.7 ± 0.2	7.9 ± 0.6	5.5 - 7.8
237	4097 ± 18	1.99 ± 0.08	1.51 ± 0.09	-0.34 ± 0.07	54.627 ± 0.065	53713.346910	1.405	-2.51	-0.816	1.93 ± 0.17	0.8 ± 0.2	18.3 ± 1.0	6.0 - 8.5
238	4802 ± 15	2.55 ± 0.05	1.38 ± 0.06	-0.27 ± 0.07	-9.253 ± 0.024	53476.216476	0.970	0.80	-0.335	1.72 ± 0.03	1.5 ± 0.1	10.5 ± 0.2	2.2 ± 0.4
239	4328 ± 15	2.13 ± 0.06	1.65 ± 0.09	-0.09 ± 0.08	-11.427 ± 0.041	53928.321788	1.264	0.74	-0.613	1.85 ± 0.29	1.1 ± 0.2	15.0 ± 1.3	8.0 ± 3.7

Table 5. continued.

No.	T_{eff} [K]	$\log g$ [cm s ⁻²]	v_t [km s ⁻¹]	[Fe/H]	RV [km s ⁻¹]	MJD +2400000 [d]	(B-V) ₀ [mag]	M_V [mag]	BC_V [mag]	$\log L/L_{\odot}$	M [M_{\odot}]	R [R_{\odot}]	Age [Gyr]
240	4546 ± 13	2.66 ± 0.05	1.44 ± 0.06	0.16 ± 0.06	-27.846 ± 0.037	54741.338582	1.160	0.77	-0.464	1.57 ± 0.21	1.6 ± 0.4	9.8 ± 0.7	2.3 ± 1.7
241	4757 ± 23	3.10 ± 0.08	1.17 ± 0.12	-0.12 ± 0.11	-4.000 ± 0.035	53600.215012	1.011	0.80	-0.354	1.13 ± 0.13	1.3 ± 0.2	5.4 ± 0.4	4.9 ± 2.2
242	4531 ± 10	2.55 ± 0.04	1.49 ± 0.09	-0.01 ± 0.07	-35.763 ± 0.041	54777.126933	1.147	0.75	-0.471	1.53 ± 0.10	1.2 ± 0.2	9.5 ± 0.4	6.0 ± 3.6
243	4920 ± 05	2.48 ± 0.02	1.46 ± 0.06	-0.53 ± 0.05	12.860 ± 0.023	54788.257517	0.877	0.88	-0.292	1.85 ± 0.20	1.5 ± 0.4	11.6 ± 0.7	2.1 ± 1.5
244	4889 ± 08	2.65 ± 0.03	1.59 ± 0.06	-0.10 ± 0.06	-8.262 ± 0.029	54014.194468	0.948	0.86	-0.300	1.82 ± 0.15	2.4 ± 0.4	11.3 ± 0.5	0.9 ± 0.5
245	4639 ± 10	2.58 ± 0.04	1.37 ± 0.06	-0.28 ± 0.06	-6.799 ± 0.033	54310.400220	1.058	0.80	-0.405	1.42 ± 0.18	0.8 ± 0.2	8.0 ± 0.5	6.4 - 9.3
246	4880 ± 10	2.82 ± 0.04	1.38 ± 0.07	0.01 ± 0.07	-18.265 ± 0.028	53744.085457	0.966	0.85	-0.303	1.65 ± 0.23	2.2 ± 0.4	9.4 ± 0.7	0.9 ± 0.5
247	4575 ± 10	2.78 ± 0.04	1.41 ± 0.08	-0.06 ± 0.07	-12.900 ± 0.034	54014.181858	1.118	0.78	-0.443	1.25 ± 0.15	1.0 ± 0.2	6.7 ± 0.4	5.9 - 8.4
248	4750 ± 10	2.67 ± 0.04	1.40 ± 0.08	-0.16 ± 0.07	-21.301 ± 0.024	53024.087332	1.010	0.55	-0.357	1.82 ± 0.38	2.1 ± 0.3	12.0 ± 1.3	1.0 ± 0.4
249	4736 ± 13	2.74 ± 0.05	1.22 ± 0.08	-0.74 ± 0.06	-55.913 ± 0.023	53601.292095	0.946	0.80	-0.366	1.37 ± 0.27	0.7 ± 0.2	7.2 ± 0.7	5.5 - 7.8
250	4512 ± 05	2.24 ± 0.03	1.33 ± 0.05	-0.30 ± 0.05	-7.505 ± 0.039	54794.209832	1.128	0.74	-0.480	1.74 ± 0.26	0.9 ± 0.3	12.2 ± 0.9	2.8 - 9.3
251	5068 ± 10	2.40 ± 0.03	1.52 ± 0.05	-0.26 ± 0.05	17.643 ± 0.024	54400.314375	0.842	0.96	-0.242	2.15 ± 0.26	2.9 ± 0.7	15.4 ± 1.0	0.5 ± 0.5
252	5046 ± 10	3.42 ± 0.04	1.18 ± 0.05	-0.11 ± 0.05	-26.394 ± 0.025	54310.384115	0.870	0.95	-0.247	1.05 ± 0.21	1.7 ± 0.2	4.4 ± 0.5	1.8 ± 0.8
253	4666 ± 13	2.71 ± 0.05	1.37 ± 0.08	-0.23 ± 0.07	-50.713 ± 0.103	54046.284722	1.049	0.80	-0.390	1.29 ± 0.27	0.8 ± 0.2	6.8 ± 0.7	4.7 - 9.2
254	4768 ± 10	2.64 ± 0.04	1.34 ± 0.04	0.02 ± 0.05	-27.619 ± 0.030	54782.294201	1.024	0.80	-0.349	1.79 ± 0.19	2.2 ± 0.4	11.5 ± 0.7	0.9 ± 0.5
255	4807 ± 20	2.18 ± 0.07	1.91 ± 0.09	-0.30 ± 0.10	-2.984 ± 0.113	53688.293125	0.964	0.09	-0.333	2.00 ± 0.57	2.8 ± 0.8	14.4 ± 2.2	0.6 ± 0.5
256	4966 ± 10	2.56 ± 0.03	1.47 ± 0.06	-0.31 ± 0.06	-31.900 ± 0.028	53937.409705	0.882	0.91	-0.274	1.91 ± 0.19	2.0 ± 0.3	12.2 ± 0.7	1.2 ± 1.1
257	4632 ± 15	2.75 ± 0.06	1.38 ± 0.10	-0.17 ± 0.09	-51.040 ± 0.030	53629.451915	1.074	0.80	-0.409	1.47 ± 0.10	1.4 ± 0.2	8.5 ± 0.3	3.5 ± 1.5
258	5026 ± 10	2.93 ± 0.03	0.97 ± 0.08	-0.22 ± 0.06	-40.233 ± 0.024	54776.118264	0.865	0.94	-0.254	1.52 ± 0.15	1.8 ± 0.2	7.6 ± 0.4	1.3 ± 0.6
259	5027 ± 10	2.64 ± 0.04	1.36 ± 0.07	-0.15 ± 0.07	-7.085 ± 0.028	53923.444317	0.874	-1.25	-0.253	2.50 ± 0.69	3.2 ± 0.8	23.5 ± 3.3	0.4 ± 0.3
260	5130 ± 08	3.11 ± 0.03	1.34 ± 0.06	-0.08 ± 0.05	9.538 ± 0.061	54773.286221	0.836	0.99	-0.222	1.49 ± 0.31	2.3 ± 0.4	7.0 ± 0.8	0.8 ± 0.6
261	4909 ± 10	2.78 ± 0.03	1.34 ± 0.06	-0.05 ± 0.06	-12.496 ± 0.026	54667.411516	0.944	0.87	-0.292	1.73 ± 0.10	2.4 ± 0.3	10.1 ± 0.3	0.7 ± 0.5
262	5069 ± 15	3.25 ± 0.05	1.36 ± 0.10	-0.09 ± 0.08	42.204 ± 0.039	53615.431447	0.862	-0.52	-0.240	2.20 ± 0.73	1.9 ± 0.3	16.4 ± 2.8	1.4 ± 0.9
263	4788 ± 13	2.84 ± 0.05	1.42 ± 0.06	-0.01 ± 0.06	-6.540 ± 0.042	54723.242784	1.010	0.80	-0.340	1.55 ± 0.20	1.9 ± 0.3	8.7 ± 0.6	1.4 ± 0.9
264	5275 ± 23	3.49 ± 0.07	1.65 ± 0.14	0.04 ± 0.10	-11.669 ± 0.244	53644.191105	0.787	1.11	-0.182	1.04 ± 0.31	1.8 ± 0.4	4.0 ± 0.6	1.8 ± 2.3
265	4791 ± 05	2.55 ± 0.02	1.40 ± 0.05	-0.36 ± 0.04	-74.362 ± 0.023	54136.403368	0.964	0.80	-0.340	1.75 ± 0.18	1.5 ± 0.3	10.9 ± 0.6	2.4 ± 1.8
266	5061 ± 15	3.14 ± 0.04	1.36 ± 0.07	-0.05 ± 0.06	-2.161 ± 0.029	53031.422054	0.871	0.99	-0.242	1.60 ± 0.20	2.0 ± 0.3	8.2 ± 0.6	1.1 ± 0.4
267	4683 ± 18	3.30 ± 0.06	1.16 ± 0.13	0.08 ± 0.09	-31.272 ± 0.036	53096.241620	1.076	0.80	-0.389	0.79 ± 0.26	0.9 ± 0.2	3.8 ± 0.7	4.4 - 8.3
268	4794 ± 08	2.78 ± 0.03	1.25 ± 0.04	-0.34 ± 0.05	34.252 ± 0.023	54577.202622	0.965	0.80	-0.339	1.39 ± 0.14	1.1 ± 0.2	7.2 ± 0.4	6.1 ± 2.7
269	4721 ± 05	2.53 ± 0.03	1.32 ± 0.06	-0.50 ± 0.05	-29.718 ± 0.037	54214.180376	0.985	0.80	-0.371	1.63 ± 0.19	1.2 ± 0.3	9.8 ± 0.6	4.6 ± 1.1
270	4777 ± 08	3.30 ± 0.03	1.05 ± 0.06	-0.07 ± 0.05	-0.886 ± 0.028	54781.448854	1.008	0.80	-0.345	0.86 ± 0.22	1.1 ± 0.2	3.9 ± 0.5	3.4 - 8.2
271	4055 ± 15	1.61 ± 0.07	1.65 ± 0.09	-0.79 ± 0.08	-69.417 ± 0.081	53742.250341	1.409	-2.54	-0.847	2.65 ± 0.14	0.8 ± 0.2	42.9 ± 1.5	5.6 - 7.9
272	4132 ± 20	2.20 ± 0.08	1.38 ± 0.11	-0.42 ± 0.09	67.737 ± 0.095	53423.333843	1.374	0.52	-0.777	1.88 ± 0.16	0.8 ± 0.2	17.0 ± 0.9	6.0 - 8.5
273	4769 ± 15	2.37 ± 0.06	1.54 ± 0.09	-0.25 ± 0.09	-8.210 ± 0.036	53193.211944	0.989	-1.05	-0.349	2.46 ± 0.62	1.9 ± 0.2	24.9 ± 3.3	1.2 ± 0.4
274	4788 ± 10	2.67 ± 0.04	1.41 ± 0.05	0.05 ± 0.06	8.262 ± 0.026	54551.469508	1.017	0.80	-0.340	1.73 ± 0.20	2.2 ± 0.4	10.7 ± 0.7	1.0 ± 0.5
275	4368 ± 10	2.51 ± 0.05	1.47 ± 0.09	0.07 ± 0.07	-19.382 ± 0.050	53941.316736	1.256	0.66	-0.586	1.35 ± 0.27	0.7 ± 0.3	8.3 ± 0.9	6.0 - 8.4
276	4645 ± 08	2.36 ± 0.03	1.57 ± 0.07	-0.53 ± 0.06	-98.989 ± 0.048	54580.426568	1.026	0.80	-0.402	1.62 ± 0.24	0.7 ± 0.2	10.0 ± 0.8	5.5 - 7.9
277	4262 ± 13	2.10 ± 0.05	1.65 ± 0.08	-0.38 ± 0.07	-88.803 ± 0.061	53513.322309	1.282	-2.50	-0.659	1.75 ± 0.15	0.9 ± 0.2	13.8 ± 0.7	6.0 - 8.4
278	4879 ± 05	2.47 ± 0.03	1.47 ± 0.06	-0.43 ± 0.06	-4.664 ± 0.035	53886.440752	0.911	0.78	-0.306	1.71 ± 0.12	2.0 ± 0.5	10.0 ± 0.4	1.0 ± 0.8
279	4550 ± 10	2.59 ± 0.04	1.50 ± 0.06	-0.04 ± 0.06	-46.471 ± 0.043	54759.091018	1.134	0.77	-0.459	1.48 ± 0.19	1.2 ± 0.3	8.9 ± 0.6	5.9 ± 1.1
280	4907 ± 05	2.72 ± 0.02	1.43 ± 0.04	-0.24 ± 0.03	-22.315 ± 0.028	54013.126047	0.921	0.87	-0.294	1.66 ± 0.19	1.7 ± 0.3	9.4 ± 0.6	1.5 ± 1.1
281	4777 ± 20	2.89 ± 0.08	1.42 ± 0.10	-0.10 ± 0.09	-27.870 ± 0.029	53158.265932	1.004	0.80	-0.345	1.48 ± 0.25	1.8 ± 0.4	8.0 ± 0.7	1.8 ± 1.6
282	4842 ± 13	3.19 ± 0.04	1.17 ± 0.08	-0.13 ± 0.06	-7.788 ± 0.027	53492.377963	0.968	0.83	-0.318	1.12 ± 0.24	1.5 ± 0.3	5.2 ± 0.6	3.2 ± 2.3
283	4322 ± 18	2.26 ± 0.08	1.58 ± 0.13	-0.12 ± 0.10	-35.375 ± 0.049	53527.447459	1.265	0.64	-0.617	1.62 ± 0.25	0.9 ± 0.4	11.5 ± 1.0	2.8 - 8.4
284	4628 ± 08	2.64 ± 0.03	1.17 ± 0.06	-0.18 ± 0.05	1.387 ± 0.025	55021.334352	1.076	0.80	-0.411	1.62 ± 0.09	1.6 ± 0.2	10.1 ± 0.3	2.4 ± 0.8
285	4760 ± 05	2.56 ± 0.02	1.33 ± 0.06	-0.48 ± 0.05	24.087 ± 0.025	54572.438889	0.965	0.80	-0.354	1.66 ± 0.13	1.3 ± 0.2	10.0 ± 0.4	3.4 ± 1.7
286	4767 ± 08	2.46 ± 0.04	1.32 ± 0.05	-0.65 ± 0.05	10.937 ± 0.024	53900.290498	0.940	0.80	-0.352	1.58 ± 0.16	0.9 ± 0.2	9.1 ± 0.5	5.5 - 7.8
287	4723 ± 30	3.33 ± 0.11	2.42 ± 0.23	-0.47 ± 0.11	-38.186 ± 0.416	53820.479502	0.987	-0.96	-0.370	2.43 ± 0.09	2.0 ± 0.3	24.5 ± 0.8	1.1 ± 0.4

Table 5. continued.

No.	T_{eff} [K]	$\log g$ [cm s ⁻²]	v_t [km s ⁻¹]	[Fe/H]	RV [km s ⁻¹]	MJD +2400000 [d]	(B-V) ₀ [mag]	M_V [mag]	BC_V [mag]	$\log L/L_\odot$	M [M_\odot]	R [R_\odot]	Age [Gyr]
288	5048 ± 15	3.35 ± 0.05	1.15 ± 0.06	-0.44 ± 0.07	-19.144 ± 0.027	53551.375394	0.829	0.95	-0.250	0.97 ± 0.14	1.3 ± 0.2	4.0 ± 0.3	3.9 ± 1.6
289	4907 ± 15	3.03 ± 0.05	1.39 ± 0.09	0.02 ± 0.08	-24.931 ± 0.031	53632.165243	0.954	0.87	-0.293	1.42 ± 0.10	2.0 ± 0.2	7.1 ± 0.3	1.1 ± 0.2
290	5624 ± 15	3.69 ± 0.03	2.01 ± 0.10	0.04 ± 0.06	-11.385 ± 0.035	54370.324722	0.653	1.39	-0.113	0.83 ± 0.18	1.4 ± 0.2	2.7 ± 0.3	3.0 ± 1.4
291	4361 ± 10	1.66 ± 0.05	2.04 ± 0.09	-0.26 ± 0.07	-24.822 ± 0.044	53722.092396	1.228	-2.50	-0.584	2.49 ± 0.20	1.7 ± 0.4	30.8 ± 1.4	2.0 ± 1.8
292	4846 ± 10	2.62 ± 0.03	1.31 ± 0.08	-0.12 ± 0.07	5.598 ± 0.024	54758.277679	0.967	0.83	-0.317	1.93 ± 0.13	2.5 ± 0.4	13.1 ± 0.5	0.8 ± 0.5
293	4820 ± 20	3.51 ± 0.06	1.14 ± 0.12	-0.04 ± 0.09	-84.229 ± 0.043	53187.404954	0.990	0.82	-0.327	0.62 ± 0.15	1.0 ± 0.1	2.9 ± 0.4	5.7 - 8.1
294	5008 ± 10	2.58 ± 0.04	1.94 ± 0.11	-0.13 ± 0.07	-7.978 ± 0.061	53545.407812	0.885	0.93	-0.259	2.12 ± 0.32	3.3 ± 0.8	15.3 ± 1.2	0.4 ± 0.4
295	5023 ± 10	2.98 ± 0.03	1.43 ± 0.06	-0.06 ± 0.06	-10.335 ± 0.023	54623.456597	0.887	0.94	-0.254	1.50 ± 0.27	2.3 ± 0.5	7.4 ± 0.7	0.8 ± 0.5
296	4297 ± 25	2.31 ± 0.11	1.67 ± 0.11	-0.18 ± 0.12	8.575 ± 0.049	53187.411007	1.276	0.62	-0.636	1.54 ± 0.23	0.8 ± 0.3	10.6 ± 0.9	6.0 - 8.4
297	4820 ± 10	2.46 ± 0.04	1.65 ± 0.08	-0.16 ± 0.06	-19.577 ± 0.039	53722.081181	0.975	-2.08	-0.327	2.86 ± 0.85	3.0 ± 0.7	38.7 ± 5.9	0.5 ± 0.6
298	5032 ± 15	3.03 ± 0.05	1.45 ± 0.08	-0.10 ± 0.08	-29.155 ± 0.027	53187.387651	0.878	0.94	-0.251	1.42 ± 0.27	2.2 ± 0.4	6.8 ± 0.7	0.9 ± 0.5
299	4701 ± 13	2.62 ± 0.05	1.35 ± 0.09	-0.33 ± 0.08	15.623 ± 0.029	53187.377124	1.017	0.80	-0.380	1.42 ± 0.14	0.9 ± 0.1	7.7 ± 0.4	6.3 - 9.3
300	4780 ± 05	2.72 ± 0.02	1.46 ± 0.06	-0.05 ± 0.05	-24.039 ± 0.048	53917.252407	1.009	0.80	-0.344	1.68 ± 0.08	2.0 ± 0.2	10.1 ± 0.3	1.1 ± 0.2
301	4652 ± 20	2.95 ± 0.08	1.36 ± 0.12	-0.08 ± 0.10	-20.228 ± 0.033	53158.311285	1.074	0.80	-0.398	1.17 ± 0.17	1.1 ± 0.2	5.9 ± 0.5	3.4 - 8.3
302	4662 ± 15	2.67 ± 0.06	1.49 ± 0.10	-0.08 ± 0.09	-39.349 ± 0.033	53158.338877	1.068	0.80	-0.392	1.63 ± 0.20	1.7 ± 0.3	10.0 ± 0.7	2.0 ± 1.6
303	4169 ± 20	1.95 ± 0.09	1.62 ± 0.09	-0.12 ± 0.10	-20.791 ± 0.060	53893.296256	1.368	-2.50	-0.751	2.09 ± 0.18	1.2 ± 0.3	21.3 ± 1.1	2.8 - 8.5
304	4915 ± 05	2.78 ± 0.03	1.50 ± 0.05	-0.22 ± 0.05	-22.791 ± 0.031	54290.361111	0.919	0.88	-0.291	1.57 ± 0.19	1.6 ± 0.3	8.4 ± 0.5	1.8 ± 1.1
305	4630 ± 10	2.64 ± 0.05	1.33 ± 0.06	-0.28 ± 0.07	-38.625 ± 0.031	53906.369468	1.063	0.80	-0.410	1.33 ± 0.28	0.8 ± 0.2	7.2 ± 0.8	4.7 - 9.3
306	4535 ± 20	2.54 ± 0.07	1.36 ± 0.11	-0.20 ± 0.10	-5.392 ± 0.031	53492.400845	1.125	0.76	-0.467	1.40 ± 0.27	0.7 ± 0.2	8.1 ± 0.9	6.4 - 9.3
307	4756 ± 15	2.84 ± 0.07	1.57 ± 0.09	-0.16 ± 0.08	-62.232 ± 0.049	53582.142176	1.007	0.80	-0.354	1.48 ± 0.19	1.7 ± 0.3	8.1 ± 0.6	1.8 ± 1.1
308	4733 ± 15	2.68 ± 0.06	1.51 ± 0.09	-0.15 ± 0.10	-45.510 ± 0.039	54276.260608	1.021	0.80	-0.365	1.69 ± 0.11	2.0 ± 0.2	10.4 ± 0.4	1.1 ± 0.4
309	4836 ± 18	3.07 ± 0.06	1.39 ± 0.10	-0.19 ± 0.09	-19.260 ± 0.027	53138.408970	0.963	0.82	-0.321	1.02 ± 0.20	0.9 ± 0.2	4.6 ± 0.5	4.6 - 9.1
310	4823 ± 13	2.97 ± 0.05	1.72 ± 0.11	-0.20 ± 0.08	-24.914 ± 0.062	53484.427789	0.968	0.40	-0.326	1.87 ± 0.22	1.1 ± 0.2	12.4 ± 0.8	2.2 - 6.3
311	4417 ± 15	2.77 ± 0.07	1.46 ± 0.11	-0.10 ± 0.08	-31.979 ± 0.041	53544.260012	1.207	0.68	-0.547	1.26 ± 0.26	0.8 ± 0.3	7.3 ± 0.8	5.9 - 8.4
312	4735 ± 15	2.73 ± 0.05	1.55 ± 0.08	-0.21 ± 0.08	-64.428 ± 0.045	53868.373067	1.012	0.80	-0.364	1.32 ± 0.16	0.9 ± 0.2	6.8 ± 0.5	4.6 - 9.2
313	4656 ± 05	2.48 ± 0.03	1.41 ± 0.05	-0.14 ± 0.05	-74.570 ± 0.030	54584.428206	1.065	0.92	-0.395	1.69 ± 0.07	2.0 ± 0.3	10.8 ± 0.2	1.3 ± 0.7
314	4688 ± 15	2.71 ± 0.06	1.45 ± 0.08	-0.06 ± 0.08	-26.834 ± 0.032	53534.338553	1.056	0.80	-0.386	1.59 ± 0.17	1.7 ± 0.3	9.5 ± 0.6	1.9 ± 1.2
315	4434 ± 20	2.27 ± 0.09	1.65 ± 0.11	-0.27 ± 0.11	-81.003 ± 0.060	54289.227500	1.180	0.70	-0.532	1.59 ± 0.31	0.7 ± 0.3	10.6 ± 1.1	4.7 - 9.3
316	4726 ± 05	2.86 ± 0.03	1.41 ± 0.08	0.00 ± 0.06	-8.634 ± 0.038	53540.244352	1.043	0.80	-0.368	1.45 ± 0.19	1.6 ± 0.3	7.9 ± 0.5	2.4 ± 1.6
317	4744 ± 13	2.75 ± 0.05	1.47 ± 0.08	-0.13 ± 0.07	-25.947 ± 0.035	53209.198003	1.017	0.80	-0.360	1.59 ± 0.07	1.8 ± 0.2	9.2 ± 0.3	1.5 ± 0.3
318	4794 ± 28	3.56 ± 0.09	1.20 ± 0.13	0.03 ± 0.12	-73.342 ± 0.042	53178.256400	1.012	0.80	-0.338	0.59 ± 0.22	1.0 ± 0.2	2.9 ± 0.6	4.3 - 8.1
319	4906 ± 23	4.58 ± 0.06	0.57 ± 0.33	-0.55 ± 0.07	26.803 ± 0.049	54309.151406	0.882	6.33	-0.297	-0.68 ± 1.04	0.6 ± 0.3	0.6 ± 0.5	5.3 - 7.5
320	4419 ± 15	2.47 ± 0.06	1.25 ± 0.08	-0.48 ± 0.08	-6.576 ± 0.035	53867.468681	1.170	1.19	-0.539	1.64 ± 0.12	0.8 ± 0.2	11.3 ± 0.5	4.7 - 9.3
321	4581 ± 10	2.59 ± 0.04	1.22 ± 0.07	-0.03 ± 0.06	-14.992 ± 0.032	54661.319769	1.118	0.79	-0.440	1.60 ± 0.13	1.4 ± 0.2	10.0 ± 0.5	3.4 ± 2.5
322	4790 ± 15	2.71 ± 0.06	1.44 ± 0.09	-0.20 ± 0.09	-31.606 ± 0.027	53509.449144	0.985	0.77	-0.340	1.73 ± 0.28	1.2 ± 0.2	10.7 ± 0.9	5.0 ± 2.6
323	5134 ± 20	3.25 ± 0.07	1.75 ± 0.13	-0.40 ± 0.08	-7.067 ± 0.967	53897.874880	0.799	0.20	-0.225	1.91 ± 0.17	1.8 ± 0.2	11.4 ± 0.6	1.4 ± 0.6
324	4815 ± 10	2.78 ± 0.04	1.53 ± 0.11	-0.12 ± 0.08	-23.115 ± 0.030	53191.283785	0.982	0.82	-0.329	1.68 ± 0.19	2.2 ± 0.3	10.0 ± 0.6	0.8 ± 0.8
325	4526 ± 13	2.70 ± 0.05	1.29 ± 0.08	0.01 ± 0.07	-46.542 ± 0.036	54641.327616	1.152	0.75	-0.475	1.33 ± 0.21	1.0 ± 0.2	7.5 ± 0.6	3.5 - 8.4
326	4499 ± 10	2.62 ± 0.04	1.45 ± 0.09	0.23 ± 0.06	-82.032 ± 0.043	54609.424595	1.194	0.73	-0.496	1.54 ± 0.12	1.4 ± 0.2	9.7 ± 0.4	3.4 ± 1.6
327	4744 ± 08	2.98 ± 0.03	1.24 ± 0.07	-0.07 ± 0.05	-9.718 ± 0.025	54639.347188	1.025	0.80	-0.360	1.27 ± 0.16	1.4 ± 0.2	6.4 ± 0.4	3.7 ± 2.3
328	4932 ± 10	2.95 ± 0.05	1.40 ± 0.08	0.04 ± 0.07	-19.548 ± 0.028	53510.417106	0.945	0.89	-0.284	1.57 ± 0.19	2.2 ± 0.3	8.4 ± 0.5	0.9 ± 0.9
329	4676 ± 15	3.41 ± 0.06	1.32 ± 0.13	0.21 ± 0.09	-66.688 ± 0.047	53552.303200	1.096	0.80	-0.385	0.66 ± 0.14	1.0 ± 0.1	3.3 ± 0.4	6.1 - 8.5
330	4842 ± 13	2.81 ± 0.05	1.46 ± 0.09	-0.19 ± 0.07	-64.210 ± 0.059	53512.420110	0.960	0.83	-0.319	1.43 ± 0.15	1.3 ± 0.2	7.4 ± 0.4	4.1 ± 2.7
331	5070 ± 13	3.27 ± 0.04	1.55 ± 0.09	-0.01 ± 0.06	-14.548 ± 0.033	53548.321262	0.872	0.96	-0.239	1.19 ± 0.12	1.9 ± 0.1	5.1 ± 0.3	1.3 ± 0.3
332	4968 ± 08	3.41 ± 0.03	1.11 ± 0.05	-0.12 ± 0.05	-9.152 ± 0.024	54254.425810	0.905	0.91	-0.272	0.91 ± 0.15	1.5 ± 0.2	3.9 ± 0.3	2.6 ± 0.7
333	4805 ± 44	2.89 ± 1.00	—	-0.15	-37.758 ± 0.025	55632.479080	1.002	0.80	-0.349	1.63 ± 0.21	2.0 ± 0.3	9.6 ± 0.7	1.3 ± 0.9
334	4626 ± 50	2.79 ± 1.00	—	-0.15	-37.076 ± 1.300	54661.266209	1.093	0.80	-0.426	1.52 ± 0.24	1.4 ± 0.3	9.1 ± 0.8	4.5 ± 3.8
335	4727 ± 24	2.85 ± 1.00	—	-0.15	-19.012 ± 0.027	53943.181887	0.922	0.89	-0.287	1.66 ± 0.06	2.3 ± 0.2	9.3 ± 0.2	0.8 ± 0.3

Table 5. continued.

No.	T_{eff} [K]	$\log g$ [cm s ⁻²]	v_t [km s ⁻¹]	[Fe/H]	RV [km s ⁻¹]	MJD +2400000 [d]	(B–V) ₀ [mag]	M_V [mag]	BC_V [mag]	$\log L/L_\odot$	M [M_\odot]	R [R_\odot]	Age [Gyr]
336	4535 ± 51	2.72 ± 1.00	–	−0.15	-12.420 ± 0.038	54640.304641	1.244	0.65	−0.594	2.12 ± 0.12	1.7 ± 0.2	20.2 ± 0.8	2.1 ± 0.9
337	4702 ± 59	2.84 ± 1.00	–	−0.15	-59.057 ± 0.170	55265.404826	1.170	0.71	−0.511	1.95 ± 0.17	1.7 ± 0.3	15.8 ± 0.9	2.2 ± 1.7
338	4818 ± 45	2.90 ± 1.00	–	−0.15	-24.091 ± 0.050	55549.226863	0.884	0.92	−0.260	1.65 ± 0.19	2.5 ± 0.3	8.9 ± 0.6	0.6 ± 0.6
339	4983 ± 49	2.97 ± 1.00	–	−0.15	-25.735 ± 0.023	55545.224213	0.712	1.23	−0.156	1.30 ± 0.25	2.0 ± 0.3	5.1 ± 0.6	1.2 ± 0.4
340	4632 ± 37	2.80 ± 1.00	–	−0.15	-32.351 ± 0.027	53024.375191	1.061	0.80	−0.393	1.69 ± 0.14	1.8 ± 0.3	10.8 ± 0.6	1.7 ± 0.8
341	4603 ± 27	2.78 ± 1.00	–	−0.15	-52.399 ± 0.039	53546.428189	1.092	0.80	−0.425	1.69 ± 0.26	1.6 ± 0.4	11.0 ± 0.9	2.6 ± 2.3
342	4040 ± 81	2.02 ± 1.00	–	−0.15	-28.550 ± 0.356	53682.221007	1.770	−0.99	−1.672	2.77 ± 0.54	2.1 ± 0.4	60.3 ± 6.0	$0.8 - 1.9$
343	4334 ± 20	2.48 ± 1.00	–	−0.15	-39.100 ± 0.505	54397.245642	1.202	0.68	−0.545	2.23 ± 0.12	2.0 ± 0.2	22.3 ± 0.7	1.4 ± 0.2
344	4636 ± 27	2.80 ± 1.00	–	−0.15	–	–	1.071	0.80	−0.403	1.58 ± 0.30	1.6 ± 0.5	9.5 ± 1.0	2.9 ± 1.9
345	4181 ± 25	2.27 ± 1.00	–	−0.15	-9.303 ± 0.443	54401.206250	1.331	0.58	−0.704	1.81 ± 0.24	1.3 ± 0.3	15.1 ± 1.1	$2.8 - 8.5$
346	4818 ± 58	2.90 ± 1.00	–	−0.15	-10.975 ± 0.026	54785.436667	0.993	0.80	−0.341	1.59 ± 0.11	1.9 ± 0.2	9.1 ± 0.5	1.2 ± 0.3
347	5162 ± 29	3.08 ± 1.00	–	−0.15	-14.062 ± 0.070	53688.266343	0.935	0.86	−0.296	1.55 ± 0.16	2.1 ± 0.2	8.3 ± 0.5	1.1 ± 0.3
348	4027 ± 138	1.99 ± 1.00	–	−0.15	-1.473 ± 0.044	53543.413843	1.715	−0.96	−1.473	2.88 ± 0.19	1.4 ± 0.3	66.3 ± 2.5	3.5 ± 1.1

Notes. The following columns present: (1) running number, (2–5) atmospheric parameters and their intrinsic uncertainties (effective temperatures, surface gravities, microturbulence velocities and metallicities), (6) radial velocity from CCF, (7) epoch (MJD) of the radial velocity, (8–10) data obtained from Alonso et al. (1999) empirical calibration (color index, absolute magnitude and bolometric correction), (11–14) derived stellar integral parameters and their uncertainties (luminosities, masses, radii and ages).